How do sister DNAs become entrapped within cohesin rings?

Charlotte Marguerite Laurent

St. Hugh's College

University of Oxford



A thesis submitted for the degree of MSc by Research

Michaelmas Term 2022

Supervised by:

Dr. Madhusudhan Srinivasan

Professor Kim Nasmyth

Abstract

Sister chromatid cohesion (cohesion) is a process that ensures accurate segregation of genetic material into daughter cells during mitosis in eukaryotic cells. Cohesion is mediated by a highly conserved ring-shaped protein complex called cohesin. Cohesion is thought to arise from the topological entrapment of replicated sister DNAs inside the cohesin ring. Although cohesin can load onto, and topologically entrap individual DNAs prior to DNA replication, cohesion is established during S-phase in concert with DNA replication. Analysis of small circular DNAs in yeast has revealed that cohesion establishment can occur by two pathways operating in parallel. Firstly, cohesin can load onto replicated sister DNAs *de novo* in a manner that is dependent on the cohesin loading protein Scc2. Secondly, there exists a 'conversion' pathway in which cohesin binds to unreplicated DNA during G1, and remains associated with DNA throughout S-phase during which it is converted into cohesive cohesin. This process is independent of Scc2 but requires a group of replisome-associated factors which include Ctf4. Whether this cohesin conversion pathway generates cohesion of yeast chromosomes, and the molecular mechanisms underlying conversion, remain largely unknown. It is thought that opening of cohesin's Smc1-Smc3 hinge is crucial for entrapment of individual DNAs, but whether this is the case for entrapment of sister DNAs is currently unclear. I have developed a unique assay to measure cohesion generated solely by cohesin rings associated with DNA from G1. Using this assay, we show for the first time that conversion of non-cohesive cohesin to cohesive cohesin occurs on *S. cerevisiae* chromosomes during DNA replication, and that this process does not require opening of the Smc1-Smc3 hinge. Furthermore, the conversion observed was significantly reduced by deletion of Ctf4 but not significantly impacted by inactivation of the cohesin loader Scc2. These data provide crucial mechanistic insight into the process of cohesin conversion, and unequivocally demonstrate that while hinge opening is required for loading of cohesin rings onto DNA, it is not required for conversion of these rings into cohesive forms.

Acknowledgements

I would firstly like to thank my supervisor, Dr. Madhusudhan Srinivasan. Without his support, guidance and frequent discussion none of the work presented in this thesis would have been possible. My laboratory training in was also delivered entirely by Dr. Srinivasan, and I am very grateful for this. I would also like to thank my second supervisor, Professor Kim Nasmyth, for his guidance, wisdom and for giving me the opportunity to work in such an exciting environment. Under these two supervisors I have learnt a great deal about the art of biological research and the field of cohesin biology.

I would like to give a special acknowledgement to all other members of the Nasmyth lab for their friendship and support, and in particular to Dr. Maurici Brunet-Roig for his help with day-to-day lab matters and his sharing of resources. I must also thank Professor Stephan Gruber, as the work that he did in the Nasmyth lab over a decade ago has formed a central part of this thesis.

Finally, I would like to thank my parents, my sisters Emma and Camille, and Benjamin for their support during this past year and for helping to maintain my sanity. Last, but most certainly not least, thank you to my Australian Shepherd, Ollie, for providing dry humor and fruitful conversations, and for simply being the best.

Declaration and contributions

- From June to September 2021 I undertook a summer studentship in the Nasmyth lab. My work during this time was completely unrelated to that presented in this thesis, and concerned the deSUMOylation of various cohesin subunits by the protease Ulp2.

- All of the data presented in the 'Results' (Chapter 2) section of this thesis was produced by me. Certain yeast strains and plasmids were available prior to my joining the lab, or were provided by other groups, and the creators are listed in the appropriate tables (See: Materials and Methods).

- Microscopy was carried out by me using the ZEISS Axio Observer Z1.

- Unless otherwise stated, figures (both schematic and data) are original and were created by me using ProCreate, Microsoft Powerpoint and Excel, GraphPad Prism and Inkscape.

Table of contents

Abstract ii
Acknowledgements iii
Declaration and contributions iv
Abbreviations vii

Chapter 1: Introduction ix

1.1 Genetic material in cellular life 1
1.2 The cell cycle 1
1.3 Sister chromatid cohesion 3
1.4 Sister chromatid segregation 4
1.5 SMC proteins 5
1.6 Cohesin complex 8
Cohesin regulation 8
Cohesin in human disease 10
1.7 Cohesin-DNA interactions and topology 11
Cohesin's DNA entry gate 14
Loading and unloading: temporal dynamics of cohesin-DNA interactions 17
1.8 DNA replication and cohesion establishment 18
1.9 Thesis objectives 22
Objective 1 22
Objective 2 23

Chapter 2: Results 24

Part A: Can non-cohesive cohesin be converted into a cohesive structure, and does this require opening of its Smc3-Smc1 hinge? 25
2.1 Developing an assay whereby cohesin loaded onto DNA during G1 gives rise to cohesion 25
Introduction 25
An assay to measure chromosomal cohesion 26
Expression of GalScc1$_{NC}$ during G1 only is sufficient to generate non-cleavable cohesin-mediated cohesion 29
2.2 Assessing the significance of the Smc1-Smc3 hinge interface in cohesion establishment 32
Introduction 32
A method to temporally control closure of the Smc1-Smc3 hinge 33
Cohesin conversion occurs *in vivo* on yeast chromosomes, and does not require opening of the Smc1-Smc3 hinge 37
2.3 Confirming that rapamycin binds to FKBP12 and FRB on DNA-bound cohesin 42
Rapamycin-induced closure of Smc3-Scc1 interface rescues Eco1 inactivation-induced lethality 43

2.4 Deletion of conversion pathway-associated protein ctf4 significantly reduces cohesion established by conversion 45
2.5 Inactivation of cohesin *de novo* loader Scc2 does not interfere with cohesion established by conversion 47
Part B: Can fusion of both Smc-kleisin interfaces support viability? 50
2.6 Expressing the Smc3-Scc1-Smc1 fusion protein *in vivo* 50
Introduction 50
Developing a Smc3-Scc1-Smc1 fusion protein for expression in *S. cerevisiae* 50
Smc3-Scc1-Smc1 fusion does not support viability in the absence of wildtype Scc1 51

Chapter 3: Discussion **57**

3.1 Results Part A: Discussion and further work 58
Wapl-mediated cohesin release in cells where the Smc1-Smc3 hinge is closed 58
Potential deficits in cohesin occupancy when cohesion is mediated only by Conversion 59
The 'topological entrapment' model of sister chromatid cohesion 59
Covalent closure of the Smc1-Smc3 hinge 61
3.2 Results Part B: Discussion and further work 61
DNA entrapment and chromatin occupancy by Smc3-Scc1-Smc1 fusion protein 61
Achieving viability upon fusion of both Smc-kleisin interfaces 62
Probing the role of the Smc-kleisin interfaces in cohesin conversion 63
3.3 Concluding remarks 64

Chapter 4: Materials and Methods **66**

4.1 Yeast strains, plasmids and antibodies used 67
4.2 Cell culture and growth conditions 69
4.3 *S. cerevisiae* genetics and strain building 70
4.4 Biochemical techniques 72
4.5 Molecular biology techniques 73
4.6 Yeast immunofluorescence 79

Bibliography **81**

Abbreviations

aa	Amino acid
ABC	ATP-binding cassette
AF	AlexaFluor
APC/C	Anaphase promoting complex/cyclosome
ATP	Adenosine triphosphate
BMOE	Bis-maleimidoethane
BSA	Bovine serum albumin
CdLS	Cornelia de Lange Syndrome
CM	Catenated monomer
CD	Catenated dimer
ChIP-seq	Chromatin immunoprecipitation sequencing
C-terminal	Carboxy terminal
Ctf4/18	Chromosome transmission fidelity protein 4/18
DAPI	4′,6-diamidino-2-phenylindole
Δ	Delta, deletion
DMSO	Dimethyl sulfoxide
dsDNA	Double-stranded DNA
E. coli	*Escherichia coli*
Eco1	Establishment of cohesion 1
EDTA	Ethylenediaminetetraacetic acid
EtBr	Ethidium bromide
FKBP12	FK506 binding protein 12
Fpr1	FK506-sensitive proline rotamase 1
g	G-force
Gal	Galactose
G1/G2-phase	Gap 1/Gap 2-phase
HAWK	HEAT repeat-containing proteins associated with kleisins
HEAT	Huntingtin-EF3-PP2A-TOR1
His	Histidine
HRP	Horseradish peroxidase
Hos1	Histone deacetylase 1
HphMX	Hygromycin
IF	Immunofluorescence
KanMX	Kanamycin
kb	Kilobases
kDa	Kilodalton
KTag	ATHIKFS**K**RD (LysineTag)
LacI	Lactose repressor protein
LacO	Lactose operon
Leu	Leucine

M phase	Mitosis
NaCl	Sodium Chloride
NatMX	Natamycin
NC (subscript)	Non-cleavable
nM	Nanomolar
NP-40	Nonyl phenoxypolyethoxylethanol
nt	Nucleotide
N-terminal	Amino terminal
OD_{600}	Optical density at 600nm
PBS	Phosphate-buffered saline
PBS	PBS + 0.05% Tween®20
PCNA	Proliferating cell nuclear antigen
PCR	Polymerase chain rection
Pds5	Precocious dissociation of sisters 5
Phos/Sorb	Phosphate/sorbitol
PK9	(GKPIPNPLLGLDST)x9
RBS	Robert's Syndrome
RFC	Replication factor C
Rpm	Rotations per minute
RT	Room temperature
SAC	Spindle assembly checkpoint
Scc:	Sister chromatid cohesion (protein)
S. cerevisiae	*Saccharomyces cerevisiae*
SDS	Sodium dodecyl-sulfate
Smc (SMC/smc)	Structural maintenance of chromosomes
S-phase	Synthesis phase
SpyTag	AHIVMVDAYKPTK
ssDNA	single stranded DNA
TAD	Topologically associating domain
tetO	tetracycline operator
TetR	Tet-repressor protein
TOR1	Target of rapamycin 1
Trp	Tryptophan
ts	Temperature sensitive
Ura	Uracil
v/v	Volume by volume (percentage)
w/v	Weight by volume (percentage)
Wapl	Wings apart-like protein homolog
WT	Wild-type
YEP	Yeast extract + peptone
YEPD	Yeast extract + peptone + 2% dextrose (glucose)
YEPG	Yeast extract + peptone + 2% galactose

Chapter I: Introduction

1.1 Genetic material in cellular life

Genetic material in all forms of cellular life is stored as double stranded DNA (dsDNA). Prokaryotes are unicellular, with non-compartmentalized genetic material comprising either single or multiple linear or circular lengths of dsDNA. In uni- and multicellular eukaryotes, DNA is stored in the nucleus and consists of one or multiple individual stretches of DNA called chromosomes. The length and number of chromosomes varies across species and is independent of size or perceived complexity. Male Australian ants have one chromosome per cell whereas some plant cells have over 700 (Keogh et al., 1998; Mayrose et al., 2021). Regardless of whether an organism is uni- or multicellular, it is crucial for its viability that all of its cells possess identical genetic material. Moreover, central to all life forms is their ability to produce new cells, both to continue the existence of their species, and if multicellular, to develop, grow and regenerate tissue. This occurs by division of an existing 'parent' cell into two 'daughter' cells. In order to ensure both cells possess complete copies of the organism's genetic material, the cell's entire genome is duplicated prior to cell division. In eukaryotes, this DNA replication, along with phases of cellular growth, protein synthesis and cell division, or mitosis, comprise what is known as the eukaryotic cell cycle.

1.2 **The cell cycle**

In basic terms, the eukaryotic cell cycle can be divided into two phases. The first is interphase, during which DNA is duplicated and cell division-specific protein synthesis occurs. After interphase, cells enter mitosis, where genetic and other cellular material are segregated in equal stoichiometry to either pole of the parent cell, and the cell

divides to give two genetically identical daughter cells. Interphase comprises three additional 'phases' termed G1 (Gap 1), S (synthesis) and G2 (Gap 2) (Figure 1). During G1, the parent cell will grow and its metabolic activity will increase, and synthesis of proteins required for DNA replication will occur. In S phase, all of the cell's genetic material is duplicated. This generates two identical molecules of DNA called sister chromatids. G2 phase occurs after S phase, and involves the synthesis of various mitosis-related proteins and cellular organelles, and migration of the nucleus to the center of the bi-lobed cell. Following G2, the cell enters mitosis (M phase). Mitosis itself can be subdivided into four stages: prophase, metaphase, anaphase and telophase. In M phase, sister chromatids are condensed and aligned as pairs along the centre of the cell. They are then segregated equally to two opposing poles of the cell, the cytoplasm divides and the cell membrane is pinched closed in the centre of the cell, giving rise to two daughter cells (Makrantoni & Marston, 2018).

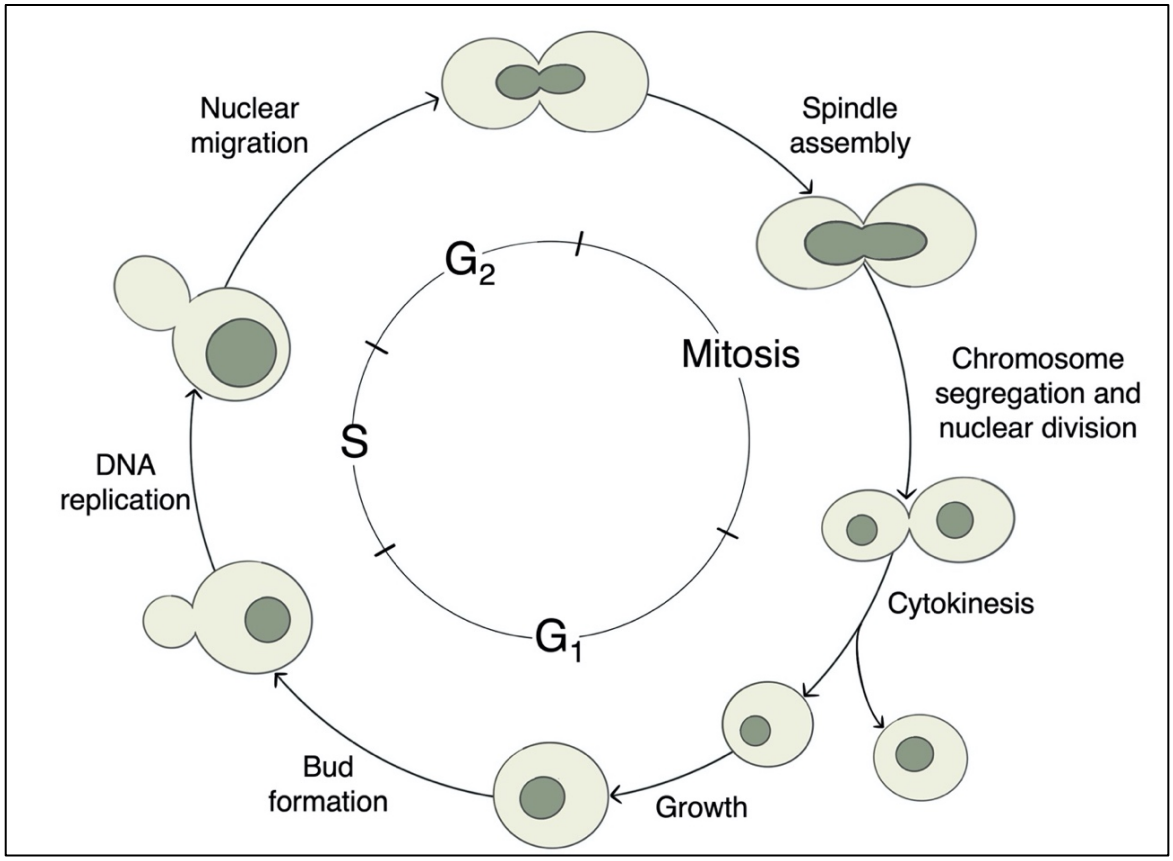


Figure 1. The *S. cerevisiae* (budding yeast) cell cycle. *G1*: cell growth, bud formation, synthesis of replisome proteins; *S*: DNA replication; *G2*: nuclear migration, protein synthesis, ***M*:** chromosome segregation and division of nuclei. G1, S and G2 comprise interphase. Adapted from Delobel & Tesniere, 2014.

1.3 **Sister chromatid cohesion:**

During interphase, despite eukaryotes possessing multiple chromatin organization mechanisms, chromosomes do not appear as distinct entities. Given chromosomes' astounding length to width ratio (in the order of 1×10^{10}), the interphase state of sister chromatids is highly 'tangled' and thus not amenable to equal segregation to opposite poles of the cell. In order to resolve this, during prophase, chromosomes are condensed into their characteristic compact and discrete rod shape (Figure 2A). In prokaryotes, the S- and M-phases of the cell cycle co-occur, meaning that prokaryotic chromosomes segregate to opposite poles of the cell whilst they are replicated (Margolin & Bernander, 2004). However, in eukaryotes, the S- and M-phases of the cell cycle are distinct. During eukaryotic cell division, sister chromatids generated in S-phase must be segregated equally into the daughter cells during mitosis. Failure of this segregation to occur properly is termed chromosome mis-segregation. This can give rise to aneuploidy, or the possession of an abnormal number of chromosomes by a cell (Orr & Compton, 2015).

Consequences of mis-segregation include cell death, and in multicellular organisms, oncogenesis and developmental disorders (Santaguida et al., 2015). To avoid these dire consequences, sister chromatids are physically tethered with one another from their replication in S phase until their separation during anaphase (Figure 2B). This phenomenon, known as sister chromatid cohesion, is a vital and highly conserved

process, and crucially, allows for the cell to identify the chromatids as sisters. During metaphase, microtubules, which emanate from opposite cell poles, attach to chromatids at the center of the cell via their centromeres, and sense tension when attached to two cohesive sister chromatids (McVey et al., 2021). Sister chromatid cohesion thus underpins orderly chromosome segregation in eukaryotes.

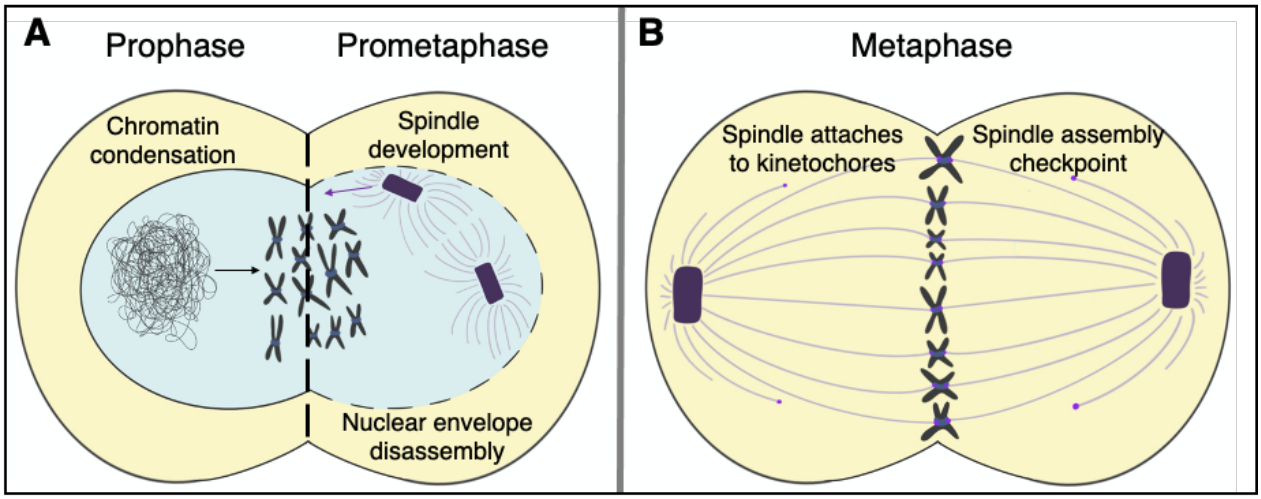


Figure 2. Prophase, prometaphase and metaphase in eukaryotic cells. A) During prophase, sister chromatids condense and are maintained as pairs. Before onset of metaphase (prometaphase) the cytoskeletal spindle forms and nuclear envelopes disassemble. B) Tension generated by spindle attachment to sister chromatids causes them to align at the centre of the cell. For progression into anaphase, spindle assembly checkpoint must be met.

1.4 **Sister Chromatid Segregation**

During mitosis, the sister chromatids align at the center of the cell. Microtubules emanating from either pole of the cell attach to sister chromatids via kinetochores, the proteinaceous scaffolds that assemble on the chromatids' centromeres. Cohesion between sister chromatids ensures that the pulling force generated by the microtubules as they depolymerize is resisted. This 'tension sensing' mechanism is known as the spindle assembly checkpoint (SAC) (Figure 2B), and its satisfaction allows for the cell to progress into anaphase (Musacchio & Salmon, 2007). Anaphase

onset is delineated by activation of the anaphase promoting complex/cyclosome (APC/C). Activation of APC/C abolishes sister chromatid cohesion, and sister chromatids are separated at their centromeres to opposite poles of the parent cell (Figure 3A) (Peters, 2006). In telophase (Figure 3B), the cytoplasm and cell membrane are pinched inwards to separate the parent cell into two daughters, and sister chromatids begin to decondense within newly formed nuclear membranes (Bouck & Cronshaw, 1965).

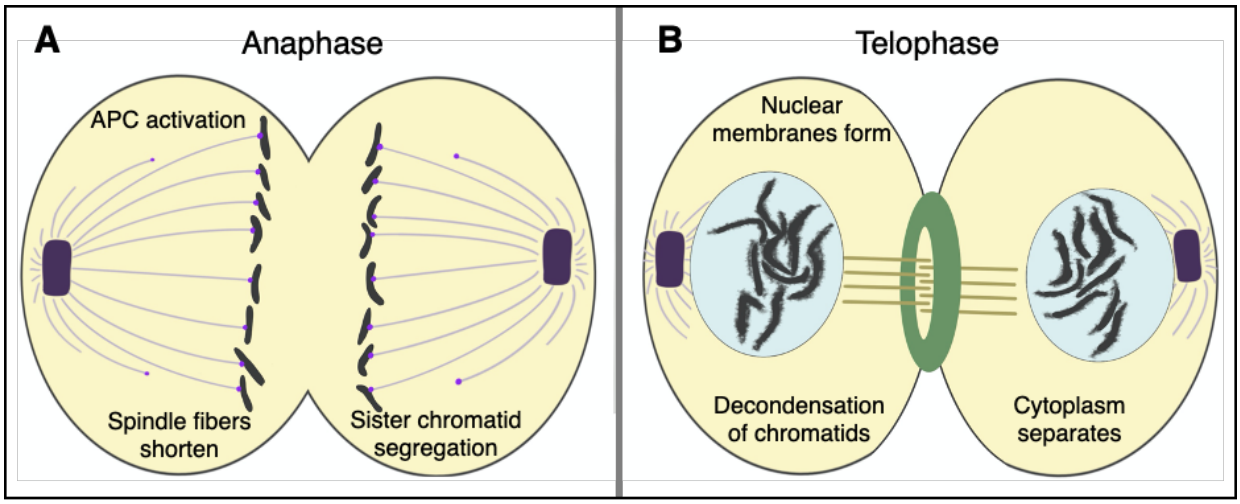


Figure 3. Anaphase and telophase in eukaryotic cells. A) During anaphase, APC is activated and Scc1 is cleaved, separating sister chromatids; their separation occurs via spindle fiber shortening. B) Nuclear membranes form around decondensing chromatids. Parent cell cytoplasm begins to separate to form daughter cells.

1.5 **SMC proteins**

Crucial to both the condensation of sister chromatids, and their cohesion from S phase until anaphase, are proteins belonging to the Structural Maintenance of Chromosomes (SMC) family. SMC proteins are highly evolutionarily conserved, with orthologs existing from archaea and bacteria, to yeast, to humans (Yoshinaga & Inagaki, 2021). All eukaryotes possess three distinct SMC complexes: cohesin, condensin and Smc5/6– these are heterotrimers comprising Smc1/3, Smc2/4 and Smc5/6

respectively, each with an additional kleisin protein subunit bound to both SMC proteins. The Smc5/6 complex is involved in DNA repair and replication fork dissolution (Atkins et al., 2020). Condensin compacts chromatin for mitotic and meiotic cell divisions (Hirano, 2012). This activity is thought to arise from the ability of SMC proteins to trap and progressively expand DNA loops in an ATP-dependent manner. This loop extrusion activity is highly conserved, and fulfilled by orthologous SMC proteins in non-eukaryotic organisms (Nichols & Corces, 2018). Cohesin mediates sister chromatid cohesion from S phase until anaphase when chromatids segregate (Rybenkov et al., 2015). In addition to mediating sister chromatid cohesion, cohesin has roles in the organization of the genome in interphase, by virtue of its ability to extrude DNA loops (Yatskevich et al., 2019). This activity facilitates contact between distal regulatory elements and their cognate genes and promoters (Schoenfelder & Fraser, 2019), and is thought to form large loop domains of DNA, called topologically associating domains (TADs). TADs are characterized by a higher frequency of contact between regions of the genome within the domain than regions outside of it (Dixon et al., 2012; Nora et al., 2012).

All SMC protein complexes and their regulatory proteins share a remarkably similar structure. Individual SMC proteins are rod-shaped (Figure 4A), with a globular dimerization domain, called the hinge, at one end and an ATP binding cassette (ABC)-like ATPase ‘head’ domain at the other (Camdere et al., 2015). Separating these two head domains is a 50nm antiparallel coiled coil; the Smc polypeptides fold in half, with their N and C termini forming the ATPase domain, and the centre of the polypeptide forming the ‘hinge’ domain (Harvey et al., 2002). Two SMC proteins dimerize via their

hinge domains, forming a V-shaped heterodimer, with the dimerization domain resembling a torus (Figure 4B) (Haering et al., 2002; Hirano & Hirano, 2002). In prokaryotes, SMC proteins form homodimers. In eukaryotes, however, each SMC protein heterodimerizes uniquely with one other SMC; highly conserved positive residues in the hinge domain allow for this interaction to occur (Figure 4C) (Kurze et al., 2011; Sakai et al., 2003).

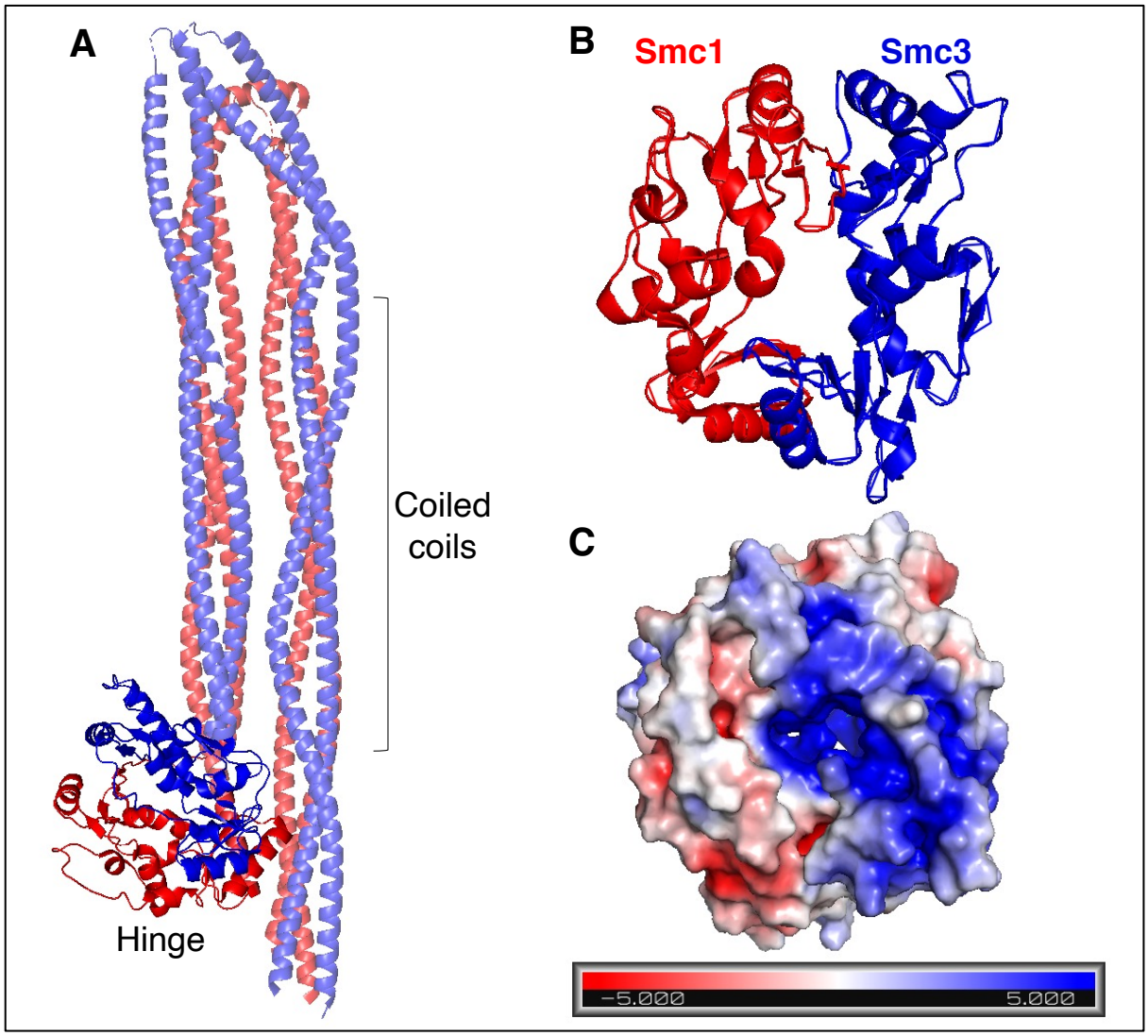


Figure 4. Cryo-EM structure of *S. cerevisiae* and *M. musculus* Smc1 and Smc3 (cohesin) coiled coils and hinge dimerization domain (Kurze et al., 2011; Petela et al., 2021). A) Schematic structure of Smc1-Smc3 coiled coil and hinge domains; hinge located in centre of both polypeptides. **B)** *Mus musculus* Smc1-Smc3 hinge domain. **C)** Electrostatic charge map of Smc1-Smc3 hinge domain. Highly conserved positively charged residues coloured in blue. Made using PyMol and APBS plugin. A: PDB 7OGT (Petela et al., 2021). B, C: PDB 2WD5 (Kurze et al., 2011).

1.6 **Cohesin complex**

Cohesin, an Smc/kleisin heterotrimer, mediates sister chromatid cohesion from S phase until anaphase (Yatskevich et al., 2019). Cohesin's functions in sister chromatid cohesion were first identified in genetic screens in budding yeast; mutation of cohesin's subunits led to chromosome condensation defects, and more notably, premature separation of sister chromatids (Guacci et al., 1997, Michaelis et al., 1997). The core cohesin heterotrimer comprises Smc1 and Smc3, and the α-kleisin protein Scc1 (Rad21 in humans). Smc1 and Smc3 interact via their hinge domains, and Scc1 binds Smc1 and Smc3's head domains via its C and N termini respectively. The cohesin heterotrimer's basic structure is thought to resemble a ring, with a lumen of diameter ~40nm. Cohesin's ATPase activity is needed to support viability; chromatin immunoprecipitation sequencing (ChIP-seq) experiments showed that mutations to Smc1 and Smc3 preventing cohesin's ability to either bind to, or hydrolyze ATP were lethal, and in the former case, abolish association between cohesin and DNA (Arumugam et al 2003, Hu et al., 2011, Weitzer et al., 2003).

Cohesin regulation

Along with its three core subunits, eukaryotic cohesin associates with three hook-shaped proteins via its Scc1 subunit. These proteins contain HEAT (**H**untingtin-**E**F3-PP2**A**-**T**OR1) repeats and associate with kleisins (Scc1/Rad21 in eukaryotes), and are thus aptly named HAWKs (**H**EAT repeat-containing proteins **a**ssociated **w**ith **k**leisins) (Wells et al., 2017). Scc3 is a HAWK that is permanently bound to Scc1, and is required for cohesin to associate with DNA (Roig et al., 2014). Scc2 (a.k.a. NIPBL) is

a HAWK that is required for the loading of cohesin onto chromosomes. Scc2 in combination with Scc4 (a.k.a. MAU2), a smaller TPR-repeat protein, forms the cohesin loading or 'kollerin' complex (Lopez-Serra et al., 2014). Both Scc2 and Scc4 are indispensable for cohesin loading *in vivo* in humans and yeast, but Scc4 was not required for cohesin-DNA association *in vitro* (Murayama and Uhlmann, 2014). Furthermore, cohesin that loaded onto DNA in an Scc2-dependent manner in G1 did not require Scc2 for cohesion to be established in S phase (Srinivasan et al., 2019). Scc2 is also required for cohesin's loop extrusion activity *in vitro* (Bauer et al., 2021).

The third HAWK protein known to associate with cohesin is Pds5. Pds5 possesses seemingly dual functions. On the one hand, it is implicated in the recruitment of a protein called *Wapl* to cohesin, causing the dissociation of cohesin from DNA (Gandhi et al., 2006; Shintomi & Hirano, 2009). On the other hand, it is crucial for stable maintenance of cohesin (Jin et al., 2009; Panizza et al., 2000) by recruitment of the acetyltransferase *Eco1* to cohesin in S phase, which prevents premature release of cohesin (Chan et al., 2013; Tedeschi et al., 2013). Wapl-mediated release occurs during prophase in human cells and throughout the cell cycle in budding yeast (Chan et al., 2012). Wapl causes cohesin to dissociate from DNA via its Smc3-Scc1 interface (Beckouet et al., 2010; Beckouet et al., 2016). In mammalian cells, this process gives rise to the characteristic X-shaped sister chromatids seen in metaphase spreads; cohesion in centromeric regions is spared of this release (Haarhuis et al., 2014).

Crucial to accurate cell division is not only the cohesion of sister chromatids, but also their timely separation at anaphase. Dictating this most markedly are the proteins

separase and securin. Separase is a cysteine protease that cleaves Scc1 at two arginine residues (R180, R268) at anaphase, causing cohesin to dissociate from DNA. Prior to anaphase, separase's proteolytic activity is inhibited through sequestration by securin. Securin is a stoichiometric inhibitor, competing with cohesin for separase binding (Hornig et al., 2002). Upon satisfaction of the SAC, inhibition of the APC/C by the MCC is relieved. APC/C is an E3 ubiquitin ligase, and upon activation it polyubiquitylates securin. This targets securin for 26S proteasomal degradation, and releases separase, which cleaves Scc1 and abolishes sister chromatid cohesion.

Cohesin in human disease

Given cohesin's crucial role in preventing aneuploidy or cell death, mutations to its core subunits and accessory proteins are associated with a number of human cancers, as well as genetic disorders known as cohesinopathies (Hill et al., 2016). Roberts Syndrome (RBS) is a cohesinopathy caused by mutation to the ESCO2 gene (Eco1 in yeast), a N-acetyltransferase that promotes maintenance of cohesion prior to M phase. RBS is characterized by limb and craniofacial deformities and delayed development. Metaphase spreads of chromosomes from RBS patients show premature separation of sister chromatids at the centromeres, designating cohesion defects (Xu et al., 2014).

Cornelia de Lange Syndrome (CdLS) is another cohesinopathy characterized, like RBS, by developmental deficiencies. In 55% of cases, CdLS is caused by mutation to NIPBL (Scc2 in yeast), a kleisin-associated protein that is required for the loading of cohesin trimers onto chromosomes (Krantz et al., 2004). Conversely to RBS, however, metaphase spreads from CdLS patients do not show significant cohesion defects.

Instead, pathology is thought to arise from deficits in cohesin's aforementioned functions in genome organization (and therefore gene expression), and perhaps due to an increased sensitivity to DNA damage (Deardorff et al., 2012; Kawauchi et al., 2009). Indeed, upon its initial discovery, cohesin's α-kleisin subunit Scc1 was named Rad21 (radiation sensitive). Rad21 mutation caused hypersensitivity to UV and ionizing radiation in fission yeast (Birkenbihl & Subramani, 1992). However, notwithstanding cohesin's various alleged roles in interphase, cohesin complexes' most highly conserved and widely reported functions are in sister chromatid cohesion. To understand mechanistically how cohesin mediates this is to understand a process that is fundamental to all cellular life.

1.7 **Cohesin-DNA interactions and topology**

It has long been debated how, mechanistically, cohesin fulfils its functions in associating with DNA and thus enabling sister chromatid cohesion. The most widely accepted theory was conceptualized due to cohesin's observed structure as a ring-shaped heterotrimer. Observations in electron micrographs that Smc3 and Smc1 form a V-shaped heterodimer, and the discovery that Scc1 binds to both via its N and C termini respectively, first alluded to this architecture (Haering et al., 2002). As such, the appropriately named 'ring model' of DNA entrapment proposes that a cohesin heterotrimer entraps two sister chromatids *topologically* within its lumen (Haering et al., 2002, Figure 5). The observation that cleavage of Scc1 resulted in a loss of cohesion was also an indicator that cohesin may exist as a ring (Uhlmann et al., 1999, Uhlmann et al., 2000). Likewise, TEV protease cleavage at an engineered Smc3's coiled coil also abolished cohesion (Gruber et al., 2003).

The development of an assay whereby cohesin can be covalently circularized and made resistant to denaturation allowed visualization of cohesin-associated DNA and thus further validated the ring model (Haering et al., 2008). Each cohesin subunit was engineered such that its 2 interaction surfaces contained a cysteine residue, giving 6 engineered cysteine residues per cohesin trimer. Treatment with a thiol-specific crosslinking agent, such as BMOE (bismaleimidoethane) leads to covalent closure of the ring that resists denaturing conditions. These modified proteins are expressed in a strain containing 2.3kb circular minichromosomes. The cells are crosslinked with BMOE, and the minichromosomes are then immunoprecipitated. The immunoprecipitate is subjected to denaturing conditions and the minichromosomes can then be detected via Southern blot. Bands will migrate at different rates according to their minichromosome stoichiometry. A single 6C cohesin trimer that is otherwise wildtype (WT) is capable of entrapping both one (catenated monomer, CM) and two (catenated dimer, CD) minichromosomes (Haering et al., 2008) (Figure 5). Similarly, linearisation of either the cohesin ring *or* the circular minichromosome destroyed cohesin and DNA's association, indicating a topological interaction (Ivanov and Nasmyth, 2005). It is thought that whilst fulfilling its loop extruding functions, cohesin's interaction with DNA is non-topological (Figure 5).

While the above mentioned experiment provides unequivocable evidence for the ring model, the assay only measures cohesion of 2.3kb minichromosomes, and not eukaryotic chromosomes which are linear and anywhere in the order of 1×10^2 to 1×10^5 times larger. This leaves the formal possibility that chromosomal cohesion is not mediated by co-entrapment of sister DNAs. Indeed, some models of cohesion

postulate that cohesion occurs through the interlocking of two cohesin rings, each of which entraps a single DNA (Zhang et al., 2008). It was proposed that Smc3 acetylation may promote dimerization of cohesin rings, but no evidence for such interactions has been obtained thus far (Xu et al., 2018). Furthermore, there is as of yet a perfect correlation between sister chromatid cohesion and minichromosome cohesion: where cohesion of minichromosomes is observed using the above described assay, chromatin immunofluorescence methods have also shown sister chromatid cohesion *in vivo* in the minichromosome-expressing cells (Srinivasan et al., 2018).

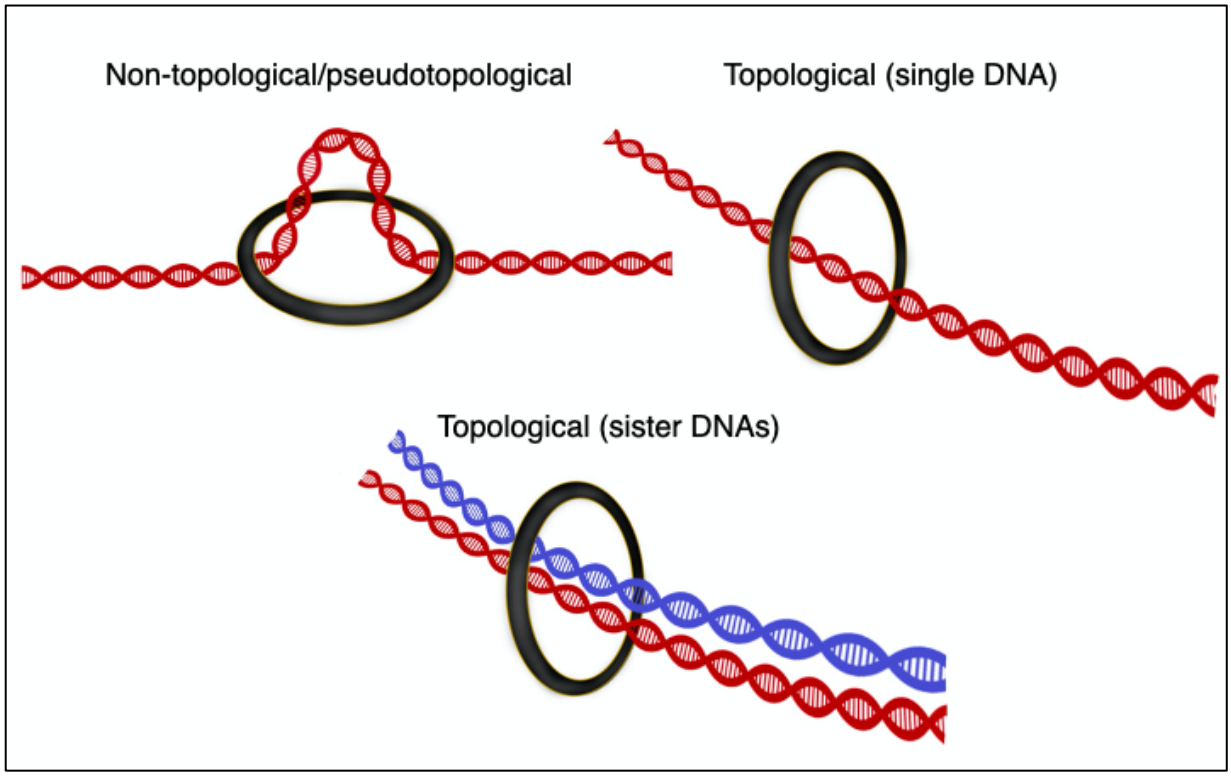


Figure 5. Putative methods of DNA entrapment by cohesin 'ring'. Non-topological entrapment: loop extrusion functions, genome organization; Topological entrapment: loading onto single DNA and sister chromatid cohesion.

Cohesin's DNA entry gate

In light of the evidence that cohesin may fulfil its function as a 'ring', it must be considered how DNA, whether linear or circular, becomes entrapped within a cohesin ring. Cohesin exists as a heterotrimer in the absence of DNA *in vitro,* and it is thus assumed that subunits do not assemble around DNA (Gruber et al., 2003). Furthermore, regardless of how many cohesin molecules are required for cohesion on a single pair of chromatids, genome-wide breakage (and subsequent repair) of DNA in multiple loci during replication is highly implausible. Thus, it is widely accepted that in order for cohesin to entrap DNA and subsequently confer cohesion, DNA must pass through one of its three interfaces. *Which* cohesin interface DNA passes through, however, is a subject of contentious debate.

It was shown that Wapl-mediated release of cohesin occurs via disruption of the Smc3-Scc1 interface, and DNA then passes through this so-called 'exit gate' interface (Beckouet et al., 2016; Murayama and Uhlmann., 2015). It is therefore conceivable that DNA might also *enter* cohesin rings via the Smc3-Scc1 interface. However, it was shown that permanent fusion of this interface did not affect cell viability or cohesin's ability to entrap single and sister minichromosome DNAs *in vivo* in yeast. Likewise, covalent fusion of the Smc1-Scc1 interface does not affect cell viability nor cohesin's ability to entrap minichromosomes (Srinivasan et al., 2018). Furthermore, cells wherein the Smc1-Scc1 gate was closed prior to DNA replication showed no major cohesion defects, as per a chromosome immunofluorescence assay (Gruber et al., 2006). This suggests that neither the Smc3-Scc1 nor the Scc1-Smc1 interfaces are *obligatory* entry gates for DNA.

By process of elimination, these data denote the hinge interface as the remaining possible entry gate. Insertion of FKBP12 and FRB domains into the Smc1 and Smc3 hinge domains respectively allows the closure of this interface upon addition of rapamycin (which binds to FKBP12, and results in a tight association between FKBP12 and FRB) (Figure 6A). Cells that contain the Smc1 and Smc3 FKBP12/FRB fusions as the sole source of Smc1 and Smc3 proliferate well in the absence of rapamycin, but die when grown in medium containing 100nM rapamycin (Gruber et al., 2006). Correspondingly, Smc1-FKBP12 and Smc3-FRB-expressing cells, when synchronized in G1 in the presence of rapamycin, displayed severe chromosomal cohesion defects (Gruber et al., 2006; Figure 6B). Furthermore, *in vitro* DNA entrapment assays showed that Smc1-Scc1 and Smc3-Scc1 fusion proteins (i.e. proteins wherein the hinge interface is open) were capable of entrapping DNA; entrapment via the hinge was dependent on Scc2. Fusion proteins in which the Smc3-Scc1 interface was open, and the hinge was not, were also able to entrap DNA independent of Scc2 (Collier & Nasmyth., 2022). The possibility of *in vitro* artefacts notwithstanding, this entrapment assay can at most determine whether a cohesin interface is required for loading onto unreplicated DNA. In the context of sister chromatid cohesion, entrapment of two DNAs must be considered. The *in vitro* and *in vivo* experiments described above shows that entrapment of DNA in cohesin rings possibly requires opening of the hinge domain. Crucially, however, these data do *not* address whether hinge opening is required for co-entrapment of sister DNAs if cohesin has already entrapped the unreplicated DNA prior to DNA replication.

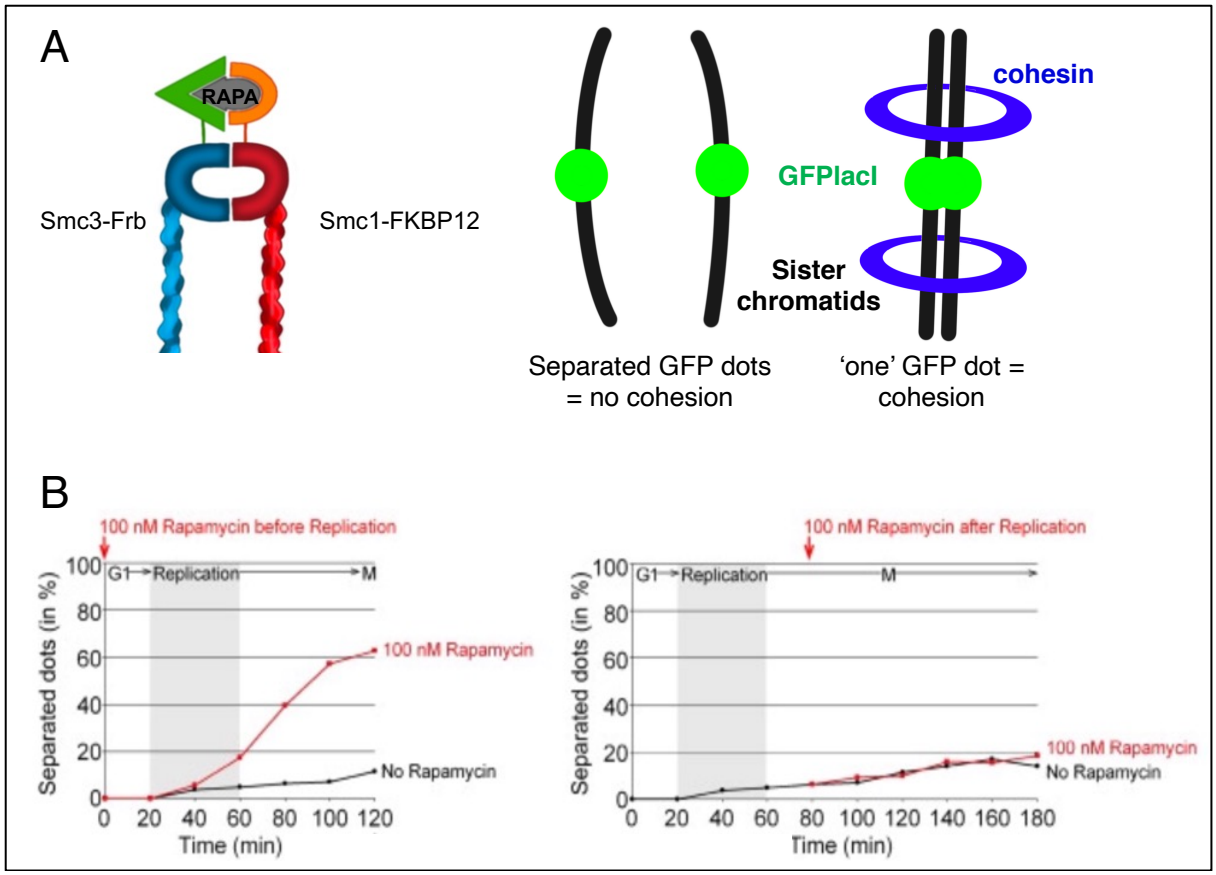


Figure 6. Closure of the Smc3-Smc1 hinge prior to DNA replication leads to severe sister chromatid cohesion defects (Gruber et al., 2006). A) Schematic outlining the principle of the assay. Smc1 and Smc3 expressed as FKBP12 and FRB fusion proteins respectively; Rapamycin causes closure of hinge domain. Cohesion measured by separation of sister chromatids, using GFP-lacI/lacO as a readout; when cohesion occurs, two GFP dots appear as one due to their close proximity. B) Addition of rapamycin before DNA replication leads to cohesion defects in ~65% of cells. Addition of rapamycin after DNA replication does not significantly affect sister chromatid cohesion. Section B adapted from Gruber et al., 2006.

Separate to the debate surrounding cohesin's DNA entry gate is evidence that two separate processes may be involved in loading and cohesion establishment respectively. Firstly, Scc2 was required for *in vitro* entrapment of DNA to occur via the hinge (Collier and Nasmyth, 2022). However, as previously mentioned, Scc2 is not needed for cohesion establishment after DNA replication has occurred (Srinivasan et al., 2019). Thus, significant alterations in cohesin's activity, or at least the regulation thereof, occur during DNA replication.

Loading and unloading: temporal dynamics of Cohesin-DNA interactions

Cohesin is crucial both in genome organization and sister chromatid cohesion, which occur in G0/G1-, and S/G2/M- phases respectively. Therefore it must be considered how, temporally, cohesin associates with DNA throughout the cell cycle. It was shown that during interphase/G1 in mammalian cells, cohesin has a mean residence time on DNA of ~20 minutes. However, upon onset of S phase, and until anaphase, one third of the cell's total population of cohesin remained stably bound to chromatin for at least 2 hours, with very little turnover; in mammalian oocytes, this binding can last for decades (Revenkova et al., 2010). This degree of protein-DNA interaction stability *in vivo* is very rare, with most DNA-binding proteins having on-off rates in the order of seconds and minutes (Gerlich et al., 2006). These data, while highlighting the increased stability of the cohesin-DNA interaction whilst cohesion is being conferred, also underline that only a relatively small fraction of available cohesin complexes become cohesive. This is in accordance with the fact that Wapl-mediated cohesin release in metazoans during prophase leaves only centromeric cohesin bound, yet cohesion is maintained until anaphase despite pulling tensions generated by the spindle (Shintomi and Hirano, 2009).

The stability of the cohesin-DNA interaction is driven in eukaryotes by the aforementioned Eco1 acetyltransferase. In vertebrate cells, necessary additional stability is imparted by binding of the protein Sororin to Pds5, which prevents Wapl recruitment (Nishiyama et al., 2010). Pds5, while serving to assist in Wapl-mediated release prior to DNA replication, recruits Eco1 thereafter, enabling acetylation of Smc3's nucleotide binding domain lysine residues K112 and K113, and subsequently

protection of this acetylation from Hos1 deacetylase (Chan et al., 2013; Ivanov et al., 2002). Smc3 acetylation by Eco1 occurs exclusively in S phase, and a PCNA binding domain within Eco1 was identified (Moldovan et al., 2006). This, among other discoveries, led to investigation of the links between DNA replication and cohesion establishment.

1.8 **DNA replication and cohesion establishment**

As of yet, available data denotes S phase as the time during which sister chromatid cohesion is established. In yeast, it was shown that restricting expression of Scc1 to only *after* S phase led to a loss of sister chromatid cohesion and did not support viability (Uhlmann and Nasmyth, 1998). Furthermore, a non-separase cleavable cohesin expressed after DNA replication was unable to entrap sister DNAs to generate cohesion, despite WT cohesin loading normally and holding sister chromatids in close proximity (Haering et al., 2004; Srinivasan et al., 2019). In the absence of Wapl, cohesin that associates with chromatin in G1 was shown to persist on chromatin during DNA replication, suggesting that cohesin rings are capable of persisting on more or less the same region of DNA even after replication fork passage (Rhodes et al., 2017). Crucially, as alluded to before, once cohesin rings are loaded onto DNA prior to DNA replication, Scc2 (which is critical for cohesin loading) becomes dispensable for cohesion establishment (Srinivasan et al., 2020).

These data indicate that it is plausible that cohesin associated with unreplicated DNA could be ‘converted’ to a cohesive structure alongside DNA replication, *without* dissociation from DNA (Figure 7). Hypothetically, this could occur firstly by passage of

the replisome through cohesin's ring. Although cohesin rings are in theory large enough to allow replisome passage, cohesin's translocation on DNA *in vitro* seems to be blocked by small roadblocks such as nucleosomes (Stigler et al., 2016). On the other hand, loop extruding cohesin *in vitro* was shown to bypass synthetic roadblocks of up to 200nm (Pradhan et al., 2022a). Therefore the capability of cohesin to allow passage of various proteins through its lumen may vary significantly according to whether it is fulfilling cohesive or loop extruding functions. During cohesion establishment, it is possible that the transient opening of one of cohesin's interfaces allows replisome passage.

There is a second mechanism known to establish cohesin that is operative during S-phase, in parallel to the above described 'conversion' pathway. This mechanism, called *de novo* loading, generates cohesion by Scc2-mediated *de novo* loading of cohesin onto replicated DNAs during S phase (Srinivasan et al., 2020; Figure 7). Given that Scc2 is dispensable for cohesion establishment after S phase (where it has already facilitated loading of cohesin onto unreplicated DNA), but indispensable prior to S phase, it is conceivable that both 'conversion' of cohesin into cohesive structures and *de novo* loading occur *in vivo*. Crucially, both pathways must operate in parallel to DNA replication in order for cohesion to be built. Indeed, it was shown that various replisome-associated proteins were involved in either cohesion establishment pathway, and that inactivation of either pathway on its own was not lethal, but inactivation of both, was (Xu et al., 2007).

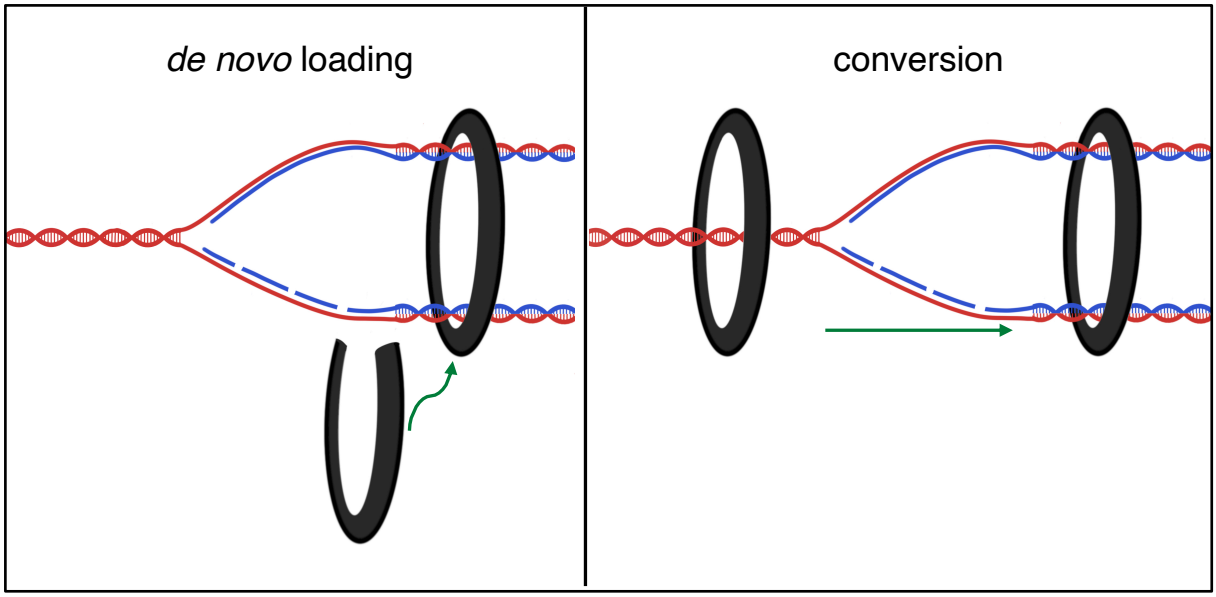


Figure 7. The two purported cohesion establishment pathways: Schematic outlining *de novo* loading (left) vs. conversion (right) hypotheses of cohesion establishment during DNA replication.

While some replisome-associated proteins, such as Chl1 and Ctf4, are thought to be required to maintain cohesin's association with DNA and thus allow cohesin conversion, others, such as Ctf18-RFC, are needed for Scc2-dependent *de novo* loading at replication forks (Srinivasan et al., 2020). Upon deletion of proteins from *one* epistasis group, cells survived and a single cohesin ring was capable of entrapping two circular minichromosomes (CD). However, deletion of proteins from both groups (conversion and *de novo*) was lethal and CD formation was greatly reduced (Srinivasan et al., 2020; Xu et al., 2007). While these minichromosome assays are as of yet the most reliable readout of cohesion *in vivo*, as mentioned previously they involve much smaller lengths of DNA that are circular, rather than linear. It is by no means certain that observations made regarding mini-chromosomes can be extrapolated to statements about sister chromatid cohesion on a genome-wide scale.

Mechanistically speaking, in the case of both cohesin conversion and *de novo* loading, it is unknown which of the cohesin ring's three interfaces are involved in sister DNA entrapment. In the case of Scc2-dependent *de novo* loading, the Smc1-Smc3 hinge is presumably involved, as previous data has highlighted the hinge as essential for Scc2-dependent loading onto unreplicated DNA (Gruber et al., 2006, Collier & Nasmyth 2022). In the case of conversion, where cohesin purportedly remains 'loaded' onto the chromosome throughout DNA replication, it is not known whether one of its interfaces opens to allow passage of the replisome and subsequent entrapment of the newly replicated DNA, or whether the cohesin ring's lumen accommodates all four strands of parent and daughter DNA at the replication fork. The replisome itself is thought to have a diameter of ~20nm, and cohesin of 40nm (Sun et al., 2015, Ivanov and Nasmyth., 2005), so this may be physically feasible. It was shown *in vitro* that in the context of its loop extrusion activity cohesin can bypass synthetic particles of up to 200nm (Pradhan et al., 2022a). However, an *in vitro* assay whereby single replication forks (+ replisomes) and their interactions with cohesin complexes on DNA were visualized, suggested differently. Instead of accommodating the replisome and allowing it to pass through its ring, it was shown that in most cases replisomes pushed cohesin along the DNA. Cohesin was observed to slide along the DNA until a converging replisome was met; after termination, both replisomes were removed, but cohesin remained on DNA, and entrapped both newly replicated sister DNAs (Cameron et al., 2022). If cohesion conversion requires opening of one of the cohesin ring's interfaces, it is not known which of the three this is. Given that cells expressing either Smc3-Scc1 or Scc1-Smc1 fusions are perfectly viable and able to establish

cohesion (Srinivasan et al., 2018), it is unlikely that these two interfaces are **essential** entry gates for co-entrapment of sister DNAs.

1.9 **Thesis objectives**

Objective 1: Thus far, cohesin conversion has only been demonstrated using small circular minichromosomes. Therefore, the first objective of this project is to determine whether cohesin conversion occurs on yeast chromosomes, and to assess the importance of the Smc1-Smc3 hinge in cohesion establishment by the conversion pathway.

Recent work in the field has hypothesized two means of sister chromatid cohesion establishment. Most pertinent to this thesis is the 'conversion' hypothesis whereby cohesin complexes associated with unreplicated DNA become cohesive during DNA replication, without re-loading onto sister DNAs. It has been established that hinge closure prior to loading onto unreplicated DNA abolishes cohesion (Gruber et al., 2006). Whether or not cohesion is observed when the hinge is closed *after* cohesin has loaded in G1, but *before* cohesion is established in S phase, will demonstrate:

1) Whether non-cohesive cohesin is converted to cohesive without dissociation from DNA

2) Whether the hinge is required to open in order for cohesion to be established

3) Whether different processes are involved in entrapment of single DNAs and sister DNAs.

In order to assess the importance of cohesin's hinge interface in cell viability and sister chromatid cohesion, I will generate a Smc1-Smc3 hinge fusion construct whereby the

closure of the hinge can be controlled temporally by addition of a drug (rapamycin) to the culture. These will be expressed alongside a separase cleavage-resistant Scc1, thus giving rise to a specific population of cohesin proteins that can be analyzed visually at anaphase using immunofluorescence methods. Crucially, this will allow for the measurement of cohesion *on chromosomes*, avoiding any uncertainty associated with the aforementioned minichromosome entrapment assay. In combining the above described system with inactivation of either cohesin conversion- or *de novo* loading-specific proteins, I will also show with greater clarity whether or not cohesin conversion is occurring *in vivo* on chromosomes.

Objective 2: To determine whether fusion of both Smc-kleisin interfaces can support viability in budding yeast.

Previously, cohesin fusion proteins whereby one Smc protein and Scc1 are expressed as a single polypeptide, have been successfully expressed *in vivo* in budding yeast. These cells were viable with some synthetic sickness compared to WT, and both cohesin fusion proteins could entrap DNA (Srinivasan et al., 2018). I aim to develop a cohesin Smc3-Scc1-Smc1 double fusion plasmid for expression *in vivo* in budding yeast. All three subunits will be expressed as a single polypeptide with short linker interspaces. The construct will be designed for integration at an ectopic locus. Expression of this construct in cells wherein a WT cohesin subunit has been deleted will effectively render the fusion protein as the cell's only available pool of cohesin. It will then be determined whether this fusion protein can indeed support viability, giving further insight into the interfaces involved in sister DNA entrapment by cohesin.

Chapter 2: Results

Part A: Can non-cohesive cohesin be converted into a cohesive structure, and does this require opening of its Smc3-Smc1 hinge?

2.1 Developing an assay whereby cohesin loaded onto DNA during G1 gives rise to cohesion

Introduction

Despite cohesin proteins being identified over two decades ago, there is still a significant lack of understanding of the processes that underly cohesion and its establishment. Most data to date seems to support that sister chromatid cohesion occurs by topological entrapment of two sister DNAs within the lumen of a cohesin trimer's 'ring'. How this entrapment comes to be, however, remains relatively unclear. It *can* be said with relative certainty however, that cohesion establishment occurs during DNA replication in S phase.

There is emerging evidence that two processes for cohesion establishment occur. The first involves the *de novo* loading of cohesin trimers onto replicated sister DNAs, a process that involves the cohesin loading complex Scc2/4 (Ciosk et al., 2000; Kogut et al., 2009). The second putative mechanism of cohesion establishment is thought to involve the 'conversion' of non-cohesive cohesin structures (bound to unreplicated G1 DNA) to cohesive structures *alongside* DNA replication, likely without dissociation from DNA. This pathway does not require the cohesin loading complex Scc2/4 (Srinivasan et al., 2020).

The work presented below concerns the characterization of the conversion pathway. The only straightforward evidence for the occurrence of cohesin conversion comes from analysis of small circular minichromosomes in yeast. It is not clear whether cohesin conversion can generate cohesion of entire chromosomes in yeast. Furthermore, it is unknown whether conversion involves passage of the replisome through cohesin's lumen. What would clarify this would be to understand whether conversion requires opening of one of cohesin's three interfaces. It was shown that opening (or flexibility) of the Smc1-Smc3 hinge dimerization domain was required *prior* to DNA replication, indicating that unreplicated DNA likely enters the cohesin ring via the hinge (Gruber et al., 2006). This manner of loading is Scc2-dependent (Collier & Nasmyth, 2022). However, Scc2 is dispensable for cohesin conversion (as measured on minichromosomes) as long as it is present for loading prior to DNA replication (Srinivasan et al., 2020). Therefore, it is currently unclear whether the cohesin hinge domain needs to open during S-phase in order for the establishment of cohesion of yeast chromosomes via the conversion pathway. In the results presented below, I address whether cohesin conversion can establish yeast chromosome cohesion, and if hinge opening is required during S phase for cohesion establishment by conversion.

An assay to measure chromosomal cohesion

Given the previously mentioned caveats of minichromosome entrapment-based assays as a readout for cohesion, I aimed to develop an assay that allowed measurement of sister chromatid cohesion *in situ* on yeast chromosomes. This would form the basis of further experiments probing the occurrence of cohesin conversion *in vivo*. Sister chromatid cohesion can be measured using immunofluorescence methods

on anaphase yeast chromosome spreads. Fixed WT cells are treated with DAPI, and visualized under a fluorescence microscope. DAPI binds to DNA and thus roughly delineates the positions of sister chromatids within the cell. Depending on the phase of mitosis in which a wildtype cell is, either one or two nuclear masses can clearly be seen. For example, in metaphase, when sister chromatids are held together at the center of the cell, one mass is seen; in anaphase or telophase, two masses can clearly be seen (Figure 8B). In cells where two masses are seen during G2, prophase, or metaphase, it can be said that cohesion has not been established, and vice versa if one mass is seen (Figure 8B).

Central to the conversion hypothesis is the persistence of cohesin on DNA throughout S phase, and the ensuing emergence of cohesive structures. Logically, this could be probed by limiting the expression of cohesin subunits to G1, using perhaps an inducible promoter system, restricting cohesin loading onto DNA to G1. However, such a system without the presence of endogenous cohesin subunits is not possible as cells are inviable. Likewise, in the presence of endogenous subunits, which could conceivably be expressed all throughout the cell cycle, we cannot discern G1-induced cohesin's cohesive structures from endogenous cohesins' (which may be loaded *de novo*) and cannot draw any conclusions about conversion. Therefore, I employed a non-cleavable Scc1(R180D, R268E) mutant ($Scc1_{NC}$ (non-cleavable) henceforth) (Uhlmann et al., 1999). $Scc1_{NC}$ is not cleaved by separase at anaphase and cells in which it is expressed experience an anaphase block, where sister chromatids remain held together for significantly longer than WT cells. Using the immunofluorescence platform described above, cells where this $Scc1_{NC}$ has formed part of a cohesive

cohesin trimer will show only one nuclear mass at anaphase (mononucleates), whereas in WT cells the sister chromatids will separate prior to cell division and show two masses (binucleates, Figure 8B). This gives us a discrete pool of cohesin proteins wherein their ability to confer cohesion can be tracked; only cells where this non-cleavable cohesin has loaded will experience an anaphase block. Furthermore, where this does occur, it can be said that cohesion has been established by this population of non-cleavable cohesin. One nuclear mass at anaphase is synonymous with sister chromatid cohesion.

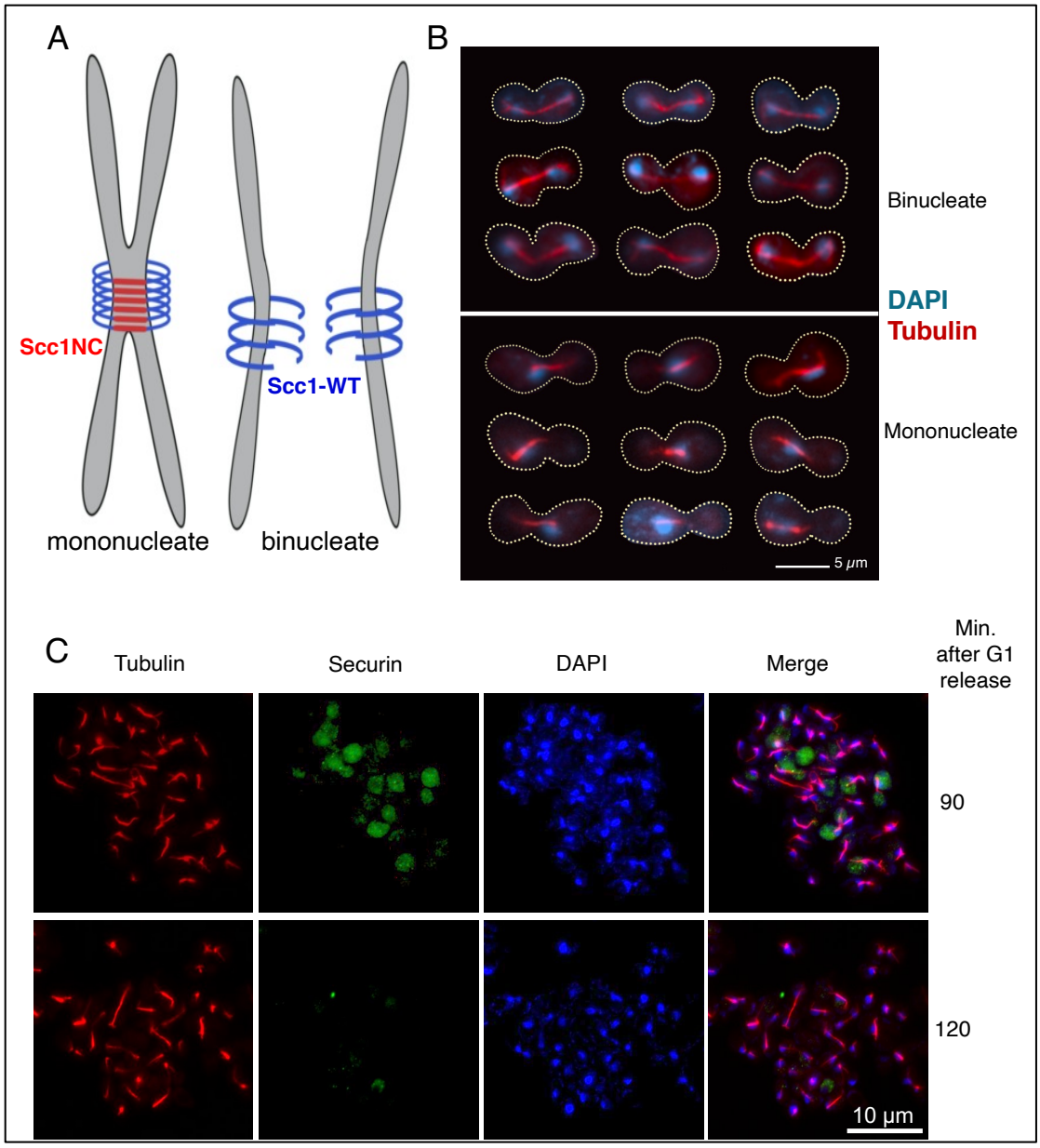


Figure 8. Schematic underpinnings of the non-cleavable Scc1-based assay **A)** At anaphase: separase cleavage-resistant cohesin maintains cohesion, giving rise to mononucleates; cohesin with Scc1-WT is cleaved and sister chromatids segregate, showing binucleates. **B)** Example images of mono and binucleate anaphase cells. Anti-tubulin (AF594) and DAPI. **C)** Tubulin (AF594), securin (AF488) and DAPI staining in cells at 90 and 120 minutes following their release from G1. Notable reduction in securin levels from 90 to 120 minutes.

A strain was built expressing $Scc1_{NC}$ under the control of a galactose (Gal)-inducible promoter. Addition of galactose to medium induces $Scc1_{NC}$ expression, and subsequent addition of glucose terminates it. *S. cerevisiae* of the mating type **a** can be treated with the mating pheromone α-factor in order to synchronize and arrest the cells in G1. By combining $GalScc1_{NC}$ induction with α-factor G1 arrest, we can restrict $Scc1_{NC}$ expression, and potentially loading onto DNA, to G1 only. Following $Scc1_{NC}$ induction, cells are released from α-factor arrest into glucose-containing medium. Samples are taken at 0, 30, 60, 90 and 120 minute timepoints and fixed in formaldehyde. Samples taken at 90 and 120 minutes were predicted to possess a large proportion of anaphase cells, given previous knowledge about the budding yeast cell cycle (Nasmyth, 1996).

Expression of $GalScc1_{NC}$ during G1 only is sufficient to generate non-cleavable cohesin-mediated cohesion.

I first determined the optimal conditions for $Scc1_{NC}$ expression in G1-arrested cells. I found that a 1-hour-long induction of $Scc1_{NC}$ during a 3-hour-long G1 arrest only led to cohesion in 33% of cells at anaphase (Figure 9A). However, upon increasing the G1 arrest time to 3.5 hours, and galactose induction to 90 minutes (which was preceded by 90 minutes α-factor arrest), 90% of cells showed cohesion at anaphase. This shows that $Scc1_{NC}$ expression only in G1 suffices for the non-cleavable cohesin

to confer cohesion. Taking this into account, along with the fact that an increase of $Scc1_{NC}$ induction time increased the amount of cells showing cohesion by nearly three-fold, it can be concluded that loading of cohesin onto DNA is occurring, at least in part, during G1 (Figure 9A). Expression of non-cleavable cohesin upon release from G1 led to cohesion in 50% of cells (Figure 9B). Some loading onto DNA may therefore also occur during S phase, or at the G1→S transition.

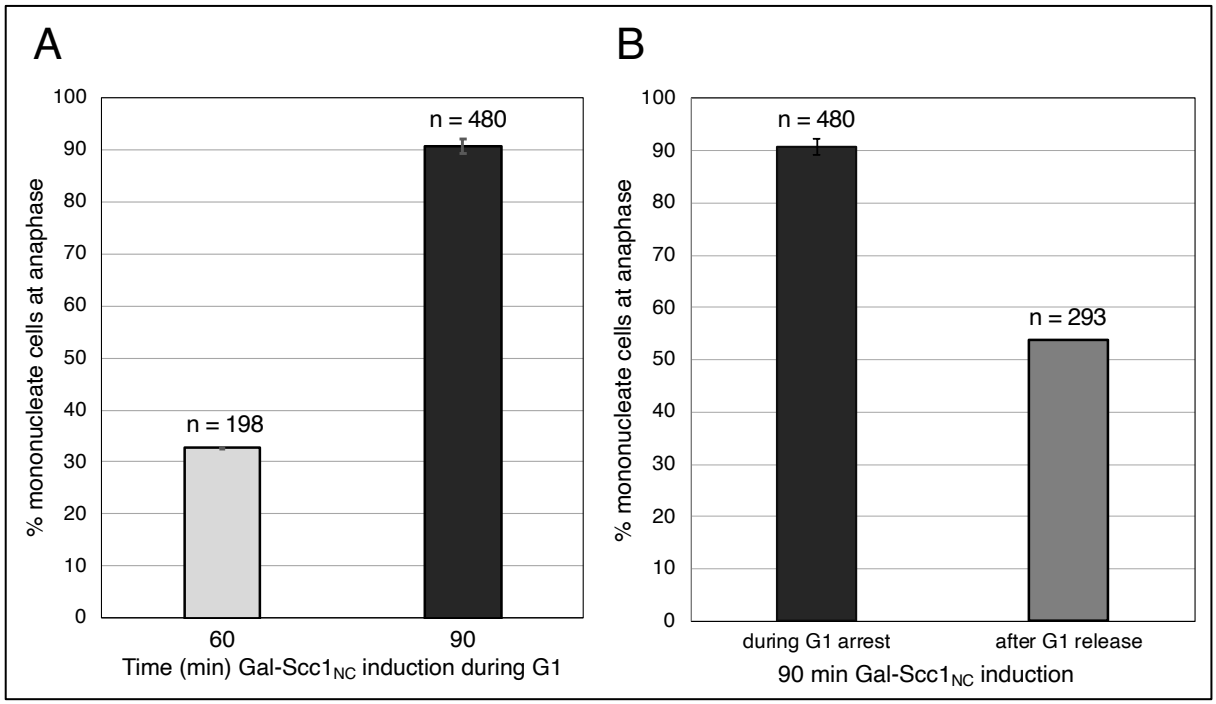


Figure 9. A) Efficiency of galactose induction of $Scc1_{NC}$ for 60 or 90 minutes, using % of mononucleate cells at anaphase as a readout. ~3 fold increase in proportion of mononucleate cells when galactose induction time increased by 30 minutes. **B)** Induction of $Scc1_{NC}$ with galactose before and after release from G1 (α-factor**)** arrest.

It is vital for the validity of this assay that anaphase cells, where only non-cleavable cohesin will give rise to cohesion, can be discerned from G2, prophase and metaphase cells. In the absence of any markers other than DAPI, these cells will look nearly identical, with only negligible variations in the size of their daughter cell buds. Securin, as previously mentioned, sequesters separase until its polyubiquitylation by the APC/C and subsequent degradation. Thus, its levels drop rapidly at anaphase onset.

Alongside $Scc1_{NC}$, the previously mentioned strain also expresses pds1 (securin) with a myc18 epitope tag. This allows for myc immunofluorescence and visualization of securin levels *alongside* DAPI. Securin levels also act as a crude indicator of cell cycle stage; levels only rise after cohesion establishment in S phase (Figure 10A). They can therefore be used to determine the time after G1 release in which the cells enter anaphase (Figure 10A/B). In addition, tubulin immunofluorescence gives some indication as to whether or not cells are in anaphase. After metaphase, and spindle assembly checkpoint passage, tubulin immunofluorescence denotes the attachment of the cytoskeleton to sister chromatids and stretches across both poles of the bi-lobed cell (Figure 8B/C).

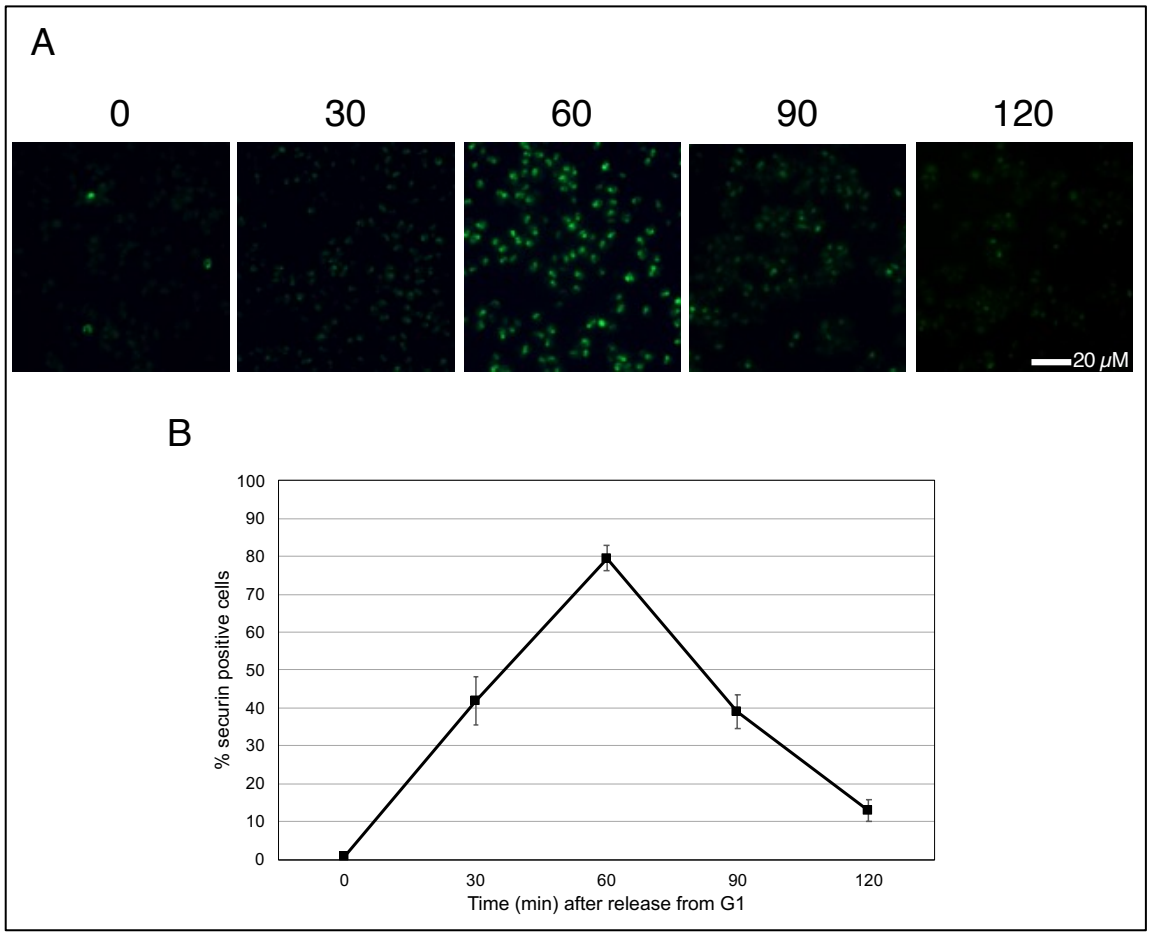


Figure 10. Securin positivity as a readout for efficiency of release from G1 arrest.
A) Immunofluorescence of securin-myc in *S. cerevisiae* cells 0, 30, 60, 90 and 120 minutes following their release from α-factor arrest. **B)** Percentage securin positive cells at five timepoints following release from α-factor arrest For each timepoint. 0: n (cells) = 1590; 30: n

= 1082; 60: n = 793; 90: n = 839; 120: n = 894. Error bars represent standard deviation per image (10 images per timepoint).

Using all of the above criteria, I was able to show that cohesin expressed (and perhaps loaded onto DNA) during G1 can give rise to sister chromatid cohesion during DNA replication. Crucially, I have not definitively shown whether or not conversion or *de novo* loading is happening, nor have I highlighted the significance of any of the cohesin heterotrimer's interfaces (Figure 9A/B). However, I now have a platform upon which to build further experiments; we can assess the ability of a specific pool of cohesin to confer cohesion, bypassing WT cohesin's effects.

2.2 **Assessing the significance of the Smc1-Smc3 hinge interface in cohesion establishment**

Introduction

Applying the principles of the assay described above, non-cleavable cohesin can be used as a readout for whether cohesion was established by cohesin exclusively expressed (and presumably loaded onto DNA) during G1 phase. Previous experimental work has highlighted cohesin's Smc1-Smc3 hinge as a vital interface for its entrapment of DNA. Crucially, however, these results do not distinguish between entrapment of single DNAs, and sister chromatid cohesion, which is widely presumed to involve entrapment of *two* DNAs. In light of the evidence that certain factors such as Scc2 and Scc4, which are vital for cohesin's functions in G1, become dispensable from DNA replication onwards, I aimed to determine with clarity the function of cohesin's hinge interface in *cohesion establishment*. By establishing a system where cohesin's hinge can be closed after cohesin's initial loading onto unreplicated DNA in

G1, but before DNA replication, when cohesion establishment occurs, I will determine whether or not hinge opening is required for cohesion establishment.

The hinge is required to be open for soluble cohesin to load onto DNA (Collier & Nasmyth, 2022; Gruber et al., 2006). Of utmost importance is the fact that the cohesion measured in these experiments will only account for that mediated by non-cleavable cohesin. By closing the hinge *after* non-cleavable cohesin has loaded in G1, I will prevent loading of any new soluble non-cleavable cohesin during S phase. Therefore, these experiments will also determine whether cohesin conversion occurs *in vivo* on yeast chromosomes.

A method to temporally control closure of the Smc1-Smc3 hinge

Rapamycin is a small-molecule drug that is capable of binding the proteins FKBP12 (FK506 and rapamycin-binding protein, 12 kDa) and FRB (FKBP rapamycin-binding, 11 kDa) simultaneously (Ho et al., 1996). FRB is a 100aa domain forming part of the cell growth regulating complex mTOR in mammalian cells, and FKBP proteins are expressed across many eukaryotic species including yeast. Rapamycin effectively induces the dimerization of FKBP12 and FRB proteins; FRB binds with high affinity to the rapamycin-FKBP12 complex (Banaszynski et al., 2005). This dimerization can be achieved *in vivo* and with nuclear proteins (Kim & Chen, 2000; Zhang et al., 2002). Given their relatively small size, FKBP12 and FRB are amenable to expression as fusions to various cellular proteins. This allows for temporal control over the dimerization of two proteins of interest by addition of rapamycin to the system. Constructs were generated whereby FKBP12 and FRB were expressed as fusions via

10aa linkers to the hinge domains of Smc1 and Smc3 respectively; the hinge domain occurs in the centre of each polypeptide. These constructs were expressed in budding yeast in the absence of WT Smc3, and cells were viable (Figure 11A, Gruber et al., 2006). In order to maximise the amount of free rapamycin available for FKBP12 and FRB binding in these cells, fpr1 (a soluble yeast rapamycin binding protein) was deleted and TOR1 mutated (TOR1-1) (Freeman & Livi, 2000). As such, the only binding partners for rapamycin within the cells are Smc1-FKBP12 and Smc3-FRB.

Previous experiments addressing the importance of the hinge domain for cohesion have shown that locking of the cohesin hinge by addition of rapamycin to G1-arrested cells abolishes cohesin loading and cohesion (pictorially summarized in Figure 11C. Gruber et al., 2006). This study, however, did not address the requirement of hinge opening for cohesion if cohesin is already loaded onto the unreplicated DNA in G1 cells. I aim to develop an assay that clarifies the hinge's role in sister DNA entrapment. By closing the hinge *after* initial loading in G1 but *before* DNA replication, I will also assess whether or not conversion can happen *in vivo* in budding yeast chromosomes (Summary in Figure 11BCD).

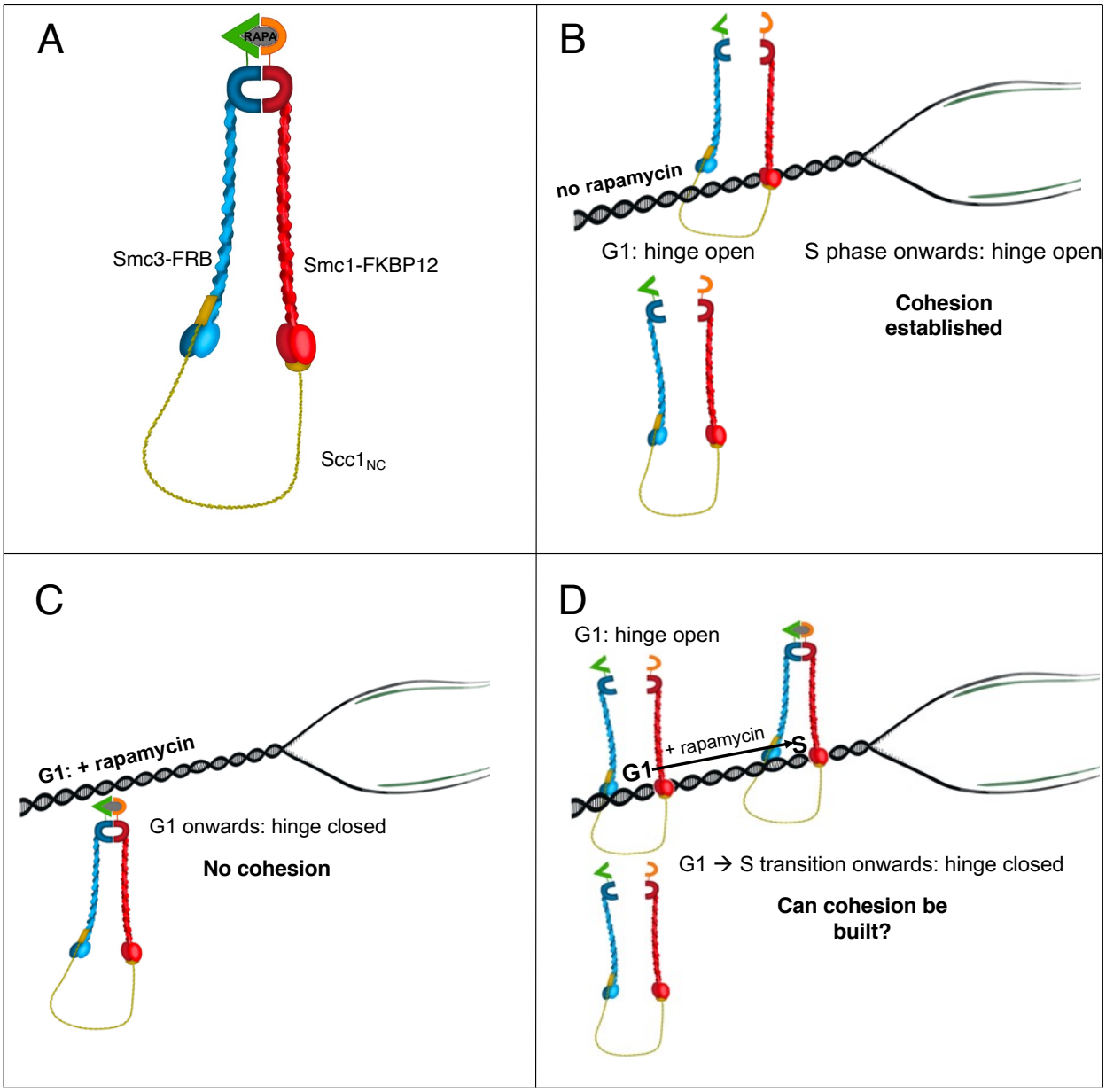


Figure 11. Cartoon depicting theoretical outcomes of the assay to be carried out. A) Cartoon of cohesin trimer to be expressed *in vivo*. **B)** Theoretical status of hinge throughout G1 and S phase when no rapamycin is added. Cohesion built. **C)** Outcome (as per Gruber et al., 2006) when rapamycin is added during G1. No cohesion built when hinge is closed in G1. **D)** Theoretical outcome of treatment with rapamycin immediately upon release from G1 arrest.

An *S. cerevisiae* strain was built to express Smc1-FKBP12 and Smc3-FRB alongside GalScc1(non-cleavable) and securin-Myc. In addition, fpr1 was deleted and TOR1 mutated as described above. The presence of labelled pds1 (securin) was confirmed via anti-Myc immunoblotting (Figure 12A) and PCR amplification of the Pds1-Myc18 locus (Figure 12B).

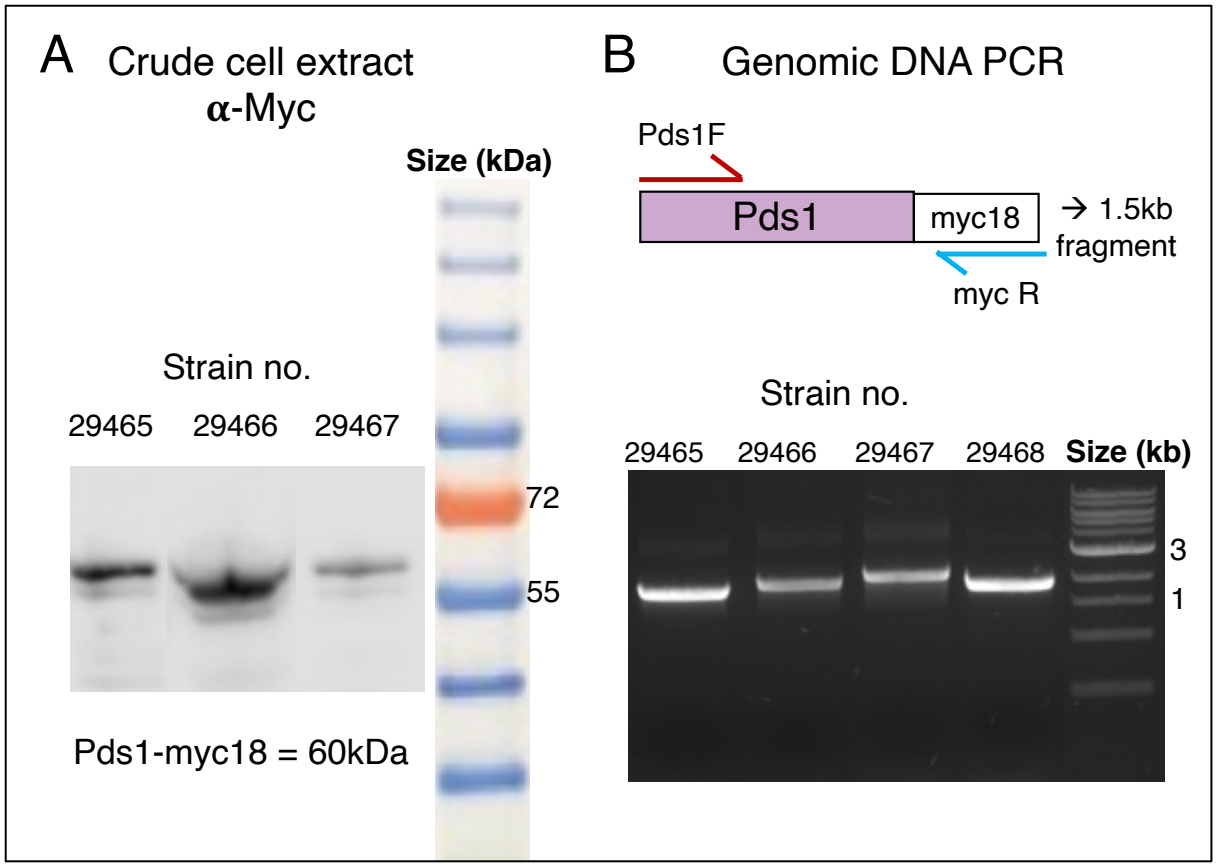


Figure 12. Confirming the presence of myc18-tagged securin in budding yeast strains. A) Western blot showing presence of myc-tagged securin in strains expressing Smc1-FKBP12 and Smc3-FRB. Crude cell extract run on NuPAGE gel and transferred to nitrocellulose membrane. Blotted with α-Myc (mouse α-Myc-HRP, Table 3)**. B)** DNA gel confirming presence of pds1-myc locus in genomic DNA extracted from strains. Pds1-myc locus amplified by PCR and run on ethidium bromide agarose gel.

The viability of these cells, as well as their sensitivity to both galactose and rapamycin, was tested compared to wildtype (Figure 13A)**.** The strain chosen for further experiments was that which showed the greatest degree of rapamycin and galactose sensitivity (=K29465) (Figure 14A).

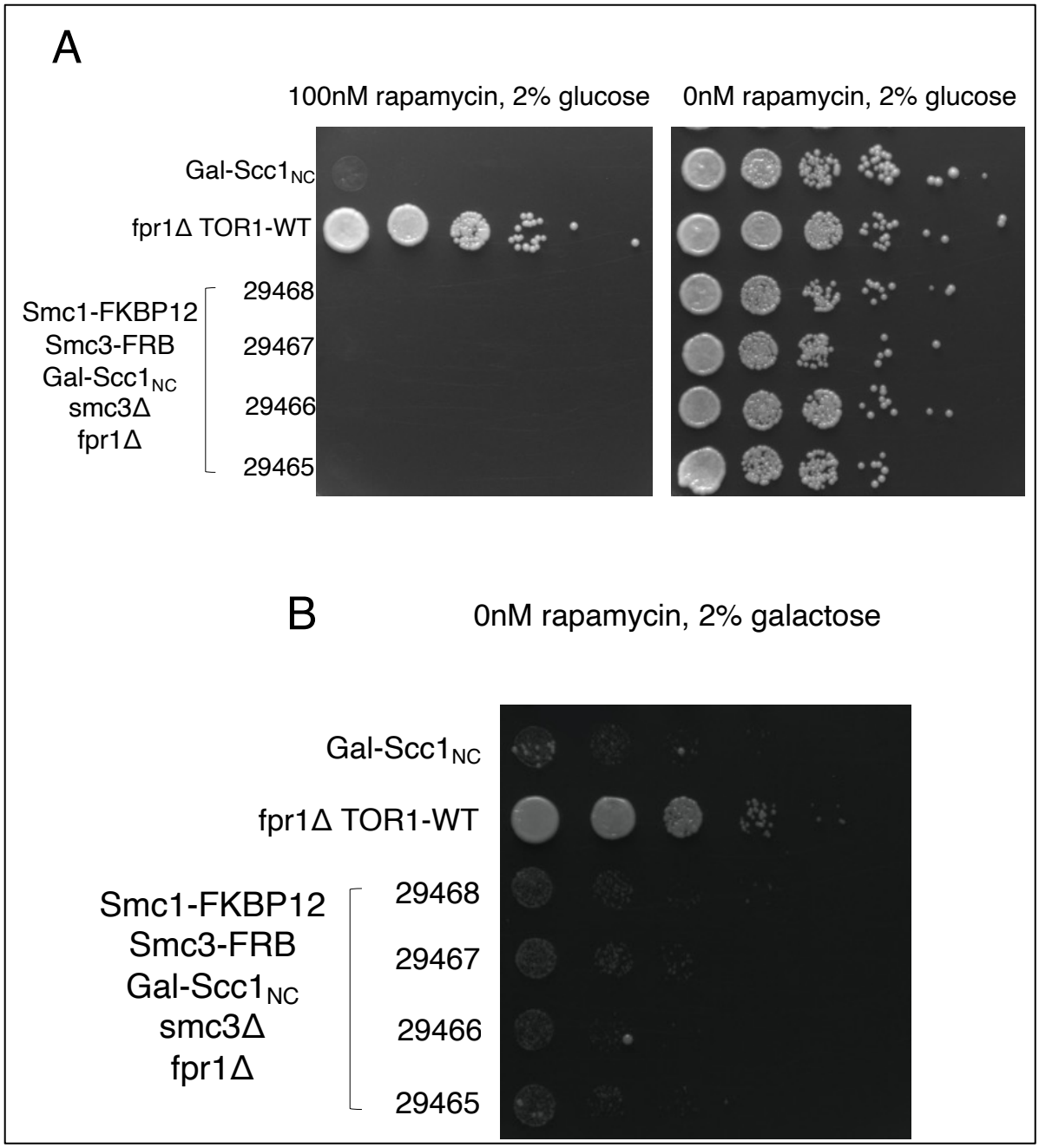


Figure 13. **Spot tests showing rapamycin and galactose-sensitivity of haploid strains.** A) Rapamycin sensitivity on glucose of candidate experimental strains (K29465-8), an otherwise WT strain expressing GalScc1$_{NC}$ (K28840) and a WT strain with an fpr1 deletion (K10599). B) Galactose sensitivity of K29465-8, K28840 and K10599; all strains but fpr1 deletion (K10599) express GalScc1$_{NC}$

Cohesin conversion occurs *in vivo* on yeast chromosomes, and does not require opening of the Smc1-Smc3 hinge domain

Galactose induction of Scc1NC, and subsequent detection of mononucleate (anaphase blocked) cells at anaphase, was carried out (Figure 14B). Securin

positivity was measured as described above in the presence and absence of rapamycin following release from α-factor arrest (Figure 14C).

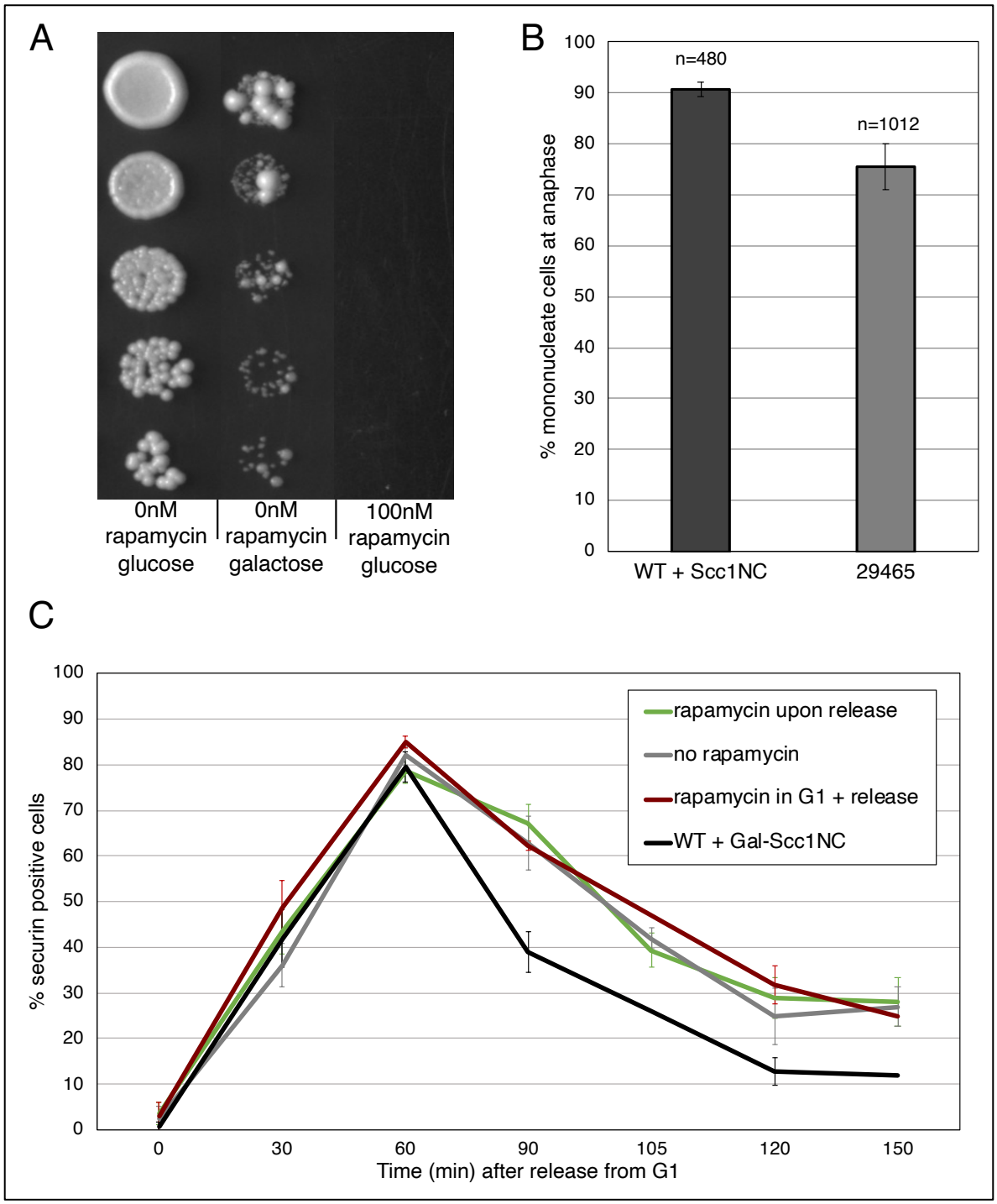


Figure 14. Viability, and efficiency of GalScc1$_{NC}$ induction and release from G1 arrest in WT vs. mutant strains. **A)** Serial dilution growth test of K29465 (GalScc1$_{NC}$, Smc1-FKBP12, Smc3-FRB) on (left to right): 0nM rapamycin with 2% glucose, 100nM rapamycin with 2% glucose and 0nM rapamycin with 2% raffinose/2% galactose. **B)** Histogram showing percentage mononucleate cells at anaphase after GalScc1$_{NC}$ induction during G1 (α-factor) arrest. Left: (K28840) WT strain + GalScc1$_{NC}$. Right: (K29465) GalScc1$_{NC}$ + Smc1-FKBP12 + Smc3-FRB. Error bars represent standard deviation per repetition (n = 3). **C)** Securin levels

at various timepoints following release from G1 (α-factor) arrest. Red, grey, green: K29465; black: K28840. Error bars represent standard deviation per image taken (n=12 for each timepoint; average n(cells) per timepoint per series = 665). Efficiency of release from G1 arrest as measured by securin levels occurs faster in WT strain (black, K28840) than K29645 (red, grey, green).

Following confirmation that G1 arrest in α-factor and GalScc1$_{NC}$ induction led to a large majority of mononucleate cells at anaphase, rapamycin was then added to culture such that hinge closure was induced either before cohesin loading onto unreplicated DNA (during G1) or afterwards (upon release from G1). Cells were fixed in formaldehyde at various timepoints following their release from G1 arrest, and anaphase cells were imaged for tubulin, DAPI and securin (Figure 15A). As previously outlined, where cohesion is established an anaphase cell will appear as a mononucleate, and where cohesion is not established as a binucleate. Consistent with previous observations (Gruber et al., 2006), when 100nM rapamycin was added to culture at the same time as GalScc1$_{NC}$ expression was induced (the concentration of rapamycin was maintained upon release from α-factor arrest), there was a loss of cohesion in 80% of cells (Figure 15B). Thus, non-cleavable cohesin was unable to load onto DNA during G1, and cohesive structures were not built in these cells.

Theoretically, treatment of cells with rapamycin only upon *release* from G1 could lead to two outcomes. Where no cohesion is established, and a majority of binucleates are seen at anaphase, it can be concluded that hinge opening or flexibility is required for cohesion establishment even *after* cohesin has loaded onto unreplicated DNA in G1. Secondly, where a majority of mononucleates are seen at anaphase, it is plausible that hinge opening is not required for cohesion establishment where cohesin has already loaded onto unreplicated DNA. Results supported the latter notion: when cells

were released from galactose with α-factor, into glucose with 100nM rapamycin, a majority of cells showed cohesion at anaphase (Figure 15C/D). This suggests that after cohesin has loaded onto unreplicated DNA, the hinge is not required to open in order for cohesion to be established. As shown by *in vitro* entrapment assays (Collier et al., 2022), in *in vivo* chromosomal cohesion assays (Gruber et al., 2006) and in Figure 15B**,** DNA entrapment cannot occur without hinge opening. This therefore refutes the possibility that the cohesion observed in Figure 15C/D has been established by *de novo* loading, and shows that conversion is happening *in vivo*. These experiments have shown for the first time that cohesion can be established on yeast chromosomes by conversion of cohesin rings that were loaded onto DNA prior to replication into cohesive forms, and that the opening of the hinge domain during S phase is not required for this process.

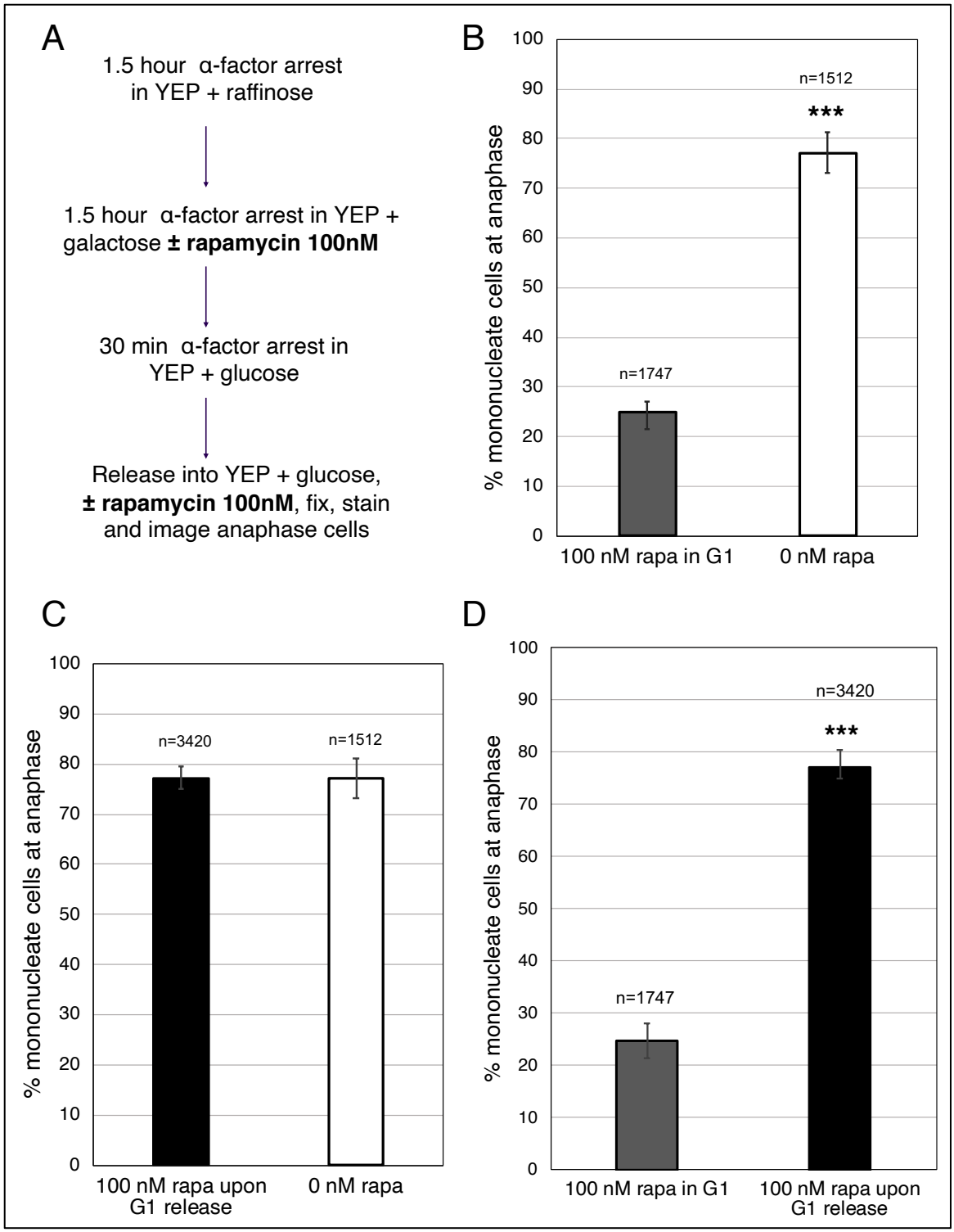


Figure 15. Cohesin conversion on chromosomes does not require opening of the Smc1-Smc3 hinge. A) Flow chart of experimental set-up for $Scc1_{NC}$ induction and hinge closure during or after G1 arrest. **B)** Histogram showing percentage mononucleate cells analyzed at anaphase; left: 100nM rapamycin added to culture at same time as galactose (during G1 arrest); right: Cells released from G1 into culture containing 2% glucose and 100nM rapamycin. One-way ANOVA carried out between series. Repeats: left n = 4, right n = 6. p-value = 1.52E-09 **C)** Histogram showing difference in % mononucleates when 0nM rapamycin added (right) or 100nM rapamycin added after release from G1. One-way ANOVA carried out between series; repeats: left n = 7, right n = 6. p-value = 0.987 (n.s.) **D)** Histogram showing difference in % mononucleates when 100nM rapamycin is added either during G1 arrest or

after release from G1. One-way ANOVA carried out between series. Repeats: left n = 4, right n = 7. p-value = 4.19E-09**. B, C, D**: error bars represent standard deviation between repeats.

2.3: **Confirming that rapamycin binds to FKBP12 and FRB on DNA-bound cohesin**

The above results show that locking of the hinge domains of pre-loaded cohesin rings by added rapamycin does not interfere with the conversion of these cohesin rings into cohesive forms. One formal possibility is that while rapamycin locks the hinges of *soluble* cohesin rings, it may be incapable of causing dimerization of the hinges of cohesin molecules bound to chromatin. That is to say that it could be that rapamycin only works on soluble and not DNA-associated cohesin. To address this possibility, I designed an experiment to test if rapamycin works on DNA-associated cohesin.

The role of Eco1 in sister chromatid cohesion maintenance has been established for some time. During G1, DNA entrapped by cohesin is released via the Smc3-Scc1 interface through the action of Wapl. During S phase, acetylation of Smc3 K112 and K113 by Eco1 acetyltransferase prevents further Wapl-mediated release and thus cohesion is maintained until Scc1 cleavage at anaphase (Ivanov et al., 2002). Eco1 deletion is lethal; in the absence of Wapl, this lethality is suppressed (Ben-Shahar et al., 2008). Eco1 deletion in the presence of Wapl, however, is suppressed by fusion of the Smc3-Scc1 interface; Wapl-mediated release of DNA occurs via this interface (Beckouet et al., 2016; Chan et al., 2012)**.** Therefore, if rapamycin can work on DNA-associated cohesin rings and induce fusion of FKBP12 and FRB, then expression of these as fusions to Scc1 and Smc3 respectively, followed by addition of rapamycin, should suppress the lethality caused by Eco1 deletion in the presence of Wapl.

Rapamycin-induced closure of smc3-scc1 interface rescues Eco1 inactivation-induced lethality

Strains were built to express FKBP12 and FRB as N-terminal fusions to Scc1 and Smc3 respectively. Alongside these constructs, the strains expressed a temperature sensitive Eco1 (G211H), fpr1 and galactose-inducible Wapl (GalWapl). At 37°C, Eco1 is inactivated. Strains expressing GalWapl are effectively WaplΔ on glucose (Figure 16A). Cells where both Eco1 and Wapl are inactivated/deleted are viable (i.e. growth on glucose at 37°C**)**, whereas presence of Wapl alongside Eco1 inactivation is lethal. In cells with GalWapl, growth on galactose leads to Wapl overexpression, and in the absence of Eco1 activity at 37°C is lethal.

Eco1 inactivation was carried out at 37°C in the presence and absence of Wapl. In the presence of Wapl at the Eco1 restrictive temperature, 100nM rapamycin should suppress Eco1G211H-induced lethality through fusion of the Smc3 and Scc1 interfaces. Indeed, in GalWapl strains at the restrictive temperature, 100nM rapamycin rescued Eco1TS-induced lethality (Figure 16B). This confirms that rapamycin *can* act by inducing dimerization of proteins when they are chromatin-bound. This also suggests that in Figure 15B/C/D rapamycin is indeed causing the observed effect through closure of the Smc1-Smc3 hinge. Wapl-mediated release occurs via the Smc3-Scc1 interface and therefore suppression of Eco1-inactivation indicates that in Figure 16A/B the Smc3-Scc1 interface is closing.

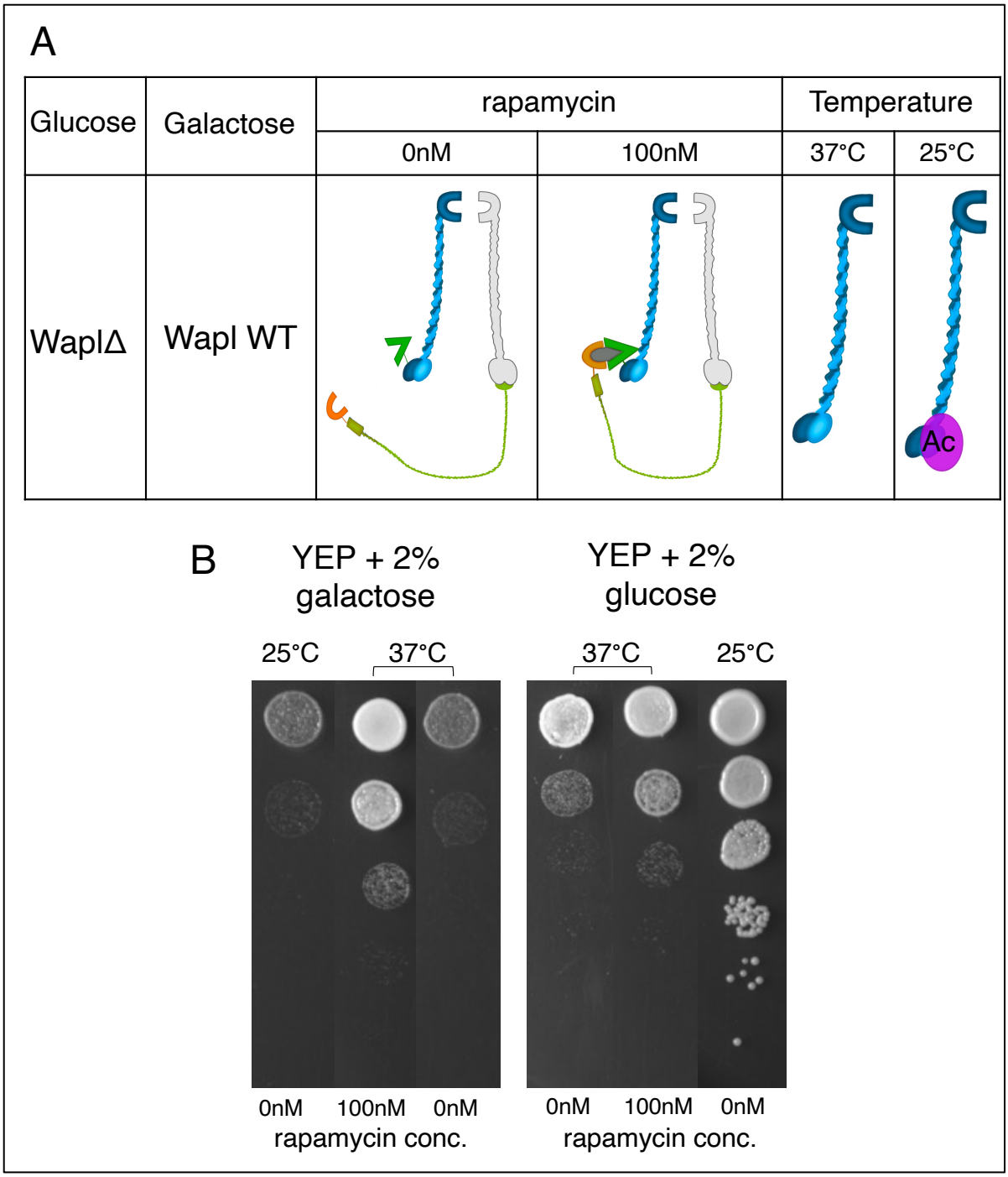


Figure 16. Rapamycin-induced fusion of Scc1-FKBP12 and Smc3-FRB suppresses lethality caused by Eco1 inactivation in the presence of Wapl. A) Schematic: Wapl expression on glucose vs. galactose, state of the Smc3-Scc1 interface in the presence and absence of rapamycin and effect of temperature on Smc3 acetylation through Eco1 inactivation. **B)** Spot test: GalWapl (effectively WaplΔ on glucose) Eco1TS cells on glucose and galactose at 37 and 25°C in the presence and absence of 100nM rapamycin.

2.4 **Deletion of conversion pathway-associated protein Ctf4 significantly reduces cohesion established by conversion**

The results depicted in Figure 15 allow us to conclude with certainty that conversion has occurred *in vivo* on yeast chromosomes, as it has been shown (Figure 15B and Gruber et al., 2006) that cohesin cannot load *de novo* onto DNA when its Smc1-Smc3 hinge is locked. As mentioned previously, several replisome-associated proteins have been shown to be involved in the process of cohesin conversion (Srinivasan et al., 2020; Xu et al., 2007). Among these is Ctf4, a DNA polymerase-interacting protein (Villa et al., 2016). Deletion of Ctf4 in yeast cells was shown to cause defects in sister chromatid cohesion (Borges et al., 2013), but ctf4Δ mutant cells were still able to entrap both one and two circular minichromosomes in the presence of Scc2 (Srinivasan et al., 2020). Seeing as the results above are in all likelihood denoting cohesin conversion, I aimed to determine whether whether cohesion established when the hinge is closed during S phase will be reduced upon deletion of Ctf4.

The strain used for experiments in section 2.2 (K29465) was crossed with a strain with deleted endogenous Ctf4 (K11689), and a haploid strain of mating type a possessing all of the required proteins was selected for on nucleotide/amino acid-deficient or antibiotic-treated agarose. The strain satisfying the criteria (K29653) showed significant synthetic sickness, which is likely cumulative from both parent strains (Figure 13A, Figure 17A). The cells were arrested in G1 and GalScc1$_{NC}$ induced as described above (Figure 15A), and released into glucose containing either 100nM or 0nM rapamycin. Anaphase cells were imaged as described previously and mononucleate cells, i.e. those showing cohesion, were quantified (Figure 17B).

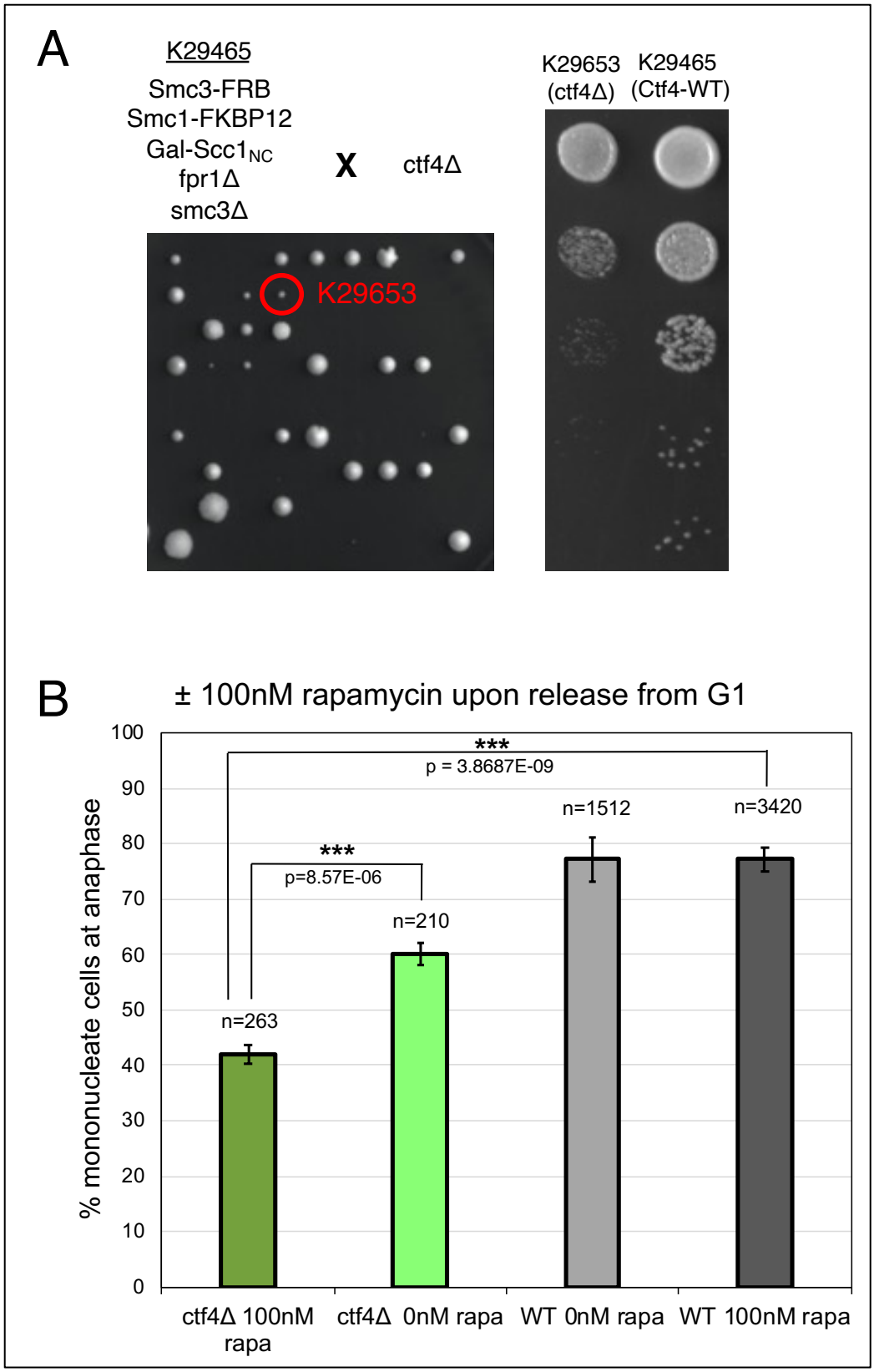


Figure 17. **Effects of ctf4 deletion on viability and cohesin conversion**. A) Left: genotypes of the two strains crossed to achieve the strain circled in red. Right: Spot test on YEPD showing sickness of circled strain compared to K29465. **B)** Histogram denoting percentage of mononucleates (i.e. percentage of cells with cohesion) seen in ctf4Δ vs. Ctf4-WT cells in the presence or absence of 100nM rapamycin upon release from G1.

As expected, deletion of the cohesin conversion pathway-associated protein Ctf4 significantly (p=3.87E-09) reduced cohesion established by conversion compared to cells expressing WT Ctf4 (Figure 17B). Cohesion established when the hinge remains open during S phase was also reduced by ~17%. This may be a consequence of the synthetic sickness of the strain, or perhaps a proportion of cohesion is established by conversion even when the hinge remains open during S phase (Figure 9A, Figure 17B). When the hinge was closed, 40% of cells still showed cohesion at anaphase in the absence of Ctf4, compared to 20% in its presence. This either signifies that cohesin conversion can take place, albeit at a reduced level, in the absence of Ctf4 (i.e. compensation by other conversion-associated factors), or that rapamycin binding to FKBP12 and FRB is reduced in the ctf4Δ strain, perhaps as a consequence of its synthetic sickness. Further work should seek to characterize if chromosomal cohesion is increasingly reduced in the absence of two or multiple conversion-associated factors.

2.5: **Inactivation of cohesin *de novo* loader Scc2 does not interfere with cohesion established by conversion.**

As the results shown in sections 2.2 and 2.4 demonstrate, the observed chromosomal cohesion that is mediated by non-cleavable cohesin has arisen due to cohesin conversion, rather than *de novo* loading of cohesin onto sister DNAs. Both processes are thought to occur in concert in the context of chromatid cohesion establishment during S-phase. Therefore, we must refute any formal possibility that the *de novo* loading of non-cleavable cohesin is still occurring in these cells, in particular when the Smc1-Smc3 hinge domain is closed. Scc2 is essential for the *de novo* entrapment of

DNA by cohesin *in vitro,* and this process requires opening of the hinge (Collier et al., 2022). Scc2 is also essential for establishment of cohesion of minichromosomes in the absence of the cohesin conversion-associated factors Ctf4, Tof1/Csm3 and Chl1 (Srinivasan et al., 2020). Therefore, I have combined the system described in sections 2.1, 2.2 and 2.4 with the temperature-sensitive inactivation of the cohesin *de novo* loading protein Scc2, in order to assess the ability of cells wherein the Smc1-Smc3 hinge is closed to establish chromosome cohesion in the absence of Scc2.

The strain used in sections 2.2 and 2.4 (K29465) was crossed with a strain expressing a Scc2 mutant, scc2-45 (L545P D575G), that is rendered completely inactive at temperatures of 37°C or greater (K21496, Petela et al., 2018)**.** A haploid strain of mating type a with the genotype detailed in (Figure 18A**)** was selected (K29654) and compared against the parent strain (K29465, Section 2.2) for temperature-sensitive synthetic sickness on at 37°C and for survival at 25°C (Figure 18A). Scc2 deletion/inactivation in cycling cells is lethal (Ciosk et al., 2000; Furuya et al., 1998). Initial loading of cohesin onto unreplicated DNA in G1 is Scc2-dependent, and as an indirect consequence so is the cohesin conversion pathway.

Cells were arrested in α-factor alongside galactose induction of $Scc1_{NC}$ as previously. Cells were released from G1 arrest into YEP+ 2% glucose containing 100nM or 0nM of rapamycin, and incubated with shaking at either 25 or 37°C. Anaphase cells were collected, fixed, stained and imaged as detailed in Figures 8C and 15A. Chromosome cohesion levels were not significantly altered in the presence or absence of rapamycin, nor at the permissive or restrictive temperatures (Figure 18B) This further refutes the

possibility that any cohesion observed in Figure 15C/D has arisen due to *de novo* loading, and even suggests that in the absence of rapamycin, i.e. when the hinge is open, the majority of cohesive structures are arising due to conversion (Figure 18B**,** Figure 15B, Figure 9A/B).

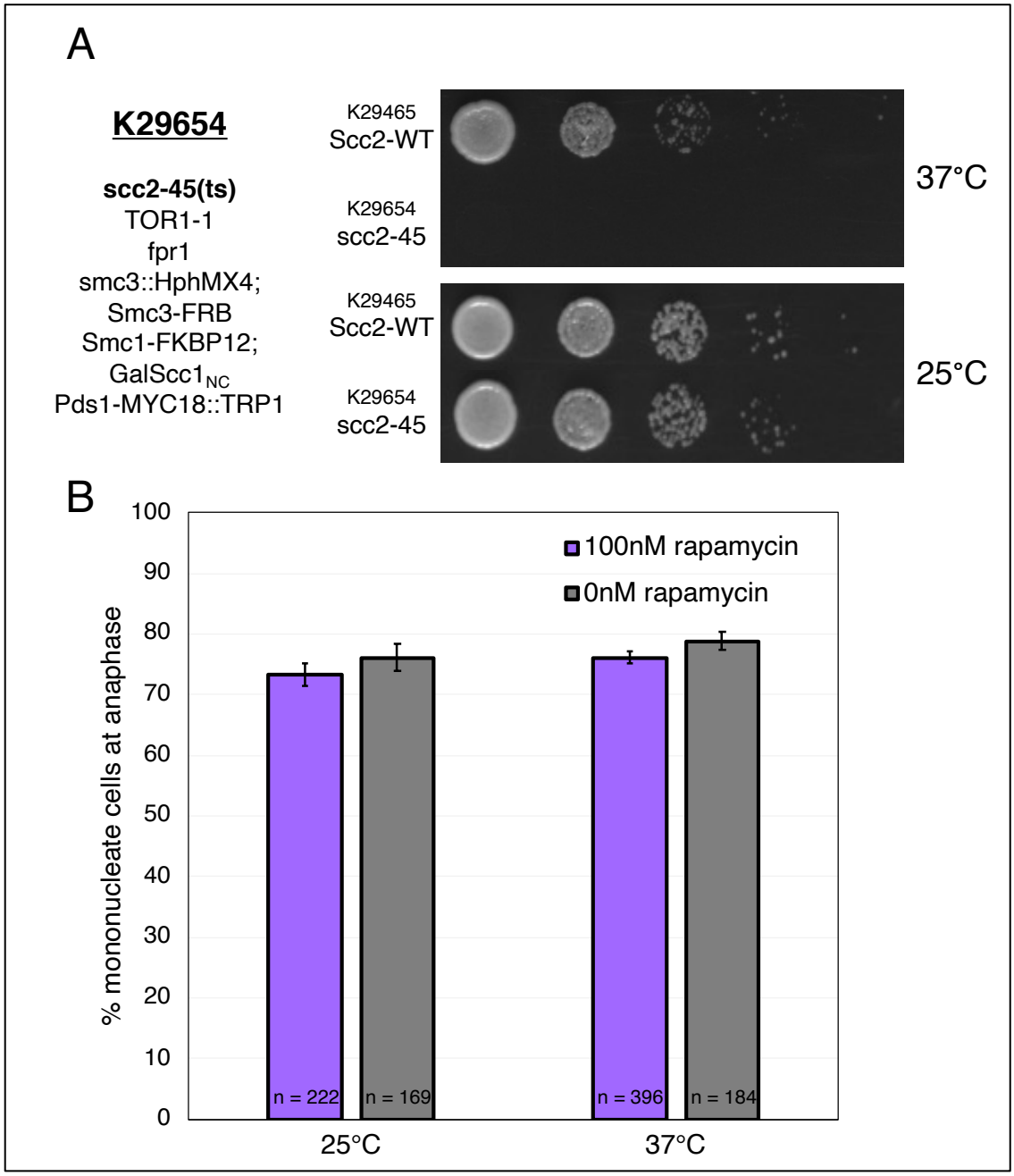


Figure 18. Scc2 inactivation does not interfere with cohesion established by the conversion pathway. A) Left: Strain genotype (hinge mutant, $Scc1_{NC}$ and scc2-45 (ts). Right: spot test on YEPD at permissive and restrictive temperatures; scc2 inactivation is lethal. **B)** K29654 cohesion assay in presence and absence of 100nM rapamycin, and at permissive or restrictive temperature. $Scc1_{NC}$-mediated chromatid cohesion at anaphase not affected by scc2 inactivation.

Part B: Can fusion of both Smc-kleisin interfaces support viability?

2.6 Expressing the Smc3-Scc1-Smc1 fusion protein *in vivo*

Introduction

Opening of the hinge is thought to be necessary for the Scc2-dependent *de novo* loading pathway of cohesion establishment (Figure 15B). However, the results presented above show that hinge opening is not required to convert chromosome-associated cohesin into a cohesive form (Figure 15CD). Therefore, it is plausible that the other two interfaces on cohesin's ring are potentially involved in cohesin conversion. The fact that Smc3-Scc1 and Scc1-Smc1 fusion strains are viable (Gruber et al., 2006; Srinivasan et al., 2018) does not rule out the possibility that either one or both interfaces are required to open for cohesion establishment by conversion. In order to address this, I aimed to build an Smc3-Scc1-Smc1 fusion protein for expression in yeast cells.

Developing a Smc3-Scc1-Smc1 fusion protein for expression in *S. cerevisiae*

Regardless of its underlying mechanism, it is possible that conversion may require the opening of one of the cohesin ring's three interfaces. Data thus far shows that opening of the hinge is not necessary for conversion to occur, however it is possible that either of the Smc-kleisin interfaces may be involved in this process. It is also possible that, where interface flexibility is required for conversion to occur, the three interfaces are redundant and that no single interface is indispensable. In order to ascertain this, I aimed to develop a Smc3-Scc1-Smc1 fusion construct for expression *in vivo* in yeast.

The only ‘open’ interface within this fusion protein is the Smc1-Smc3 hinge, and it is fully capable of entrapping individual DNAs *in vitro* (Collier & Nasmyth, 2022). Whether or not this fusion protein can support viability in the absence of WT cohesin subunits will demonstrate whether or not these interfaces within the cohesin rings are vital for cohesion.

Smc3-Scc1-Smc1 fusion does not support viability in the absence of wildtype Scc1

DNA fragments for construction of the double fusion construct (Figure 19B) were obtained from existing vectors in the Nasmyth collection (6972) and yeast genomic DNA (K795, Bin Hu). Fragments were assembled into a vector (Figure 19BC**).** The vector was amplified by transformation into *E. coli,* purified from the bacterial culture, sequenced and aligned to the previously generated vector map. The plasmid shown in Figure 18C was transformed into a WT *S. cerevisiae* strain (K700) and integrated into the URA3 locus.

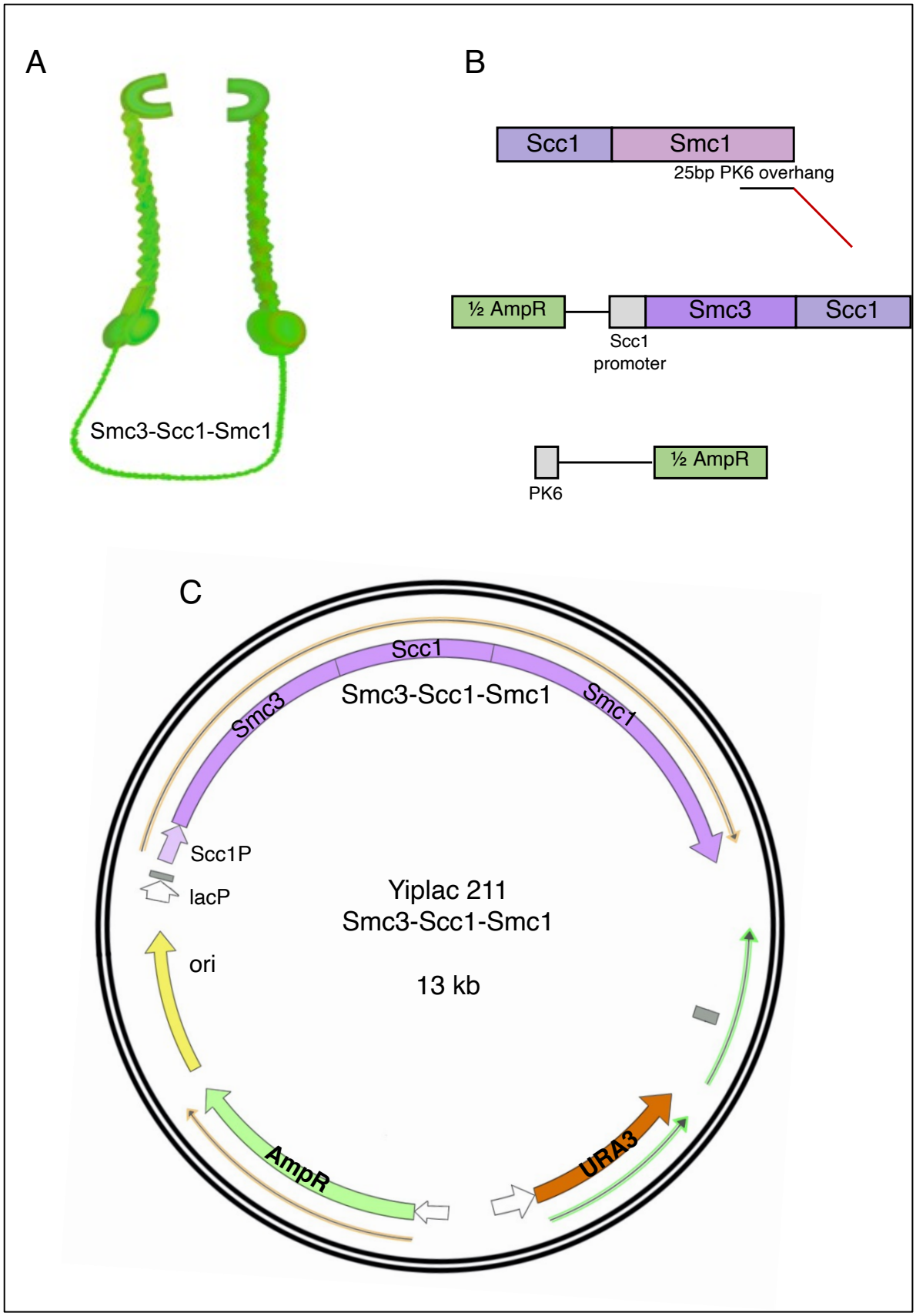


Figure 19. Double fusion plasmid construction schematic. **A)** Cartoon of Smc3-Scc1-Smc1 fusion protein; putatively expressed as a single polypeptide **B)** Composition of the three fragments used to assemble plasmid. Plasmid backbone denoted by thin black line. **C)** Map of Yiplac211 plasmid encoding Smc3-Scc1-Smc1 fusion protein.

Nine successful transformants were selected on uracil – (minus) plates and each crossed with a strain containing one ectopic (LEU2/leucine locus) WT copy of Scc1 and a deleted endogenous Scc1 with a natamycin (NAT) resistance cassette in its place. Diploids were selected and allowed to sporulate. Spore tetrads were separated to form haploid strains (648 new haploid strains generated in total). These strains were scored for their ability to grow on NAT, uracil – and leucine – plates.

Strains wherein scoring denoted the presence of the double fusion protein (growth on uracil –), the presence of deleted endogenous Scc1 (growth on NAT) and the absence of WT ectopic Scc1 (no growth on leucine –) were assessed for their growth on rich medium (YPD) in comparison to wildtype (Figure 20A). In a majority of the seven strains, synthetic sickness was at least somewhat apparent. One clone in particular, clone C, showed a high degree of sickness (Figure 20A). This is to be expected; previous work has shown that budding yeast are sick even when expressing single Smc-kleisin fusions. If all of the alleles selected for in this cross were to have no detriment to the health of the strain in which they are expressed, and were to segregate according to Mendelian genetics, then one in every six new haploid strains should possess the aforementioned desired genotype. Given that in the 648 newly generated haploid strains, only ~twelve met the scoring criteria described above, it is highly likely some form of gene conversion has occurred. Such an event at the Leu2 locus or the scc1Δ-NAT locus, could have afforded the strains a copy of WT Scc1 without the Leu2 marker.

Genomic DNA was extracted from the seven clones shown in Figure 19A, in order to test for the presence of both the double fusion protein DNA sequence, and a WT Scc1 sequence. Wildtype genomic DNA wherein Scc1 was amplified from its promoter to 300 nucleotides past its stop codon showed a ~3.5 kilobase band. All clones but one possessed bands of varying sizes that were significantly smaller than this at ~1.5-2 kb (Figure 20B). Two clones possessed multiple sequences of DNA within this range of sizes, as did the parental strain (K24413; Scc1WT::LEU2, scc1Δ-NAT), albeit much more faintly. The sequence spanning from Smc3 5' end to the middle of the Scc1 coding sequence was amplified, and shown to be present in six of the seven clones, as well as in the original double fusion-encoding plasmid, and not in WT DNA (K700) or in the parental strain (K24413) (Figure 20C). All clones that possessed the DNA sequence corresponding to an Smc3-Scc1 fusion also possessed, in some form, the wildtype Scc1 sequence. Therefore, it can be concluded that the Smc3-Scc1-Smc1 fusion protein likely does not support viability in the absence of WT cohesin.

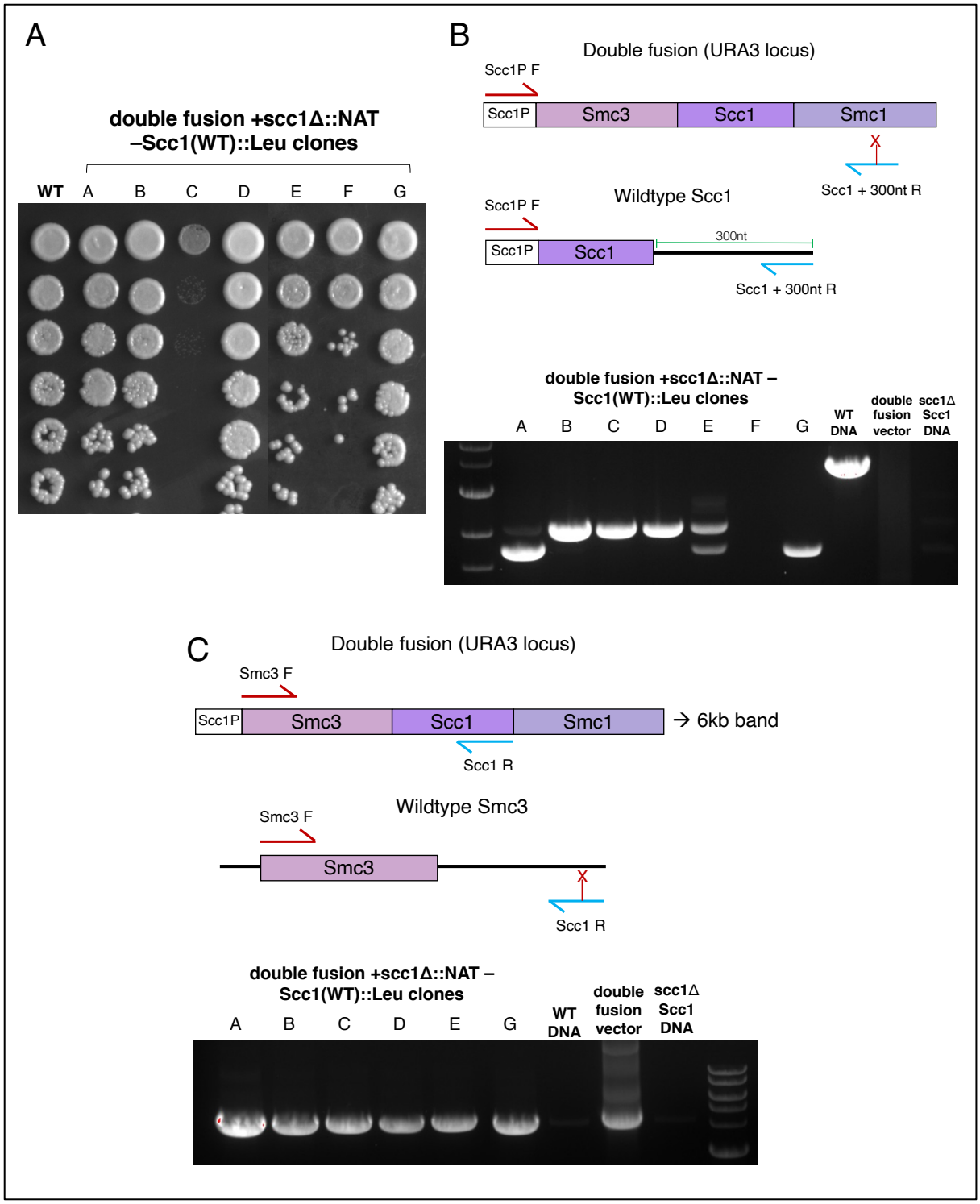


Figure 20. Growth test and validation of genomic content in double fusion haploid clones. A) Serial dilution growth test of seven clones alongside WT on YPD plates. B) Schematic and gel displaying fragment corresponding to WT Scc1. C) Schematic and gel displaying fragment corresponding to Smc3-Scc1 fusion.

The bands corresponding to Scc1 that are seen in the double fusion clones in Figure 20B are significantly smaller than that seen in the wildtype DNA. It is evident that a

gene conversion event has taken place, but with which allele or ectopic sequence this exchange has occurred is unclear. The DNA of the parental strain K24413 does not contain the sequence corresponding to WT Scc1, yet all of the clones do. Of particular note are clones A and G in Figure 20B: at 1.5kb, they represent at the very least a truncated Scc1 sequence; the fragment amplified by the primers used would be at a minimum 2 kilobases long. Ideally, analysis of the size of the cognate proteins of these sequences would reveal the presence or absence of WT Scc1. However, due to the lack of antibodies against *S. cerevisiae* Scc1, this is not possible. Considering all of the above, and in particular the fact that only a very small fraction of the 648 clones generated displayed the appropriate genetic markers, it can be concluded that the Smc3-Scc1-Smc1 fusion protein does not support viability in the absence of WT Scc1.

Chapter 3: Discussion

3.1 **Results part A: Discussion & further work**

Wapl-mediated cohesin release in cells where the Smc1-Smc3 hinge is closed

When considering the dynamics of cohesin on DNA in WT cells, one must take into account the Wapl-mediated release activity that occurs during G1. Here, DNA 'exits' the cohesin ring via its Smc3-Scc1 interface, and cohesin reloads onto DNA thereafter or during DNA replication. One could posit that the cohesion observed when rapamycin-induced closure of the hinge occurs after release from G1 is due to reloading of cohesin onto DNA, and not 'converted' structures that have remained associated with DNA from their initial loading in G1. However, given the *in vitro* evidence that hinge opening is required for entrapment of DNA, and that closure of the hinge prior to loading onto DNA abolishes cohesion (Collier et al., 2022; Gruber et al., 2006; Figure 15B), it is highly implausible here that any *de novo* loading of cohesin onto DNA occurs in the presence of rapamycin. Thus, it is very probable that the cohesion observed at anaphase is imparted by cohesin trimers that are not removed by Wapl prior to DNA replication. This is not to say, however, that this population of cohesive trimers form a majority of cohesin molecules in the cell. It is thought that only one third of a cell's available pool of cohesin contribute to sister chromatid cohesion (Gerlich et al., 2006)**,** and the minimum amount of cohesin trimers required to mediate cohesion of two sister chromatids may well be even less than this.

Potential deficits in cohesin occupancy on DNA where sister chromatid cohesion is mediated only by conversion

A crucial caveat to the results presented in Section 2 is that, the fact that sister chromatid cohesion established by conversion alone is observed, does not refute the possibility that there is a significant deficit in cohesin's activity in these cells. That is to say that much fewer hinge-fusion/Scc1$_{NC}$ cohesin rings may be loaded onto sister DNAs compared to WT cells (where conversion and *de novo* loading occur in parallel), but perhaps *just enough* cohesin is loaded onto sister DNAs in order to confer cohesion. Scc4 inactivation upon release from G1 led to a drastic reduction in chromosomal cohesin levels at centromeric regions in G2 and M phases (Petela et al., 2021). The cohesin loading complex Scc2/Scc4 facilitates the loading of cohesin at the centromeres through interactions between Scc4 and the kinetochore protein Ctf19 (Hinshaw et al., 2017). So in the absence of *de novo* loading, when the hinge is closed and the cells are effectively 'forced' to produce cohesion only by conversion, there may indeed be a significant reduction in chromosomal cohesion levels, particularly at centromeres, in diploid cells. In order to verify this, GalScc1$_{NC}$ chromatin immunoprecipitation sequencing (GalScc1$_{NC}$-PK9 is expressed in K29465) should be carried out. This will also give insight into the lower limits of cohesin occupancy on DNA that are required to confer sister chromatid cohesion.

The 'topological entrapment' model of sister chromatid cohesion

The immunofluorescence system used (Section 2.1, Figure 8) relies in large part on the visual assessment of sister chromatid cohesion, rather than measurement of topological entrapment (e.g. minichromosome assay). Sister chromatid cohesion has

as of yet perfectly correlated with entrapment of minichromosomes, and the proven importance of cohesin's hinge and Smc3-Scc1 interface in both the loading and dissociation of cohesin from chromosomes suggests topological entrapment is occurring. There is a formal possibility that chromosome cohesion does not involve DNA entrapment, and certain models of cohesion such as the handcuff model (Zhang et al., 2008) propose as such. However, significant further work is needed to categorically settle this debate; the more recently discovered links between cohesion establishment and the replisome, and the upsurge in investigation of cohesin's loop extrusion activity have only complicated existing models of cohesion establishment. It was shown that during DNA replication, nascent sister DNAs become intertwined, purportedly through the rotation of the replisome. This caused the catenation of circular 26kb minichromosomes; topoisomerase II removes the majority of the entanglement, but some remains until sister chromatid separation at anaphase (Farcas et al., 2011). This persistence of minichromosome entanglement was shown to be cohesin-dependent, meaning that without functional cohesin, the intertwining of minichromosomes was not maintained, nor was it sufficient to confer minichromosome cohesion (Farcas et al., 2011). This further supports the notion that the cohesion observed in results presented in Section 2 is a result of sister DNA entrapment by cohesin, and not some ulterior mechanism. Nonetheless, it would be interesting to compare the levels of minichromosome catenation by wildtype cohesin and hinge-fusion, $Scc1_{NC}$ cohesin, to see if some compensation for lower cohesin occupancy is occurring through sister chromatid intertwining.

Covalent closure of the Smc1-Smc3 hinge

While the major pitfalls of the rapamycin-based fusion system used have been addressed (Section 2.3), it is still desirable to achieve fusion of the hinge interface *covalently*. Rapamycin binds to FKBP12 and FRB with relatively high affinity (Banaszynski et al., 2005), but this interaction is reversible and the non-specific (i.e. not FKBP12 and FRB-related) contributions of the rapamycin drug to the strain's synthetic sickness are still somewhat unclear. The SpyTag/KTag/SpyLigase system can be used in order to achieve covalent and irreversible closure of the hinge in a time-controllable manner (Hatlem et al., 2019). SpyTag and KTag are small (13aa and 10aa respectively) peptides that can be covalently linked by docking to the 11kDa SpyLigase protein (Fierer et al., 2014). By expressing SpyTag and KTag as fusions to the Smc1 and Smc3 hinges, and expressing the SpyLigase inducibly, closure of the hinge can be controlled temporally as in the rapamycin system, and this closure is irreversible. Furthermore, the SpyTag/KTag/SpyLigase system is approximately half the size of the FKBP12-FRB system, and this may mitigate some synthetic sickness (Figure 13A) arising from fusion of bulky moieties to the Smc1-Smc3 hinge.

3.2 **Results Part B: Discussion & further work**

DNA entrapment and chromatin occupancy by Smc3-Scc1-Smc1 fusion protein

It is pertinent to the understanding of the results presented in Section 2.6 that the properties of the double fusion protein are analyzed. If translated properly, the fusion protein would be approximately 345kDa, which certainly nears the upper limit of budding yeast protein mass. Its molecular weight should be assessed in order to first determine that the full-sized protein is being expressed, given its expression in the

absence of Scc1 was lethal. Despite this, *in vitro* evidence shows that Smc3-Scc1-Smc1 fusion proteins are still capable of entrapping DNA (Collier and Nasmyth, 2022). Without viability, there is no way to measure chromosome cohesion that is mediated purely by the double fusion construct *in vivo*. However, by addition of an epitope tag to Smc1's N terminus, its ability to entrap circular minichromosomes and its occupancy on chromosomes can be measured using minichromosome-IP and ChIP-seq respectively. Whether the double fusion polypeptide overwhelmed the budding yeast's protein synthesis machinery and was not properly translated, or fusion of both Smc-kleisin interfaces was indeed lethal is unclear. In order to mitigate this, double fusion of Smc-kleisin interfaces should be achieved *in vivo* in a different manner.

Achieving viability upon fusion of both Smc-kleisin interfaces

It was shown that both Smc1-Scc1 and Smc3-Scc1 single fusion proteins are viable, implying that neither interface is indispensable for cohesion establishment (Srinivasan et al., 2018). Furthermore, *in vitro* evidence shows that DNA can enter cohesin via the Smc3-Scc1 interface. As established in this study, the hinge interface is also not required for cohesion establishment, at least not that established by conversion. The Smc3-Scc1-Smc1 fusion protein did not support viability in budding yeast in the absence of WT Scc1 (Figure 20BC). While it is unclear as to what caused this lethality, it is still highly pertinent to dissect the roles of both Smc-kleisin interfaces in chromosomal cohesion establishment. In order to bypass the lethality of double fusion expression *in vivo*, FRB can be fused to Smc1 and Smc3 C- and N-termini respectively, and this can be expressed alongside a *single* fusion of the other Smc protein with Scc1 (non-cleavable) (Figure 21) *in vivo*. In doing this, we will avoid

lethality from expression of the double fusion protein, and gain temporal control over closure of one Smc-kleisin interface.

Probing the role of the Smc-kleisin interfaces in cohesin conversion

Robust previous evidence highlights S phase as crucial in the establishment of cohesion. The work presented here underlines this with regards to cohesin conversion, and has demonstrated that conversion does not require opening of the Smc1-Smc3 hinge. Thus, applying the assay described in Section 2.2 to the setup summarized in Figure 21 will further probe the roles of each cohesin interface in cohesion establishment. *In vitro* evidence shows that, unlike the hinge, entrapment of DNA through the Smc3-Scc1 interface does not require Scc2 (Collier and Nasmyth, 2022). Taken together with the evidence that cohesin dissociates from DNA via this interface *in vivo* (Chan et al., 2012), it is technically possible that this observation *in vitro* is artefactual. Therefore, expression of an Smc-kleisin single fusion (Smc3-Scc1 and Smc1-Scc1) should also accompany the rapamycin-induced closure of the Smc1-Smc3 hinge (Figure 21) and the subsequent measurement of sister chromatid cohesion. This will clarify the mechanisms of cohesin conversion with respect to the involvement of cohesin's various interfaces in the entrapment of sister DNAs.

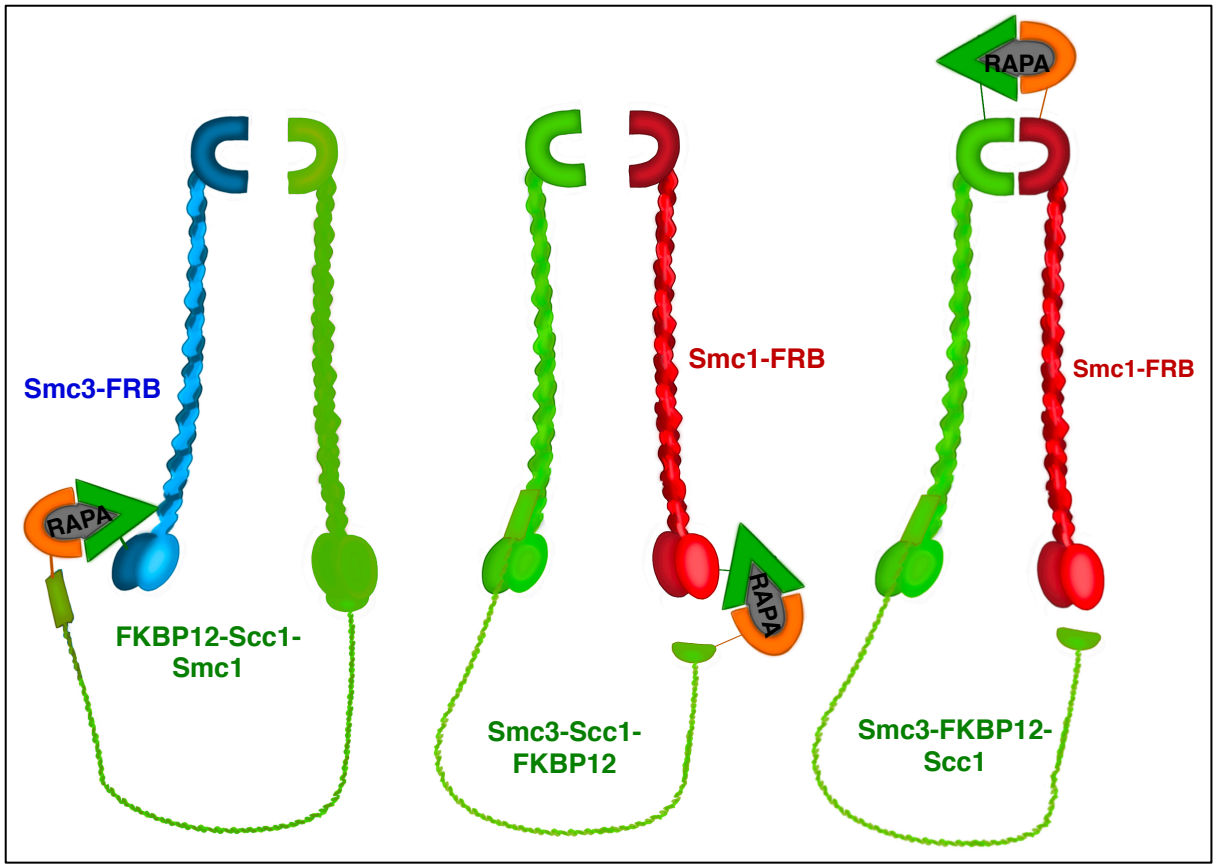


Figure 21. Schematic of Smc-kleisin single fusions with rapamycin-induced closure of a second interface . (Left to right) N-terminal fusion of FKBP12 to Scc1, C terminal fusion of Scc1 to Smc1; C-terminal Scc1-FRB fusion, N-terminal

3.3 **Concluding remarks**

The *de novo* and conversion cohesion establishment pathways occur in parallel during DNA replication, and cohesion can still be established upon abrogation of one pathway (Xu et al., 2007). *De novo* loading requires hinge opening, whereas conversion does not, and both single Smc-kleisin fusions support viability and CD entrapment in yeast (Srinivasan et al., 2018). Therefore, it seems that there is both redundancy in terms of the pathways through which chromatid cohesion is established, *and* in terms of cohesin's three interfaces in the context of enabling DNA entry into the cohesin ring. This apparent versatility in cohesin's means of DNA entry further adds to the ever-growing list of cohesin's purported mechanisms. Despite this, the work presented in

this thesis provides categorical evidence for cohesin conversion on eukaryotic chromosomes, and has clarified the Smc1-Smc3 hinge's involvement (or lack thereof) therein. Moreover, the tools and systems used will continue to prove important in probing the roles of cohesin's interfaces in chromosomal cohesion. The results presented here, and the data that downstream work will generate, delineate a straightforward trajectory towards a detailed mechanistic understanding of how cohesin confers sister chromatid cohesion.

Chapter 4: Materials and Methods

4.1 **Yeast strain, plasmid, antibody and oligonucleotide tables**

S. cerevisiae **strains**

Number	Genotype	Description	Creator
K700	Mat α	Wildtype mat α strain	Kim Nasmyth
K11689	Mat α; URA3::tetR::GFP-LEU2; Rec8-HA3::URA3; his3::hisG; trp1::hisG; ADE2; Pds1-MYC18::TRP1; ctf4::KanMX	Endogenous ctf4 deletion and myc-tagged securin.	Barbara Chwalla
K28840	Hura3::3XURA3 tetO112; his3::HIS3tetR-GFP; Pds1-MYC18::TRP1; leu::GalScc1(R180E, R268D)-HA3::LEU; wapl::hphMX4	Expresses non-cleavable Scc1, Myc-tagged securin and Wapl deletion with hygromycin resistance.	Madhusudhan Srinivasan
K29465 **K29466** **K29467** **K29468**	Mat a; TOR1-1; fpr1::NatMx4; smc3::HphMX4; leu2::Smc3-insmFRB-HA3::LEU2 Smc1-FKBP12; ura3::GalScc1(R180E, R268D, A547C)-PK6::URA3; Pds1-MYC18::TRP1	Rapamycin-induced fusion of Smc1 and Smc3 hinge domains. Non-cleavable Scc1 expression induced with galactose. Myc-tagged securin. Endogenous smc3 deletion. TOR1-1 and fpr1 mutations for increased rapamycin sensitivity.	Madhusudhan Srinivasan
K21496	Mat α; scc2-45::KanMX (L545P D575G)	Expresses Scc2 that is inactivated at 37°C	Bin Hu
K10599	Mat a; fpr1::NatMX4	Fpr1 deletion with Natamycin resistance	Stephan Gruber
K16522	Mat α; eco1(G211H) (ts); Scc1-PK9::KanMX	Expresses Eco1 that is inactivated at 37°C and PK-tagged WT Scc1	Chris Chan
K18388	Mat α; ura3::FKBP12-GL-Scc1::URA3; Smc3-GL-mFRB::HIS3; scc1::NatMX4	N-terminal fusions of FKBP12 and FRB to Scc1 and Smc3 respectively. Endogenous Scc1 deletion with natamycin resistance.	Pelin Uluocak
K16496	Mat a; GalWapl::HphMX4; ADE2; ura3::3XURA3 tetO112; his3::His3tetR-GFP	Endogenous Wapl promoter replaced with Gal promoter (strain is effectively WaplΔ on glucose).	Benjamin Rowland
K795	Scc1-TEV-Smc1::KanMX	Expresses Scc1-Smc1 fusion with short linker; used to generate fragments for double fusion plasmid assembly	Bin Hu
K29654	Mat a; fpr1::NatMX4; Smc1-FKBP12; Smc3-insmFRB-HA3::LEU2; GalScc1(R180E, R268D, A547C)-PK6::URA3; Pds1-MYC18::TRP1; scc2-45::KanMX	Cycling cells dead at 37°C, viable if inactivated upon release from G1. Pds1-myc and $Scc1_{NC}$ for IF assay	Charlotte Laurent
K29653	Mat a; fpr1::NatMX4; Smc1-FKBP12; Smc3-insmFRB-HA3::LEU2; GalScc1(R180E,	Cells viable with synthetic sickness. Pds1-myc and $Scc1_{NC}$ for IF assay.	Charlotte Laurent

	R268D, A547C)-PK6::URA3; Pds1-MYC18::TRP1; ctf4::KanMX		
Figure 16, Section 2.3	Eco1(G211H); fpr1::NatMX4; Scc1-PK9::KanMX4; Smc3-GL-mFRB::HIS3; ura3::FKBP12-GL-Scc1::URA3; GalWapl::HphMX	Dead on galactose at 37°C, rescued with rapamycin. Viable on glucose at 37°C.	Charlotte Laurent

Table 1. *S. cerevisiae* strains used in this study. All strains listed are haploid and genotypes were verified by scoring on selective growth medium and, where relevant, by validation of genomic or proteomic content

Plasmids

Number	Description	Use	Source
6972	Yiplac211 Scc1P-Smc3(E570C)-TEV3-Scc1(A547C)-PK9::KanMX AmpR	Amplification of: 1/2AmpR–Scc1P–Smc3–Scc1; and PK9–1/2AmpR for construction of double fusion protein	Nasmyth lab
7674	Yiplac211 Scc1P-Smc3(E570C)-TEV3-Scc1(A547C)-TEV3-Smc1-PK9::KanMX; URA3 AmpR	Cohesin double fusion plasmid for transformation into yeast	Nasmyth lab

Table 2. Plasmids used in this study

Antibodies

Antibody	Origin	Source	Use
α-tubulin	Rat	BioRad	Immunofluorescence
α-myc	Rabbit	Santa Cruz Biotechnology	Immunofluorescence
α-myc	Mouse	Santa Cruz Biotechnology	Immunofluorescence
α-myc-HRP	Mouse	EMC Millipore Corp	Western Blot
α-rat-AF594	Donkey	Life Technologies	Immunofluorescence
α-rabbit-AF488	Donkey	Invitrogen	Immunofluorescence

Table 3. Antibodies used in this study.

4.2 **Cell culture and growth conditions**

S. cerevisiae **culture**

Unless stated otherwise, *S. cerevisiae* were cultured in Yeast extract + Peptone (YEP) and 2% Glucose/Dextrose by volume at 25°C. Liquid cultures were agitated at 200rpm. The optical density was measured on a standard spectrophotometer at 600nm wavelength (OD_{600}) with a correction factor of 0.54. For cell cycle arrest or culture synchronization, OD_{600} 0.15-0.3 was used. For transformation with linearized plasmids and extraction of genomic DNA, OD_{600} 0.5-0.8 was used. G1 arrest was achieved by adding α-factor to liquid culture at OD_{600} 0.15-0.3 at 1mg/L every 30 minutes, for 210 minutes or as otherwise specified. Release from G1 or other cell cycle arrest was achieved by filtration through Millipore filter paper and washing with YEP (no sugar source). Washed filter paper with cells was placed in YEP+glucose (unless stated otherwise) and cells were resuspended.

For expression of galactose inducible genes, cells were first cultured to OD_{600} 0.15-0.3 in YEP with 2% raffinose. Galactose was added to form 2% by volume of the final culture. Galactose-induced expression was terminated by addition of 2% glucose by volume to the culture. Galactose induction-dependent phenotypes were screened by growing on YEP agarose plates supplemented with raffinose and galactose.

E.coli **culture**

E.coli was used to amplify plasmids for use in the development of constructs for expression in *S. cerevisiae.* The *E. coli* strains XL1-Blue and TOP10 were cultured in 2x TY (tryptone-yeast extract) with antibiotics where appropriate at 37°C with 200rpm

agitation. For liquid cultures and suspensions of both *E. coli* and *S. cerevisiae*, plating onto agarose was achieved using borosilicate beads; 150uL of culture was placed on the plate along with 6-10 beads, and the plate was agitated horizontally until liquid was spread evenly. Beads were discarded afterwards.

Yeast growth assay: Serial dilution spot test

Aliquots of cells from *S. cerevisiae* strains of interest were suspended in water and diluted until an OD_{600} = 1 was achieved. This suspension was then serially diluted 10-fold six times. 3uL of each dilution was plated in a vertical line on an agarose plate with the appropriate carbon source, marker or drug. The plates were left to grow at 25°C (unless otherwise stated) for 48 hours and imaged on a bioRad GelDoc XR in the absence of a UV filter.

4.3 *S. cerevisiae* strain building and genetics

Crossing of two strains:

Haploid strains of opposite mating types (a or α-**)** with known genotypes were mixed in a patch on a YEPD plate and left to grow for ~24 hours. Diploids were selected by sequential plating of the crossed patch onto medium containing resistance markers carried by each strain; where possible, this selection occurred on rich medium supplemented with antibiotics (e.g. kanamycin, hygromycin), rather than nucleotide or amino acid-depleted medium. The cross was then patched onto a sporulation plate, which is nitrogen and carbon-depleted and induces meiosis, and left for 2-4 days at 25°C

Tetrad dissection:

A wide-ended toothpick was used to collect a small amount of cells from the sporulation plate. These cells were resuspended in a spheroplasting solution comprising 1M sorbitol and 1mg/ml zymolyase; spheroplasting digests the ascus surrounding a tetrad of spores and allows for their separation. Spores were incubated for 30 minutes at 30°C**.** The tube was then mixed very gently by inversion and 10uL suspension was pipetted onto a YEPD plate using a large pipette tip and allowed to drip down in a straight line. The plate was then loaded onto the MSM 300 Singer Instruments light microscope and spores from 18 tetrads were plated individually onto a grid using the needle attachment. Spores were allowed to grow for ~48-72 hours at 25°C.

Replica plating:

Tetrad dissection grid plates were pressed firmly onto sterile velvet sheets such that each clone from the plate was transferred onto the velvet. The appropriate selection plates were then stamped onto the velvet containing the transferred cells, and left to grow at 25°C (unless otherwise stated) for 24 hours. The mating type of haploid strains was determined by replica plating the dissection plate onto a minimal agarose plate containing a lawn of either K216 (mating type a) or K217 (mating type α) and left to grow at 25°C for 48 hours. All parent strain alleles used (apart from temperature-sensitive ones) carried linked resistance markers. Strains were scored for their survival on the various replica plates and their genotypes were characterized as such. Mating type was determined by growth or lack thereof on the aforementioned K216/K217 plates.

4.4 **Biochemical techniques:**

Yeast lysis and cell extract preparation

50ml cells growing in YPD were harvested at OD600 0.5-0.8 (exponential growth phase) by centrifugation at 3500 rpm for 3 minutes. The pellet was washed in 50ml 1X PBS, and resuspended in 200uL EbX lysis buffer (150mM NaCL, 50mM Tris-HCl pH 7.5, 0.5% w/v NP-40, 5mM EDTA, 1.25mM DTT, 1mM PMSF, 1 complete protease inhibitor cocktail tablet (Roche) per 50 ml prepared buffer) in a 2ml screw-top plastic tube. Acid-washed glass beads were added to the tube to 1ml volume. Cells were lysed at 4°C using a FastPrep-24 benchtop homogenizer at 6.5m/s, in 3x 60 second increments with 5 minutes on an ice block in between each interval. Cell lysate was drained from 2ml tube into a 4ml glass FACS tube by piercing a small hole in the bottom and loosening the lid. Lysate was collected in the glass tube by centrifugation at 3500rpm for 3 minutes. The lysate was then transferred to a microfuge tube and centrifuged at 16,600g for 15 minutes at 4°C, and the pellet was discarded.

Protein concentration measurement from yeast crude cell extracts

The Bradford protein assay was used to estimate the protein concentration in yeast whole cell extracts (WCE). 2uL WCE was added to 1ml Bradford reagent (diluted 1:4 from dye concentrate, Bio-Rad). Absorbance was measured at 595nm relative to Bradford reagent with 2uL EbX lysis buffer. Concentrations were calculated based on a standard curve obtained from serially diluted BSA.

Protein gel electrophoresis and western blotting

WCE was mixed with 2X Laemmli buffer to achieve the desired final concentration of protein (typically 40mg/ml). Samples were then loaded onto a 3-8% Tris-acetate gel (pre-made, NuPAGE Life Technologies) and run alongside a molecular weight ladder at 150V until the ladder had traversed ~75% of the length of the gel. The proteins were then transferred from the gel onto a nitrocellulose membrane. Transfer was carried out with prepared Trans-blot Turbo packs (incl. buffer) and transfer system. The membrane was blocked in PBST 3% skimmed milk powder (w/v) for 1 hour. Primary antibody was diluted in PBST (PBS + Tween/polysorbate 20) + 3% milk and membrane was incubated in primary antibody overnight at 4°C with gentle shaking. The membrane was then washed in PBST 3x for 10 minutes with gentle shaking. The secondary antibody was diluted in PBST + 3% milk and membrane was incubated in secondary antibody for 1-2 hours at RT with gentle shaking. The membrane was washed 3x as previously stated, and incubated with Immobilon Western Chemiluminescent HRP substrate (Millipore, luminol + hydrogen peroxide) for <20 seconds. Excess substrate was removed and the membrane was imaged using the ODYSSEY Fc imaging system (LI-COR).

4.5 **Molecular biology techniques**

Extraction of genomic material from yeast:

7.5-10 ODs of yeast cells were harvested from liquid or solid culture and resuspended in 200uL SCE buffer (1M sorbitol, 100nM sodium citrate, 60mM EDTA, 1mg/ml zymolyase, 0.1M β-mercaptoethanol) in an 1.5ml microfuge tube and incubated on a thermomixer at 37°C with 850rpm shaking. 200uL lysis buffer was added (2%SDS,

100mM Tris (pH 8.8), 5mM EDTA) and cells were incubated at 65°C for 5 minutes with shaking. SDS and other debris was precipitated by addition of 200uL 5M potassium acetate and incubation on ice, followed by centrifugation at 16,000g for 10 minutes. Genomic material was precipitated by addition of 1ml 20°C 70% isopropanol and 200uL 5M NH4OAc to 450uL supernatant in a new 2ml microfuge tube. DNA was pelleted by centrifugation at 2,300g for 30-60sec and pellet dissolved in 90uL 1X TE (Tris-EDTA) buffer for 30 minutes at 37°C. Pellet reprecipitated with 200uL 70% isopropanol (°C) and 10uL 5M NH4OAc. Pellet centrifuged as above, washed once in 1ml 70% ethanol, and resuspended in 50uL 1XTE + 2mg/ml RNAse.

Yeast transformation

The vector encoding the construct for transformation into yeast was incubated with the appropriate restriction endonuclease for 2 hours at 37°C. A cut was made within the selection marker (e.g. URA3) locus of the plasmid for ectopic expression within the transformant cells; the selection marker within the vector is in between homology arms that flank the desired insertion site in the transformed strain, and proper integration thus allows for selection of successfully transformed strains on the appropriate depleted growth medium. Unless stated otherwise, transformed DNA was integrated into the URA3 locus of an otherwise WT strain (K700).

The cells to be transformed were harvested from culture in YEP + 2% glucose at OD600=0.5-0.8 by centrifugation at 3500rpm for 3 minutes in 50ml falcon tubes. The pellet was washed twice in 50ml 0.1M LiOAc and resuspended in ~200uL remaining liquid. 50uL aliquots were transferred into 1.5ml microfuge tubes and incubated at

30°C for 15 minutes. In the meantime, ssDNA (salmon sperm DNA) was heated at 95°C for 5-10 minutes and cooled on ice. To each 50uL aliquot was added: 240uL PEG, 36uL 1M LiOAc, 25uL ssDNA, 30-40ng DNA (diluted to 50uL in 1xTE) **or** 50uL TE. Cells were incubated at 30°C for 60 minutes, and then heat shocked at 42°C for 15 minutes. Cells were harvested at 6000rpm for 5 minutes and resuspended in 1ml YEP + 2% glucose by gently vortexing. Cells were then incubated on a ThermoMixer for 90 minutes at 30°C with 800rpm shaking, and harvested by 5 min centrifugation at 2000rpm. The pellet was washed in 1ml ddH2O, and resuspended in 600uL ddH2O. 150uL of cell suspension was plated onto YEP agarose plates possessing the appropriate selection marker using glass beads, and cells were left to grow for 48-72 hours. Individual colonies were streaked onto new plates for isolation of individual colonies.

Transformation with and extraction of plasmid DNA from *Escherichia coli*.

100uL XL1-Blue or TOP10 competent cells were incubated on ice with <50ng DNA for 20 minutes. Cells were heat shocked at 42°C for 1 minute and incubated on ice for 2 minutes, after which 800uL 2xTY was added and cells were incubated with 900rpm shaking at 37°C for 1 hour. Cells were then plated onto 2xTY agarose plates possessing the appropriate resistance marker (typically ampicillin or gentamicin) and grown at 37°C for 48 hours. Individual colonies were resuspended in 4ml2xTY + 100ug/ml antibiotic in round-bottomed 15ml plastic tubes, and cultured at 37C with 200rpm shaking for 16-24 hours.

Cells were harvested by centrifugation at 3,500 rpm for 4 minutes. The pellet was resuspended in 250uL resuspension buffer P1 (50mM Tris-Cl, 10mM EDTA, 100ug/mL RNase A, Lyseblue) in a clean 1.5ml microfuge tube. 250uL lysis buffer P2 (200nM NaCl, 1% SDS) was added and tube was inverted 5-10 times until uniformly blue in color. 350uL neutralization buffer N3 (3M KOAc) was added and tubes were inverted 5-10 times until all traces of blue had disappeared, and a white precipitate was visible. SDS and other debris were pelleted by centrifugation at 16,600g for 10 minutes. 800uL supernatant was applied to a QIAprep 2.0 spin column (placed within a 2ml collection tube). Tubes were spun at 16,600g for 30-60seconds and flow-through was discarded. For endA+ strains such as TOP10, 0.5ml buffer PB was applied to the column, and flowthrough was collected and discarded as above. For all strains, 750uL buffer PE (wash buffer) was applied to the column and spun as above. After flowthrough was discarded, the column was spun for an additional 1min and all flowthrough was discarded. The column was placed into a 1.5ml microfuge tube, and 50uL buffer EB (10mM Tris-HCl) at 50°C was applied. Columns were incubated for 2-3 minutes at RT and then spun as above for collection into the microfuge tubes. dsDNA concentration was measured (normalized to EB) using a NanoDrop spectrophotometer.

PCR amplification of plasmid and genomic DNA

25/50 µL PCR reactions set up with

- <1000ng template DNA for genomic samples
- <200ng template DNA for plasmid samples
- 100/200µM each dNTP (800µM total)

- 0.25/0.5µM forward primer
- 0.25/0.5µM reverse primer
- 1x Q5 reaction buffer (5/10µL per reaction, stock is 5x)
- Q5 polymerase 0.02 units/L. (20 units/µL)

PCR cycle:

- Denaturation 98°C 2 min
    - 98°C 30s
    - 50°C 30s
    - Extension: 72°C 30 seconds per kb up to 6kb; 40 seconds per kb >6kb
    - Repeat indented steps 30-35x
- Final extension 72°C 5 minutes
- 10°C pause ∞

DNA Agarose gel electrophoresis

TAE (Tris-acetate-EDTA) buffer and 1% agarose (w/v) were heated until boiling and cooled slightly in an ice bath. Ethidium bromide was added to a concentration of 0.5µg/ml and the agarose was then poured into a mold fit with gel combs and left to set for 20 minutes. The combs were removed and the gel was placed into a tank and covered with TAE buffer. Tubes containing PCR samples were spun in a mini-centrifuge and DNA loading dye (typically 6X) was added to samples such that 1X concentration was achieved. Samples were mixed well. 30µL sample was loaded into each well alongside 10µL 1kb DNA ladder (10-0.5kb range). The gel was run at 120V for 1h20 minutes or until the ladder migrated ~75% of the gel's length. Gels were imaged on a bioRAD GelDocXR imager fitted with a UV filter. The gel was

transilluminated with UV. Bands of interest were excised with a scalpel, and incubated in 2ml microfuge tubes with 1ml buffer QG (Solubilization buffer). The dissolved agarose-Buffer QG solution was applied to Zymoclean™ DNA Recovery columns in 750µL aliquots and spun at 16,600g for 30-60seconds. Flow through was discarded and centrifugation was repeated until all of the dissolved agarose solution had been passed through the column. Columns were washed with 750 µL wash buffer PE and spun at 16,600g for 30-60seconds, and flow through was discarded. The empty columns were spun again as above to discard residual flowthrough. Each column was placed into a clean 1.5ml microfuge tube and 20 µL warm (50°C) ddH2O was applied to the centre of each column and left for 2-3 minutes. Columns were then spun at 16,600g for 1 minute. DNA concentration was quantified on a nanodrop.

Gibson assembly of plasmids for expression in *S. cerevisiae*

50bp forward and reverse oligonucleotide primers were designed with 25bp complementary sequence to the template and a 25bp overlap with the sequence with the desired sequence to which it will be fused. DNA fragments for Gibson Assembly were generated by PCR amplification with Q5 polymerase. 50ng of vector and 100ng insert fragments were added to equal parts by volume NEBuilder HiFi DNA Assembly Master Mix and incubated at 50°C for 30 minutes

4.5 **Yeast immunofluorescence**

Preparing cells and slides for immunofluorescence

Cells were fixed by 120 minute incubation in 10% (v/v) formaldehyde with rolling. Cells were pelleted by centrifugation at 3,500 rpm for 3 minues and washed once in 10ml 1XPBS and once in Phos/Sorb (1X PBS/1M sorbitol) before resuspension in 1ml Phos/Sorb. 100 µL cells were added to 385 µL Phos/Sorb + 10 µL zymolyase + 5 µL β-mercaptoethanol and incubated for 20-30 minutes at RT. In the meantime, 15 µL poly-lysine was applied to each well in a 15 well slide and incubated for 15 minutes at RT before being aspirated, washing 2x with ddH2O and leaving to air dry. Spheroplasted cells were harvested by spinning for 3 minutes at 0.8g, and washed 2x with 1ml Phos/Sorb before being resuspended in 200 µL Phos/Sorb. 20 µL cells were applied to each well and left to settle for 20-30 minutes. Cells were then aspirated and the slides were plunged into methanol at -20°C for 6 minutes, followed by -20°C acetone for 30 seconds. Slides were left to air dry for 2-3 minutes after removal from acetone. 20 µL 1X PBS/1% BSA were applied to each well and the slide was kept in a humid chamber to block for 1 hour at RT. PBS/BSA was removed by aspiration prior to application of primary antibodies.

Immunofluorescence and imaging

Primary antibodies were diluted in PBS/BSA and applied to each well in 15 µL aliquots. The slide was left in a humid chamber at 4°C overnight. Wells were washed 5x with 20 µL PBS/BSA. Secondary antibodies were diluted in PBS/BSA and applied to wells in 15µL aliquots. Slides were incubated in the dark at RT for 3-4 hours, after which wells were washed 5x with PBS/BSA as above. 10 µL DAPI at 1mg/ml

concentration was applied to each well and incubated for 5 minutes at room temperature. The wells were then washed a further 2x in PBS/BSA before leaving the slide to air dry for 1-2 minutes. The slide was mounted in vectashield and a large coverslip was used to cover all 15 wells. The edges of the coverslip were made watertight by sealing with transparent varnish. Slides were stored at 4°C when not being used for fluorescence microscopy. Cells stained with fluorescent antibody markers were imaged using a Zeiss Axio Observer.Z1 microscope using a 40x oil immersion objective and a numerical aperture of 1.40. Samples were illuminated at the corresponding wavelengths to DAPI and the fluorophore-conjugated secondary antibodies used. Images were taken using the coolSNAP HQ camera.

Image analysis

Images were saved as RGB stacks in jpeg format. Merge stacks were generated in ImageJ in order to exclude securin positive anaphase and G1 cells. Blue (DAPI only) images of the resulting securin negative anaphase cells were then analyzed manually in ImageJ. Mono and binucleate cells were quantified as total numbers per independent repeat (Figures 9, 14 and 15) or per well in a 15-well plate (Figures 17 and 18). The percentage of mononucleate cells was calculated per repeat and the standard deviation was calculated, and a one way ANOVA performed for each experimental condition. For analysis of securin positivity across the cell cycle (Figures 10 and 14), independent time-course experiments were carried out at the conditions described in figure 14C and cells were stained only with securin antibodies. Images using only the 488nm (green) channel were obtained and analyzed manually in ImageJ.

Bibliography

Arumugam, P., Gruber, S., Tanaka, K., Haering, C.H., Mechtler, K. and Nasmyth, K. (2003) 'ATP Hydrolysis Is Required for Cohesin's Association with Chromosomes', *Current Biology*, 13(22), 1941-1953, available: http://dx.doi.org/10.1016/j.cub.2003.10.036.

Atkins, A., Xu, M.J., Li, M., Rogers, N.P., Pryzhkova, M.V. and Jordan, P.W. (2020) 'SMC5/6 is required for replication fork stability and faithful chromosome segregation during neurogenesis', *eLife*, 9, available: http://dx.doi.org/10.7554/elife.61171.

Banaszynski, L.A., Liu, C.W. and Wandless, T.J. (2005) 'Characterization of the FKBP·Rapamycin·FRB Ternary Complex', *Journal of the American Chemical Society*, 127(13), 4715-4721, available: http://dx.doi.org/10.1021/ja043277y.

Bauer, B.W., Davidson, I.F., Canena, D., Wutz, G., et al. (2021) Cohesin mediates DNA loop extrusion by a “swing and clamp” mechanism. *Cell*. 184 (21), 5448–5464.e22. Available from: doi:10.1016/j.cell.2021.09.016.

Beckouët, F., Hu, B., Roig, M.B., Sutani, T., Komata, M., Uluocak, P., Katis, V.L., Shirahige, K. and Nasmyth, K. (2010) 'An Smc3 Acetylation Cycle Is Essential for Establishment of Sister Chromatid Cohesion', *Molecular Cell*, 39(5), 689-699, available: http://dx.doi.org/10.1016/j.molcel.2010.08.008.

Beckouët, F., Srinivasan, M., Roig, B., Maurici, Chan, K.-L., Scheinost, C., Johanna, Batty, P., Hu, B., Petela, N., Gligoris, T., Smith, C., Alexandra, Strmecki, L., Rowland, D., Benjamin and Nasmyth, K. (2016) 'Releasing Activity Disengages Cohesin’s Smc3/Scc1 Interface in a Process Blocked by Acetylation', *Molecular Cell*, 61(4), 563-574, available: http://dx.doi.org/10.1016/j.molcel.2016.01.026.

Birkenbihl, R.P. and Subramani, S. (1992) 'Cloning and characterization of rad21an essential gene of Schizosaccharomyces pombe involved in DNA double-strand-break repair', *Nucleic Acids Research*, 20(24), 6605-6611, available: http://dx.doi.org/10.1093/nar/20.24.6605.

Borges, V., Smith, D.J., Whitehouse, I. and Uhlmann, F. (2013) 'An Eco1-independent sister chromatid cohesion establishment pathway in S. cerevisiae', *Chromosoma*, 122(1-2), 121-134, available: http://dx.doi.org/10.1007/s00412-013-0396-y.

Bouck, G.B. and Cronshaw, J. (1965) 'The Fine Structure of Differentiating Sieve Tube Elements', *Journal of Cell Biology*, 25(1), 79-95, available: http://dx.doi.org/10.1083/jcb.25.1.79.

Çamdere, G., Guacci, V., Stricklin, J. and Koshland, D. (2015) 'The ATPases of cohesin interface with regulators to modulate cohesin-mediated DNA tethering', *eLife*, 4, available: http://dx.doi.org/10.7554/elife.11315.

Cameron, G., Gruszka, D., Xie, S., Nasmyth, K.A., Srinivasan, M. and Yardimci, H. (2022) 'Sister chromatid cohesion establishment during DNA replication termination'. *Internal Cold Spring Harbor Laboratory Report*, unpublished. Available: https://doi.org/10.1101/2022.09.15.508094

Chan, K.-L., Gligoris, T., Upcher, W., Kato, Y., Shirahige, K., Nasmyth, K. and Beckouët, F. (2013) 'Pds5 promotes and protects cohesin acetylation', *Proceedings of the National Academy of Sciences*, 110(32), 13020-13025, available: http://dx.doi.org/10.1073/pnas.1306900110.

Chan, K.-L., Roig, B., Maurici, Hu, B., Beckouët, F., Metson, J. and Nasmyth, K. (2012) 'Cohesin's DNA Exit Gate Is Distinct from Its Entrance Gate and Is Regulated byAcetylation', *Cell*, 150(5), 961-974, available: http://dx.doi.org/10.1016/j.cell.2012.07.028.

Ciosk, R., Shirayama, M., Shevchenko, A., Tanaka, T., Toth, A., Shevchenko, A. and Nasmyth, K. (2000) 'Cohesin's Binding to Chromosomes Depends on a Separate Complex Consisting of Scc2 and Scc4 Proteins', *Molecular Cell*, 5(2), 243-254, available: http://dx.doi.org/10.1016/s1097-2765(00)80420-7.

Collier, J.E. and Nasmyth, K.A. (2022) 'DNA passes through cohesin's hinge as well as its Smc3–kleisin interface', *eLife*, 11, available: http://dx.doi.org/10.7554/elife.80310.

Deardorff, A., Matthew, Wilde, J., Jonathan, Albrecht, M., Dickinson, E., Tennstedt, S., Braunholz, D., Mönnich, M., Yan, Y., Xu, W., Gil-Rodríguez, C., María, Clark, D., Hakonarson, H., Halbach, S., Michelis, D., Laura, Rampuria, A., Rossier, E., Spranger, S., Maldergem, V., Lionel, Lynch, A., Sally, Gillessen-Kaesbach, G., Lüdecke, H.-J., Ramsay, G., Robert, Mckay, J., Michael, Krantz, D., Ian, Xu, H., Horsfield, A., Julia and Kaiser, J., Frank (2012) 'RAD21 Mutations Cause a Human Cohesinopathy', *The American Journal of Human Genetics*, 90(6), 1014-1027, available: http://dx.doi.org/10.1016/j.ajhg.2012.04.019.

Delobel, P. and Tesnière, C. (2014) 'A Simple FCM Method to Avoid Misinterpretation in Saccharomyces cerevisiae Cell Cycle Assessment between G0 and Sub-

G1', *PLoS ONE*, 9(1), e84645, available: http://dx.doi.org/10.1371/journal.pone.0084645.

Dixon, J.R., Selvaraj, S., Yue, F., Kim, A., Li, Y., Shen, Y., Hu, M., Liu, J.S. and Ren, B. (2012) 'Topological domains in mammalian genomes identified by analysis of chromatin interactions', *Nature*, 485(7398), 376-380, available: http://dx.doi.org/10.1038/nature11082.

Dorsett, D. and Krantz, I.D. (2009) 'On the Molecular Etiology of Cornelia de Lange Syndrome', *Annals of the New York Academy of Sciences*, 1151(1), 22-37, available: http://dx.doi.org/10.1111/j.1749-6632.2008.03450.x.

Farcas, A.-M., Uluocak, P., Helmhart, W. and Nasmyth, K. (2011) 'Cohesin's Concatenation of Sister DNAs Maintains Their Intertwining', *Molecular Cell*, 44(1), 97-907, available: http://dx.doi.org/https://doi.org/10.1016/j.molcel.2011.07.034

Fierer, J.O., Veggiani, G. and Howarth, M. (2014) 'SpyLigase peptide–peptide ligation polymerizes affibodies to enhance magnetic cancer cell capture', *Proceedings of the National Academy of Sciences*, 111(13), E1176-E1181, available: http://dx.doi.org/10.1073/pnas.1315776111.

Furuya, K., Takayashi, K. and Yanagida, M. (1998) 'Faithful anaphase is insured by Mis4, a sister chromatid cohesion molecule required in S phase and not destroyed in G1 phase', *Genes & Development*, 12(21), 3408-3418, available: http://dx.doi.org/10.1101/gad.12.21.3408.

Gandhi, R., Gillespie, P.J. and Hirano, T. (2006) 'Human Wapl Is a Cohesin-Binding Protein that Promotes Sister-Chromatid Resolution in Mitotic Prophase', *Current Biology*, 16(24), 2406-2417, available: http://dx.doi.org/10.1016/j.cub.2006.10.061.

Gerlich, D., Hirota, T., Koch, B., Peters, J.-M. and Ellenberg, J. (2006) 'Condensin I Stabilizes Chromosomes Mechanically through a Dynamic Interaction in Live Cells', *Current Biology*, 16(4), 333-344, available: http://dx.doi.org/10.1016/j.cub.2005.12.040.

Gruber, S., Arumugam, P., Katou, Y., Kuglitsch, D., Helmhart, W., Shirahige, K. and Nasmyth, K. (2006) 'Evidence that Loading of Cohesin Onto Chromosomes Involves Opening of Its SMC Hinge', *Cell*, 127(3), 523-537, available: http://dx.doi.org/10.1016/j.cell.2006.08.048.

Gruber, S., Haering, C.H. and Nasmyth, K. (2003) 'Chromosomal Cohesin Forms a Ring', *Cell*, 112(6), 765-777, available: http://dx.doi.org/10.1016/s0092-8674(03)00162-4.

Guacci, V., Koshland, D. and Strunnikov, A. (1997) 'A Direct Link between Sister Chromatid Cohesion and Chromosome Condensation Revealed through the Analysis of MCD1 in S. cerevisiae', *Cell*, 91(1), 47-57, available: http://dx.doi.org/10.1016/s0092-8674(01)80008-8.

Haarhuis, H.I., Judith, Elbatsh, M.O., Ahmed and Rowland, D., Benjamin (2014) 'Cohesin and Its Regulation: On the Logic of X-Shaped Chromosomes', *Developmental Cell*, 31(1), 7-18, available: http://dx.doi.org/10.1016/j.devcel.2014.09.010.

Haering, C.H., Farcas, A.-M., Arumugam, P., Metson, J. and Nasmyth, K. (2008) 'The cohesin ring concatenates sister DNA molecules', *Nature*, 454(7202), 297-301, available: http://dx.doi.org/10.1038/nature07098.

Haering, C.H., Löwe, J., Hochwagen, A. and Nasmyth, K. (2002) 'Molecular Architecture of SMC Proteins and the Yeast Cohesin Complex', *Molecular Cell*, 9(4), 773-788, available: http://dx.doi.org/10.1016/s1097-2765(02)00515-4.

Haering, C.H., Schoffnegger, D., Nishino, T., Helmhart, W., Nasmyth, K. and Löwe, J. (2004) 'Structure and Stability of Cohesin's Smc1-Kleisin Interaction', *Molecular Cell*, 15(6), 951-964, available: http://dx.doi.org/10.1016/j.molcel.2004.08.030.

Harvey, S.H., Krien, M.J. and O'Connell, M.J. (2002) 'Structural maintenance of chromosomes (SMC) proteins, a family of conserved ATPases', *Genome Biology*, 3(2), reviews3003.1, available: http://dx.doi.org/10.1186/gb-2002-3-2-reviews3003.

Hatlem, D., Trunk, T., Linke, D. and Leo, J.C. (2019) 'Catching a SPY: Using the SpyCatcher-SpyTag and Related Systems for Labeling and Localizing Bacterial Proteins', *International Journal of Molecular Sciences*, 20(9), 2129, available: http://dx.doi.org/10.3390/ijms20092129.

Hill, V.K., Kim, J.-S. and Waldman, T. (2016) 'Cohesin mutations in human cancer', *Biochimica et Biophysica Acta (BBA) - Reviews on Cancer*, 1866(1), 1-11, available: http://dx.doi.org/10.1016/j.bbcan.2016.05.002.

Hirano, M. (2002) 'Hinge-mediated dimerization of SMC protein is essential for its dynamic interaction with DNA', *The EMBO Journal*, 21(21), 5733-5744, available: http://dx.doi.org/10.1093/emboj/cdf575.

Hirano, T. (2012) 'Condensins: universal organizers of chromosomes with diverse functions', *Genes & Development*, 26(15), 1659-1678, available: http://dx.doi.org/10.1101/gad.194746.112.

Hornig, N.C., Knowles, P.P., McDonald, N.Q. and Uhlmann, F. (2002) 'The Dual Mechanism of Separase Regulation by Securin', *Current Biology*, 12(12), 973-982, available: http://dx.doi.org/https://doi.org/10.1016/S0960-9822(02)00847-3.

Hu, B., Itoh, T., Mishra, A., Katoh, Y., Chan, K.-L., Upcher, W., Godlee, C., Roig, M.B., Shirahige, K. and Nasmyth, K. (2011) 'ATP Hydrolysis Is Required for Relocating Cohesin from Sites Occupied by Its Scc2/4 Loading Complex', *Current Biology*, 21(1), 12-24, available: http://dx.doi.org/10.1016/j.cub.2010.12.004.

Ivanov, D., Schleiffer, A., Eisenhaber, F., Mechtler, K., Haering, C.H. and Nasmyth, K. (2002) 'Eco1 Is a Novel Acetyltransferase that Can Acetylate Proteins Involved in Cohesion', *Current Biology*, 12(4), 323-328, available: http://dx.doi.org/10.1016/s0960-9822(02)00681-4.

Ivanov, D. and Nasmyth, K. (2005) 'A Topological Interaction between Cohesin Rings and a Circular Minichromosome' *Cell*, 122(6), 849-860, available: http://dx.doi.org/10.1016/j.cell.2005.07.018

Jin, H., Guacci, V. and Yu, H.-G. (2009) 'Pds5 is required for homologue pairing and inhibits synapsis of sister chromatids during yeast meiosis', *Journal of Cell Biology*, 186(5), 713-725, available: http://dx.doi.org/10.1083/jcb.200810107.

Kawauchi, S., Calof, A.L., Santos, R., Lopez-Burks, M.E., Young, C.M., Hoang, M.P., Chua, A., Lao, T., Lechner, M.S., Daniel, J.A., Nussenzweig, A., Kitzes, L., Yokomori, K., Hallgrimsson, B. and Lander, A.D. (2009) 'Multiple Organ System Defects and Transcriptional Dysregulation in the Nipbl+/– Mouse, a Model of Cornelia de Lange Syndrome', *PLoS Genetics*, 5(9), e1000650, available: http://dx.doi.org/10.1371/journal.pgen.1000650.

Keogh, R., Seouighe, C. and Wolfe, K. (1998) 'Evolution of gene order and chromosome number in Saccharomyces, Kluyveromyces and related fungi', *Yeast*, 14(5), 443-457, available: http://dx.doi.org/10.1002/(SICI)1097-0061(19980330)14:5<443::AID-YEA243>3.0.CO;2-L.

Kim, J.E. and Chen, J. (2000) 'Cytoplasmic–nuclear shuttling of FKBP12-rapamycin-associated protein is involved in rapamycin-sensitive signaling and translation initiation', *Proceedings of the National Academy of Sciences*, 97(26), 14340-14345, available: http://dx.doi.org/10.1073/pnas.011511898.

Kogut, I., Wang, J., Guacci, V., Mistry, R.K. and Megee, P.C. (2009) 'The Scc2/Scc4 cohesin loader determines the distribution of cohesin on budding yeast chromosomes', *Genes & Development*, 23(19), 2345-2357, available: http://dx.doi.org/10.1101/gad.1819409.

Krantz, I.D., Mccallum, J., Descipio, C., Kaur, M., Gillis, L.A., Yaeger, D., Jukofsky, L., Wasserman, N., Bottani, A., Morris, C.A., Nowaczyk, M.J.M., Toriello, H., Bamshad, M.J., Carey, J.C., Rappaport, E., Kawauchi, S., Lander, A.D., Calof, A.L., Li, H.-H., Devoto, M. and Jackson, L.G. (2004) 'Cornelia de Lange syndrome is caused by mutations in NIPBL, the human homolog of Drosophila melanogaster Nipped-B', *Nature Genetics*, 36(6), 631-635, available: http://dx.doi.org/10.1038/ng1364.

Kurze, A., Michie, K.A., Dixon, S.E., Mishra, A., Itoh, T., Khalid, S., Strmecki, L., Shirahige, K., Haering, C.H., Löwe, J. and Nasmyth, K. (2011) 'A positively charged channel within the Smc1/Smc3 hinge required for sister chromatid cohesion', *The EMBO Journal*, 30(2), 364-378, available: http://dx.doi.org/10.1038/emboj.2010.315.

Lopez-Serra, L., Kelly, G., Patel, H., Stewart, A. and Uhlmann, F. (2014) 'The Scc2–Scc4 complex acts in sister chromatid cohesion and transcriptional regulation by maintaining nucleosome-free regions', *Nature Genetics*, 46(10), 1147-1151, available: http://dx.doi.org/10.1038/ng.3080.

Makrantoni, V. and Marston, A.L. (2018) 'Cohesin and chromosome segregation', *Current Biology*, 28(12), R688-R693, available: http://dx.doi.org/10.1016/j.cub.2018.05.019.

Margolin, W. and Bernander, R. (2004) 'How Do Prokaryotic Cells Cycle?', *Current Biology*, 14(18), R768-R770, available: http://dx.doi.org/10.1016/j.cub.2004.09.017.

Mayrose I, Lysak MA. (2021) 'The Evolution of Chromosome Numbers: Mechanistic Models and Experimental Approaches', *Genome Biol Evol*. 13(2). Available: http://dx.doi.org/10.1093/gbe/evaa220.

Mcvey, S.L., Cosby, J.K. and Nannas, N.J. (2021) 'Aurora B Tension Sensing Mechanisms in the Kinetochore Ensure Accurate Chromosome Segregation', *International Journal of Molecular Sciences*, 22(16), 8818, available: http://dx.doi.org/10.3390/ijms22168818.

Michaelis, C., Ciosk, R. and Nasmyth, K. (1997) 'Cohesins: Chromosomal Proteins that Prevent Premature Separation of Sister Chromatids', *Cell*, 91(1), 35-45, available: http://dx.doi.org/10.1016/s0092-8674(01)80007-6.

Moldovan, G.-L., Pfander, B. and Jentsch, S. (2006) 'PCNA Controls Establishment of Sister Chromatid Cohesion during S Phase', *Molecular Cell*, 23(5), 723-732, available: http://dx.doi.org/10.1016/j.molcel.2006.07.007.

Murayama, Y. and Uhlmann, F. (2014) 'Biochemical reconstitution of topological DNA binding by the cohesin ring', *Nature*, 505(7483), 367-371, available: http://dx.doi.org/10.1038/nature12867.

Murayama, Y. and Uhlmann, F. (2015) 'DNA Entry into and Exit out of the Cohesin Ring by an Interlocking Gate Mechanism', *Cell*, 163(7), 1628-1640, available: http://dx.doi.org/10.1016/j.cell.2015.11.030.

Musacchio, A. and Salmon, E.D. (2007) 'The spindle-assembly checkpoint in space and time', *Nature Reviews Molecular Cell Biology*, 8(5), 379-393, available: http://dx.doi.org/10.1038/nrm2163.

Nasmyth, K. (1996) 'At the heart of the budding yeast cell cycle', *Trends in genetics*, 12(10), 405-412, available: http://dx.doi.org/doi:10.1016/0168-9525(96)10041-x.

Nichols, M.H. and Corces, V.G. (2018) 'A tethered-inchworm model of SMC DNA translocation', *Nature Structural & Molecular Biology*, 25(10), 906-910, available: http://dx.doi.org/10.1038/s41594-018-0135-4.

Nishiyama, T., Ladurner, R., Schmitz, J., Kreidl, E., Schleiffer, A., Bhaskara, V., Bando, M., Shirahige, K., Hyman, A.A., Mechtler, K. and Peters, J.-M. (2010) 'Sororin Mediates Sister Chromatid Cohesion by Antagonizing Wapl', *Cell*, 143(5), 737-749, available: http://dx.doi.org/10.1016/j.cell.2010.10.031.

Nora, E.P., Lajoie, B.R., Schulz, E.G., Giorgetti, L., Okamoto, I., Servant, N., Piolot, T., Van Berkum, N.L., Meisig, J., Sedat, J., Gribnau, J., Barillot, E., Blüthgen, N., Dekker, J. and Heard, E. (2012) 'Spatial partitioning of the regulatory landscape of the X-inactivation centre', *Nature*, 485(7398), 381-385, available: http://dx.doi.org/10.1038/nature11049.

Orr, B., Godek, K.M. and Compton, D. (2015) 'Aneuploidy', *Current Biology*, 25(13), R538-R542, available: http://dx.doi.org/10.1016/j.cub.2015.05.010.

Panizza, S., Tanaka, T., Hochwagen, A., Eisenhaber, F. and Nasmyth, K. (2000) 'Pds5 cooperates with cohesin in maintaining sister chromatid cohesion', *Current Biology*, 10(24), 1557-1564, available: http://dx.doi.org/10.1016/s0960-9822(00)00854-x.

Petela, N.J., Gligoris, T.G., Metson, J., Lee, B.-G., Voulgaris, M., Hu, B., Kikuchi, S., Chapard, C., Chen, W., Rajendra, E., Srinivisan, M., Yu, H., Löwe, J. and Nasmyth, K.A. (2018) 'Scc2 Is a Potent Activator of Cohesin's ATPase that Promotes Loading by Binding Scc1 without Pds5', *Molecular Cell*, 70(6), 1134-1148.e7, available: http://dx.doi.org/10.1016/j.molcel.2018.05.022.

Petela, N.J., Gonzalez Llamazares, A., Dixon, S., Hu, B., Lee, B.-G., Metson, J., Seo, H., Ferrer-Harding, A., Voulgaris, M., Gligoris, T., Collier, J., Oh, B.-H., Löwe, J. and Nasmyth, K.A. (2021) 'Folding of cohesin's coiled coil is important for Scc2/4-induced association with chromosomes', *eLife*, 10, available: http://dx.doi.org/10.7554/elife.67268.

Peters, J.-M. (2006) 'The anaphase promoting complex/cyclosome: a machine designed to destroy', *Nature Reviews Molecular Cell Biology*, 7(9), 644-656, available: http://dx.doi.org/10.1038/nrm1988.

Pradhan, B., Barth, R., Kim, E., Davidson, I.F., Bauer, B., Van Laar, T., Yang, W., Ryu, J.-K., Van Der Torre, J., Peters, J.-M. and Dekker, C. (2022a) 'SMC complexes can traverse physical roadblocks bigger than their ring size', *Cell Reports*, 41(3), 111491, available: http://dx.doi.org/10.1016/j.celrep.2022.111491.

Revenkova, E., Herrmann, K., Adelfalk, C. & Jessberger, R. (2010) 'Oocyte Cohesin Expression Restricted to Predictyate Stages Provides Full Fertility and Prevents Aneuploidy'. *Current Biology*. 20 (17), 1529–1533, available: doi:10.1016/j.cub.2010.08.024.

Rhodes, J.D.P., Haarhuis, J.H.I., Grimm, J.B., Rowland, B.D., Lavis, L.D. and Nasmyth, K.A. (2017) 'Cohesin Can Remain Associated with Chromosomes during DNA Replication', *Cell Reports*, 20(12), 2749-2755, available: http://dx.doi.org/10.1016/j.celrep.2017.08.092.

Roig, M.B., Löwe, J., Chan, K.-L., Beckouët, F., Metson, J. and Nasmyth, K. (2014a) 'Structure and function of cohesin's Scc3/SA regulatory subunit', *FEBS Letters*, 588(20), 3692-3702, available: http://dx.doi.org/10.1016/j.febslet.2014.08.015.

Roig, M.B., Löwe, J., Chan, K.-L., Beckouët, F., Metson, J. and Nasmyth, K. (2014b) 'Structure and function of cohesin's Scc3/SA regulatory subunit', *FEBS Letters*, 588(20), 3692-3702, available: http://dx.doi.org/10.1016/j.febslet.2014.08.015.

Rolef Ben-Shahar, T., Heeger, S., Lehane, C., East, P., Flynn, H., Skehel, M. and Uhlmann, F. (2008) 'Eco1-dependent cohesin acetylation during establishment of sister chromatid cohesion', *Science*, 321(5888), 563-566, available: http://dx.doi.org/doi: 10.1126/science.157774.

Rybenkov, V.V., Herrera, V., Petrushenko, Z.M. and Zhao, H. (2014) 'MukBEF, a Chromosomal Organizer', *Microbial Physiology*, 24(5-6), 371-383, available: http://dx.doi.org/10.1159/000369099.

Sakai, A. (2003) 'Condensin but not cohesin SMC heterodimer induces DNA reannealing through protein-protein assembly', *The EMBO Journal*, 22(11), 2764-2775, available: http://dx.doi.org/10.1093/emboj/cdg247.

Santaguida, S., Vasile, E., White, E. and Amon, A. (2015a) 'Aneuploidy-induced cellular stresses limit autophagic degradation', *Genes & Development*, 29(19), 2010-2021, available: http://dx.doi.org/10.1101/gad.269118.115.

Schoenfelder, S. and Fraser, P. (2019) 'Long-range enhancer–promoter contacts in gene expression control', *Nature Reviews Genetics*, 20(8), 437-455, available: http://dx.doi.org/10.1038/s41576-019-0128-0.

Shintomi, K. and Hirano, T. (2009) 'Releasing cohesin from chromosome arms in early mitosis: opposing actions of Wapl–Pds5 and Sgo1', *Genes & Development*, 23(18), 2224-2236, available: http://dx.doi.org/10.1101/gad.1844309.

Srinivasan, M., Fumasoni, M., Petela, N.J., Murray, A. and Nasmyth, K.A. (2020) 'Cohesion is established during DNA replication utilising chromosome associated cohesin rings as well as those loaded de novo onto nascent DNAs', *eLife*, 9, available: http://dx.doi.org/10.7554/elife.56611.

Srinivasan, M., Petela, N.J., Scheinost, J.C., Collier, J., Voulgaris, M., B Roig, M., Beckouët, F., Hu, B. and Nasmyth, K.A. (2019) 'Scc2 counteracts a Wapl-independent mechanism that releases cohesin from chromosomes during G1', *eLife*, 8, available: http://dx.doi.org/10.7554/elife.44736.

Srinivasan, M., Scheinost, J.C., Petela, N.J., Gligoris, T.G., Wissler, M., Ogushi, S., Collier, J.E., Voulgaris, M., Kurze, A., Chan, K.-L., Hu, B., Costanzo, V. and Nasmyth, K.A. (2018) 'The Cohesin Ring Uses Its Hinge to Organize DNA Using Non-topological as well as Topological Mechanisms', *Cell*, 173(6), 1508-1519.e18, available: http://dx.doi.org/10.1016/j.cell.2018.04.015.

Stigler, J., Çamdere, G., Koshland, D. and Greene, E. (2016) 'Single-Molecule Imaging Reveals a Collapsed Conformational State for DNA-Bound Cohesin', *Cell Reports*, 15(5), 988-998, available: http://dx.doi.org/https://doi.org/10.1016/j.celrep.2016.04.003.

Sun, X., Huang, L., Markowitz, T.E., Blitzblau, H.G., Chen, D., Klein, F. and Hochwagen, A. (2015) 'Transcription dynamically patterns the meiotic chromosome-axis interface', *eLife*, 4, available: http://dx.doi.org/10.7554/elife.07424.

Tedeschi, A., Wutz, G., Huet, S., Jaritz, M., Wuensche, A., Schirghuber, E., Davidson, I.F., Tang, W., Cisneros, D.A., Bhaskara, V., Nishiyama, T., Vaziri, A., Wutz, A.,

Ellenberg, J. and Peters, J.-M. (2013) 'Wapl is an essential regulator of chromatin structure and chromosome segregation', *Nature*, 501(7468), 564-568, available: http://dx.doi.org/10.1038/nature12471.

Uhlmann, F., Lottspeich, F. and Nasmyth, K. (1999) 'Sister-chromatid separation at anaphase onset is promoted by cleavage of the cohesin subunit Scc1', *Nature*, 400(6739), 37-42, available: http://dx.doi.org/10.1038/21831.

Uhlmann, F. and Nasmyth, K. (1998) 'Cohesion between sister chromatids must be established during DNA replication', *Current Biology*, 8(20), 1095-1102, available: http://dx.doi.org/10.1016/s0960-9822(98)70463-4.

Villa, F., Simon, C., Aline, Bazan, O., Angeles, Maria, Kilkenny, L., Mairi, Wirthensohn, D., Wightman, M., Matak-Vinkovíc, D., Pellegrini, L. and Labib, K. (2016) 'Ctf4 Is a Hub in the Eukaryotic Replisome that Links Multiple CIP-Box Proteins to the CMG Helicase', *Molecular Cell*, 63(3), 385-396, available: http://dx.doi.org/10.1016/j.molcel.2016.06.009.

Weitzer, S., Lehane, C. and Uhlmann, F. (2003) 'A Model for ATP Hydrolysis-Dependent Binding of Cohesin to DNA', *Current Biology*, 13(22), 1930-1940, available: http://dx.doi.org/10.1016/j.cub.2003.10.030.

Wells, J.N., Gligoris, T.G., Nasmyth, K.A. and Marsh, J.A. (2017) 'Evolution of condensin and cohesin complexes driven by replacement of Kite by Hawk proteins', *Current Biology*, 27(1), R17-R18, available: http://dx.doi.org/10.1016/j.cub.2016.11.050.

Xu, B., Lu, S. and Gerton, J.L. (2014) 'Roberts syndrome', *Rare Diseases*, 2(1), e27743, available: http://dx.doi.org/10.4161/rdis.27743.

Xu, H., Boone, C. and Brown, G. (2007) 'Genetic dissection of parralel sister-chromatid cohesion pathways', *Genetics*, 176(3), 1417-1429, available: http://dx.doi.org/10.1534/genetics.107.072876.

Xu, X., Kanai, R., Nakazawa, N., Wang, L., Toyoshima, C. and Yanagida, M. (2018) 'Suppressor mutation analysis combined with 3D modeling explains cohesin's capacity to hold and release DNA', *Proceedings of the National Academy of Sciences*, 115(21), E4833-E4842, available: http://dx.doi.org/10.1073/pnas.1803564115.

Yatskevich, S., Rhodes, J. and Nasmyth, K. (2019) 'Organization of Chromosomal DNA by SMC Complexes', *Annual Review of Genetics*, 53(1), 445-482, available: http://dx.doi.org/10.1146/annurev-genet-112618-043633.

Yoshinaga, M. and Inagaki, Y. (2021) *Ubiquity and origins of structural maintenance of chromosomes (SMC) proteins in eukaryotes*, Internal Cold Spring Harbor Laboratory Report, unpublished.

Zhang, N., Kuznetsov, S.G., Sharan, S.K., Li, K., Rao, P.H. and Pati, D. (2008) 'A handcuff model for the cohesin complex', *Journal of Cell Biology*, 183(6), 1019-1031, available: http://dx.doi.org/10.1083/jcb.200801157.

Zhang, X., Shu, L., Hosoi, H., Murti, K.G. and Houghton, P.J. (2002) 'Predominant Nuclear Localization of Mammalian Target of Rapamycin in Normal and Malignant Cells in Culture', *Journal of Biological Chemistry*, 277(31), 28127-28134, available: http://dx.doi.org/10.1074/jbc.m202625200.